



People's Democratic Republic of Algeria
Ministry of Higher Education and Scientific Research
University Djilali Bounaâma - Khemis Miliana
Faculty of Nature and Life Sciences and Earth Sciences
Earth Sciences Department



Field: Applied Geology
Speciality: Engineering Geology and Geotechnics

Thesis presented for obtaining a Master's degree
in Engineering Geology and Geotechnics

Theme

**Numerical Modeling of the Roadway Stabilized with
Lime: Case of the Harchoun Highway Section, W.
Chlef**

Prepared by :

Mr. **Jane-Molemo Joseph**
Mrs. **Tjimbueti-Joana Doroteia**

Posted on: 26/09/2021

Supervised by:

Dr. GADOURI Hamid	MCB	Khemis-Miliana University	Supervisor
Dr. MEZIANI Brahim	MCB	Khemis-Miliana University	Co-supervisor

Reviewed remotely by :

Dr. Kellouche Yasmina	MCB	Khemis-Miliana University	President
Dr. FILALI Mira	MCB	Khemis-Miliana University	Examiner

University Year : 2020/2021

Dedication

I want to dedicate this modest piece of work above all;

*In memory of my father **Motebang**, may he continue to rest in peace,*

*To my dear Mother **Mamolemo** for everything she has done for me, God bless and grant her more life,*

*To my dear sister and niece, **Liteboho** and **Naleli**,*

To all my closest friends without any exception,

*And to **Monica** who has been extremely helpful in all aspects through her mentorship.*

Molemo. J.J

Dedication

Je dédie ce modeste travail :

*À mes très chers parents **Luciano Tjimbueti** et **Amélia Songo** qui n'ont jamais cessé, de me soutenir et prier pour moi dans cette étape plus importante dans ma vie et pas seulement.*

*À mes sœur adorées **Veronica, Filipa, Teresa, Luisa, Lúcia** et **Clara,***

*À mes très chers frères **Francisco, Joaquim** et mon cher **neveu Real,***

*À ma chère tante **Mulembe,***

*À mes chères amis **Justina, Darlene** et **Jesna,***

*À mes chers amis **Mutilifa** et **Tomé,***

*À mes cher collègue **Molemo** et tous mes collègues de ma promotion 2020-2021*

Et à tous ceux qui m'ont aidé de près ou de loin à accomplir ce travail.

**Joana
Tjimbueti**

Acknowledgements

First of all, we want to thank the Almighty and Merciful God, who has given us the strength and the patience to do this modest work.

In the first place, we take this opportunity to address our warmest thanks and express our deep gratitude to our thesis Supervisor **Dr. Gadouri Hamid**, Lecturer and researcher at the University of Khemis-Miliana and member of the research laboratory “Geomaterials” from the University of Chlef, for having offered us an ambitious and motivating subject, for his constant support, these encouragements and these golden advice, for his patience, his generosity and for having trusted us throughout this project, for his benevolent supervision and for these constructive criticisms and his interest which he carried throughout the development of this thesis project.

My most sincere thanks to our Co-supervisor **Dr. Meziani Brahim**, Lecturer and researcher at the University of Khemis-Miliana for having guided us throughout this work, we warmly thank for his availability, his generosity and for his wise advice and his invaluable help in writing this brief.

We are pleased to sincerely thank **Dr. Kellouche Yasmina**, Lecturer and Researcher at the University of Khemis Miliana, and member of the “Geomaterials” research laboratory of the University of Chlef, for accepting to chair the jury,

We also extend our sincere thanks and expressions of all our gratitude to **Dr. Filali Mira**, Lecturer and Researcher at the University of Khemis-Miliana, for agreeing to give careful consideration to this work.

Finally, we thank all those who have helped us from near or far to all those who encouraged us to carry out this work.

ملخص

تساهم ، ذلك إلى بالإضافة .العالم أنحاء جميع في البلدان اقتصاد لتطور الرئيسي السبب وهو أساسية ضرورة الطرق إنشاء يعد ثباتها من للتحقق قوية وسيلة أيضاً الطرق لأرصفة الرقمية النمذجة تعد .للكاب ومأمونة أمنة قيادة في كبير بشكل الطرق هذه البناء ووقت البناء تكاليف تقليل وبالتالي (الطرق على المرور حركة) المركبات مرور حركة تجلبها التي الأحمال مواجهة في خام أرضية طبقة (PLAXIS-2D برنامج باستخدام الرقمية النمذجة طريق عن) استجابة دراسة هو المشروع هذا من الهدف بطبقة A -نموذج (1) :هما هندسيين نموذجين اقتراح تم ، الواقع في .الطرق على المرور حركة تأثير تحت بالجبر ومعالجتها لمحاكاة (باسكال كيلو 600) كبير وحمل (باسكال كيلو 200) بسيط لحمل تتعرض (CDF) متر 0.9 بسبك معالجة غير أساس يتم حيث A للنموذج الهندسي الشكل نفس له الذي B -النموذج (2) و التوالي على ، والثقيلة الخفيفة المركبات مرور حركة بنفس المعالجة التربة أعمدة على أيضاً هذا يعتمد .(م 0.6 و 0.3) مختلفة بسماكات الجبر من % 8 مع به الخاص CDF معالجة فيزيائية معلمة (1) :وهي ، الاعتبار في معلمات ثلاث تأثير أخذ تم ، ذلك ومع م. 2.1 و 1.4 و 0.7 بمسافات الجبر محتوى الجبر من % 8 مع لا أم معالجتها تمت (CDF) ميكانيكية معلمة (2) ، (المرور حركة تدفق لمحاكاة المطبقة الأحمال) إزاحة أن عليها الحصول تم التي النتائج أظهرت .(CDF سمك تباين) هندسية معلمة (3) و ، (الجيوتقنية والخصائص بالجبر والمعالج متر 0.6 بسبك CDF حالة في ، الإزاحة لعمليات بالنسبة ، ذلك ومع .(سم 3 >) مقبولة غير النموذجين متر 0.6 بسبك CDF حالة اختيار تم .سم 3 من أقل أنها الواضح فمن ، الجبر محتوى بنفس المعالجة الأعمدة على والراحة أمان وبالتالي مقبولة إزاحة ولديها اقتصادا الأكثر لأنها حدة على متر 2.1 و المعالجة الأعمدة على بناءً ، كلس % 8 ب معالج .باسكال كيلو 600 من كبيرة حمولة تأثير تحت $F_s = 1.2$ أمان معامل على الحصول تم حيث كاف

النموذج طبقة ، PLAXIS-2D رمز ، الرقمية النمذجة ، الجيوتقنية الخصائص ، الطرق على المرور أحمال :الرئيسية الكلمات .الإزاحات ، بالجبر المعالجة التربة أعمدة ، (CDF)

Abstract

The construction of roads is an indispensable necessity and is the main reason for the development of the economy of countries all over the world. In addition, these roads significantly contribute to a safe and secure driving for passengers. Numerical modelling of road pavements is also a powerful way to check their stability against the loads brought by vehicle traffic (road traffic) and thus to reduce construction costs and construction time. The purpose of this project is to study the response (by numerical modelling using PLAXIS-2D software) of a roadway with untreated and lime-treated subbase layer under the effect of road traffic. Indeed, two geometric models have been proposed namely: (1) Model-A with an untreated subbase layer (SL) of 0.9m thickness subjected to a minor load (200kPa) and a major (600kPa) load to simulate light and heavy vehicle traffic, respectively and (2) Model-B which has the same geometry as Model-A where its SL is treated with 8% lime at different thicknesses (0.3 and 0.6m). This is also based on soil columns treated with the same lime content with spaces of 0.7, 1.4 and 2.1m. However, the effect of three parameters was taken into account, namely: (i) a physical parameter (the loads applied to simulate the traffic flow), (ii) a mechanical parameter (SL treated or not with 8% lime and geotechnical properties), and (iii) a geometric parameter (variation in the thickness of SL). The results obtained showed that the displacements for both Models are inadmissible ($> 3\text{cm}$). However, for displacements, in the case of a SL with 0.6m thickness treated with lime and based on columns treated with the same lime content, are clearly less than 3cm. The case of a 0.6m thickness SL treated with 8% lime, based on treated columns and spaced by 2.1m was chosen because it is the most economic and presents admissible displacements and consequently, sufficient safety where a safety coefficient of $F_s = 1.2$ was obtained under the effect of a major load of 600kPa.

Keywords: Road traffic loads, Geotechnical properties, Numerical modelling, PLAXIS-2D software, Subbase layer (SL), Soil columns treated with lime, Displacements.

Résumé

La construction de routes est une nécessité essentielle et est la principale raison du développement de l'économie des pays du monde entier. De plus, ces routes contribuent de manière significative à une conduite sûre et sécurisée pour les passagers. La modélisation numérique des chaussées routières est également un moyen puissant de vérifier leur stabilité face aux charges apportées par la circulation des véhicules (trafic routier) et ainsi de réduire les coûts de construction et le temps de construction. Le but de ce projet est d'étudier la réponse (par modélisation numérique à l'aide du logiciel PLAXIS-2D) d'une chaussée à couche de fondation brute et traitée à la chaux sous l'effet du trafic routier. En effet, deux modèles géométriques ont été proposés à savoir : (1) Modèle-A avec une couche de fondation (CDF) non traitée de 0.9m d'épaisseur soumise à une charge mineure (200kPa) et une charge majeure (600kPa) pour simuler le trafic des véhicules légers et lourds, respectivement et (2) Modèle-B qui a la même géométrie que le Modèle-A où son CDF est traité avec 8% de chaux à différentes épaisseurs (0,3 et 0,6m). Ceci est également basé sur des colonnes de sol traitées avec la même teneur en chaux avec des espaces de 0,7, 1,4 et 2,1 m. Cependant, l'effet de trois paramètres a été pris en compte, à savoir : (i) un paramètre physique (les charges appliquées pour simuler le flux de trafic), (ii) un paramètre mécanique (CDF traité ou non avec 8% de chaux et propriétés géotechniques), et (iii) un paramètre géométrique (variation de l'épaisseur de CDF). Les résultats obtenus ont montré que les déplacements pour les deux modèles sont inadmissibles ($> 3\text{cm}$). Cependant, pour les déplacements, dans le cas d'un CDF de 0,6m d'épaisseur traité à la chaux et reposant sur des colonnes traitées avec la même teneur en chaux, sont nettement inférieurs à 3cm. Le cas d'un CDF d'épaisseur 0,6m traité à la chaux à 8%, à base de poteaux traités et espacés de 2,1m a été choisi car il est le plus économique et présente des déplacements admissibles et par conséquent, une sécurité suffisante où un coefficient de sécurité de $F_s = 1,2$ a été obtenu sous l'effet d'une charge importante de 600kPa.

Mots-clés : Charges du trafic routier, Propriétés géotechniques, Modélisation numérique, Code PLAXIS-2D, Couche de forme (CDF), Colonnes de sol traitées à la chaux, Déplacements.

Table of contents

Dedication	
Acknowledgements	
ملخص	
Abstract	
Résumé	
Table of contents	
List of figures	
List of tables	
List of notations and abbreviations	
General introduction.....	1
Chapter 1 : Road traffic and Pavement structures	
1.1. Introduction.....	3
1.2. Road Traffic.....	3
1.2.1. Different types of traffic.....	3
1.2.2. Different classes of traffic.....	3
1.2.3. Presentation of traffic models.....	4
1.2.4. Existing traffic analysis and Traffic counting methods.....	5
1.2.5. Classification of vehicles.....	6
1.2.6. Traffic stream parameters.....	8
1.2.6.1. Speed.....	11
1.2.6.1. Flow.....	11
1.2.6.1. Density.....	12
1.3. The different types of pavement structures.....	12
1.3.1. Flexible pavements.....	13
1.3.2. Semi-rigid pavements.....	14
1.3.3. Rigid pavements.....	15
1.4. Materials used in the construction of road pavements.....	15
1.4.1. Soil.....	15

1.4.2. Aggregate.....	14
1.4.3. Asphalt and bitumen.....	14
1.4.4. Concrete.....	15
1.4.5. Composite pavement.....	16
1.5. Conclusion.....	16

Chapter 2 : Summary of road pavement simulation models

2.1. Introduction.....	17
2.2. Road pavement simulation models.....	17
2.2.1. Behaviour Models.....	17
2.2.2. Types of Behaviour Model.....	18
2.2.2.1. Empirical Model.....	19
2.2.2.2. Establishment of Empirical Model.....	20
2.2.2.3. Analytical-Empirical Models.....	24
2.2.3. Analytical Models.....	24
2.2.3.1. Boussinesq Model (1885).....	24
2.2.3.2. Westergaard Bilayer Model (1926).....	25
2.2.3.3. Hogg’s Bilayer Model (1938).....	26
2.2.3.4. Burmister Model (1943).....	27
2.2.3.5. Jeuffroy Model (1955).....	28
2.3. Conclusion.....	29

Chapter 3 : Presentation of PLAXIS Software

3.1. Introduction.....	30
3.2. PLAXIS-2D code simulation.....	30
3.2.1. Plaxis calculation code.....	30
3.2.2. Default options and approximate solutions.....	31
3.2.3. Plaxis sub-programs.....	31
3.2.3.1. The data input program (Input).....	31
3.2.3.2. The calculation program (Calculations).....	32
3.2.3.3. The output programmes.....	33
3.2.3.4. The programme curves.....	33
3.2.4. The modelling approach with PLAXIS.....	34
3.2.4.1. Geometry.....	34
3.2.4.2. Boundary conditions.....	35

3.2.4.3. Definition of material parameters.....	35
3.2.4.4. Mesh Size.....	35
3.2.4.5. The initial conditions.....	35
3.2.4.6. Calculation phase.....	36
3.2.4.7. Visualisation of Results.....	36
3.3. Behavioural laws in PLAXIS.....	36
3.3.1. Mohr-Coulomb's model.....	37
3.3.1.1. Young's Modulus.....	39
3.3.1.2. Poisson's ratio.....	40
3.3.1.3. Friction Angle.....	40
3.3.1.4. Cohesion.....	40
3.3.1.5. The angle of dilatancy.....	41
3.3.1.6. Tensile stresses.....	41
3.3.1.7. Advanced settings.....	41
3.3.2. Hardening Soil Model (H.S.M).....	42
3.4. Conclusion.....	44

Chapter 4 : Presentation of study area, Numerical Modelling, Results and Interpretation

4.1. Introduction.....	45
4.2. Presentation of study area.....	45
4.3. Identification and characterization of soil used.....	46
4.4. Geotechnical parameters used.....	47
4.5. Geometric models.....	48
4.6. Numerical Modelling.....	49
4.6.1. Mesh generation.....	49
4.6.2. Boundary conditions.....	49
4.6.3. Pore pressure generation.....	50
4.6.4. Effective stress generation.....	51
4.7. Results and discussion.....	52
4.7.1. Case of the untreated subbase layer "Model-A".....	52
4.7.1.1. Extreme total displacement in the untreated subbase layer.....	52
4.7.1.2. Coefficient security obtained with Min and Max loads for Model-A.....	53
4.7.2. Case of the treated subbase layer "Model-B".....	55
4.7.2.1. Extreme total displacement in the untreated subbase layer.....	56
4.7.2.1.1. Extreme total displacement for lime-treated subbase layer without....	56

treated columns

4.7.2.1.2. Extreme total displacement for lime-treated subbase layer based on lime-treated columns.....	58
4.7.2.2. Coefficient security obtained with Min and Max loads for Model-A.....	61
4.8. Conclusion.....	64
General Conclusions & recommendations.....	65
List of references.....	67

List of figures

Figure 1.1: Traffic classification (SETRA)

Figure 1.2. Light vehicles

Figure 1.3. Intermediate vehicles

Figure 1.4. Heavy goods vehicles and coaches with 2 axles

Figure 1.5. Heavy goods vehicles and coaches with 3 axles

Figure 1.6. Illustration of density (Tom V. Mathew and K V Krishna Rao)

Figure 1.7. Typical structure of a flexible pavement

Figure 1.8. Typical structure of a semi-rigid pavement

Figure 1.9. Typical structure of a Rigid pavement

Figure 2.1. An example of a degradation behaviour model

Figure 2.2. Example of the evolution of a degradation

Figure 2.3. Types of behavioural models (LAVOC, EPF Lausanne Suisse)

Figure 2.4. Fatigue rides at EPFL and EPFZ

Figure 2.5. Typical representation of a photo method

Figure 2.6. Description of the photo method

Figure 2.7. Typical representation of a video method

Figure 2.8. Description of the video method

Figure 2.9. Diagram of Boussinesq Model

Figure 2.10. Diagram of Westergaard Model

Figure 2.11. Diagram of Hogg's Model

Figure 2.12. Diagram of Burmister Model

Figure 2.13. Diagram of Jeuffroy Model

Figure 2.14. Parameters influencing the appearance and evolution of degradation

Figure 3.1. Main window of the Input program (geometric creation).

Figure 3.2. Main window of the calculation program.

Figure 3.3. Calculation window.

Figure 3.4. Toolbar of the main window of the Output program.

Figure 3.5. Toolbar in the main window of the curve's program.

Figure 3.6. Modelling of a triaxial compression test with the Mohr Coulomb model (a) and representation of the stresses in the Mohr plane (b).

Figure 3.7. Mohr-Coulomb pyramid plotted for $C=0$.

Figure 3.8. Mohr-Coulomb window setting.

Figure 3.9. Definition of modulus at 50% failure.

Figure 3.10. Angle of Dilatancy (ψ).

Figure 3.11. Mohr-Coulomb advanced window settings.

Figure 3.12. Representation of the hyperbolic relation managing the hardening of the HSM model.

Figure 3.13. Definition of the parameter E from the results of an oedometer test.

Figure 3.14. Hardening Soil Model window settings.

Figure 4.1. Sampling of red clay soil from a depth of 5m in the region of Harchoun, Algeria.

Figure 4.2. Model-A suggested for subbase layer without treatment.

Figure 4.3. Model-B suggested for subbase layer treated with 8% lime based on columns treated with the same lime content.

Figure 4.4. Mesh generation for Model-A.

Figure 4.5. Mesh generation for Model-B.

Figure 4.6. Boundary conditions for Model-A.

Figure 4.7. Boundary conditions for Model-B.

Figure 4.8. Pore pressure generation for Model-A.

Figure 4.9. Pore pressure generation for Model-B.

Figure 4.10. Effective stress generation for Model-A.

Figure 4.11. Effective stress generation for Model-B.

Figure 4.12. Different calculation phases made for the untreated subbase layer by the application of Min (200kPa) and Max (600kPa) loads (Model-A).

Figure 4.13. Extreme total displacement of the untreated subbase layer obtained from the application of Min-load (200kPa) (Model-A).

Figure 4.14. Extreme total displacement made on the untreated subbase layer obtained from the application of Max-load (600kPa) (Model-A).

Figure 4.15. Coefficient security obtained by the application of Min-load (200 kPa) for Model-A.

Figure 4.16. Coefficient security obtained by the application of Max-load (600 kPa) for Model-A.

Figure 4.17. Different calculation phases made for lime-treated subbase layer (0.3 m thick) by the application of Min (200kPa) and Max (600kPa) loads (Model-B).

Figure 4.18. Different calculation phases made for lime-treated subbase layer (0.6 m thick) by the application of Min (200kPa) and Max (600kPa) loads (Model-B).

Figure 4.19. Extreme total displacement of lime-treated subbase layer (0.3 m thick) caused by the application of Min-load (200kPa) (Model-B).

Figure 4.20. Extreme total displacement of lime-treated subbase layer (0.3 m thick) caused by the application of Min-load (600kPa) (Model-B).

Figure 4.21. Extreme total displacement of lime-treated subbase layer (0.6 m thick) caused by the application of Max-load (200kPa) (Model-B).

Figure 4.22. Extreme total displacement of lime-treated subbase layer (0.6 m thick) caused by the application of Max-load (600kPa) (Model-B).

Figure 4.23. Extreme total displacement of lime-treated subbase layer (0.3 m thick) made by the application of Min-load (200kPa) based on lime-treated columns spaced by 0.7 m (Model-B).

Figure 4.24. Extreme total displacement of lime-treated subbase layer (0.3 m thick) made by the application of Min-load (200kPa) based on lime-treated columns spaced by 1.4 m (Model-B).

Figure 4.25. Extreme total displacement of lime-treated subbase layer (0.3 m thick) made by the application of Min-load (200kPa) based on lime-treated columns spaced by 2.1 m (Model-B).

Figure 4.26. Extreme total displacement of lime-treated subbase layer (0.3 m thick) made by the application of Max-load (600kPa) based on lime-treated columns spaced by 0.7 m (Model-B).

Figure 4.27. Extreme total displacement of lime-treated subbase layer (0.3 m thick) made by the application of Max-load (600kPa) based on lime-treated columns spaced by 1.4 m (Model-B).

Figure 4.28. Extreme total displacement of lime-treated subbase layer (0.3 m thick) made by the application of Max-load (600kPa) based on lime-treated columns spaced by 2.1 m (Model-B).

Figure 4.29. Extreme total displacement of lime-treated subbase layer (0.6 m thick) made by the application of Min-load (200kPa) based on lime-treated columns spaced by 0.7 m (Model-B).

Figure 4.30. Extreme total displacement of lime-treated subbase layer (0.6 m thick) made by the application of Min-load (200kPa) based on lime-treated columns spaced by 1.4 m (Model-B).

Figure 4.31. Extreme total displacement of lime-treated subbase layer (0.6 m thick) made by the application of Min-load (200kPa) based on lime-treated columns spaced by 2.1 m (Model-B).

Figure 4.32. Extreme total displacement of lime-treated subbase layer (0.6 m thick) made by the application of Max-load (600kPa) based on lime-treated columns spaced by 0.7 m (Model-B).

Figure 4.33. Extreme total displacement of lime-treated subbase layer (0.6 m thick) made by the application of Max-load (600kPa) based on lime-treated columns spaced by 1.4 m (Model-B).

Figure 4.34. Extreme total displacement of lime-treated subbase layer (0.6 m thick) made by the application of Max-load (600kPa) based on lime-treated columns spaced by 2.1 m (Model-B).

Figure 4.35. Effects of different applied loads on the untreated and lime-treated subbase layer with different thicknesses.

Figure 4.36. Effects of both different applied loads and lime-treated columns under different spacing on the behaviour of lime-treated subbase layer with 0.3m thickness (LTSL-WC: lime-treated subbase layer without treated columns; LTSL-SC: lime-treated subbase layer based on lime-treated columns under different spacing).

Figure 4.37. Effects of both different applied loads and lime-treated columns under different spacing on the behaviour of lime-treated subbase layer with 0.6m thickness (LTSL-WC: lime-treated subbase layer without treated columns; LTSL-SC: lime-treated subbase layer based on lime-treated columns under different spacing).

List of tables

Table 1.1. Different classes of traffic.

Table 4.1. Physico-mechanical and chemico-mineralogical properties of red soil used as a subbase soil.

Table 4.2. Geotechnical and geometrical parameters.

Table 4.3. General information from mesh generation.

Table 4.4. Displacements for untreated subbase layer.

Table 4.5. Displacement for lime-treated subbase layer without lime-treated columns.

Table 4.6. Displacement for lime-treated subbase layer with different spacing distance of lime-treated columns soil (LTCS).

List of notations and abbreviations

- C : KN/m^2 : cohesion (effective)
- AADT : Average Annual Daily Traffic
- AAWT : Average Annual Weekday Traffic
- ADT : Average Daily Traffic
- ADR : Annual Daily Average
- ALT. : Accelerating, Landing Test
- AWT : Average Weekday Traffic
- Φ : Effective friction angle
- Ψ : Angle of dilatancy
- Ds cm : Displacement
- E KN/m^2 : Young's modulus
- Fs : Safety Coefficient
- GNP : Gross national product
- K m^2 : coefficient of permeability
- LTSL : Lime-treated Subbase Layer
- LCPC : Laboratoire Centrale des Ponts et Chaussées
- σ' KPa : Effective stress
- σ KPa : Normal stress
- SETRA : Services d'études Techniques des Routes et Autoroutes (road and motorway technical study services)
- SL : Subbase Layer
- USL : Untreated Subbase Layer
- v : Poisson's ratio
- γ KN/m^3 : Density

General

Introduction

General introduction

The construction of roads is an indispensable necessity and is the main reason for the development of the economy of countries around the world (Gadouri et al. 2017a). In addition, these roads contribute significantly to providing passengers with a safe and secure ride when moving from one place to another.

However, these types of engineering structures require a huge financial outlay and a very long construction time (Gadouri et al. 2017b). The choice of destination (layout), the type of materials to be used (materials for the construction of different layers of the road pavement), the type of road (category and environmental friendliness) is based on catalogues (B40, 1977), technical guides (LCPC-SETRA, 1994) and other manuals which should be followed. For all these reasons, the choice of the most appropriate design method for road construction is a very important factor. Indeed, the chosen design method can contribute considerably to reducing construction costs and construction time and thus guaranteeing the sustainability of the project, while ensuring maximum traffic flow and comfort for people during travel.

In fact, a large number of methods are used for the structural design of road pavements and the type of materials to be used in road infrastructure (Manoj and Sharad, 2019). The choice of the most appropriate method is based on compliance with the above-mentioned requirements (construction costs, construction time and durability of the project/life span). Numerical modelling of road pavements is also an effective means of verifying their stability against loads from vehicle traffic.

Objective

The main objective of this project is to study the response, by numerical modelling, of a lime-stabilised road pavement. Indeed, the collection of data from the literature or from a completed or ongoing road project is very important in order to study a real case using the **PLAXIS 2D** software.

Work plan

This thesis is structured in four chapters namely:

A general introduction outlining the problem and defining the objectives to be achieved;

- **The first chapter** presents in the first part an overview on road traffic, traffic models and traffic stream parameters while the second part presents an overview on different types of road pavements and the materials commonly used in the construction of those pavements.
- **The second chapter** presents a literature review on the summary of road pavement simulation models developed, their types and choice depending the problem posed.
- **The third chapter** gives a general presentation on the PLAXIS software.
- **The fourth chapter** presents the study area, data collected and the response of a lime-stabilized road pavement based on the numerical modelling with PLAXIS-2D software.

Finally, essential conclusions and recommendations will be drawn.

Chapter 1

Road traffic and Pavement structures

1.1. Introduction

This chapter presents a bibliographic study on road traffics and pavement structures with further details on the types of traffic, classification of pavements, as well as materials used in the construction of pavement structures.

1.2. Road Traffic

Traffic on roads is made up of road users including vehicles, streetcars, buses, pedestrians, ridden or herded animals and other conveyances. Therefore, in order to keep a flexible and efficient flow of traffic on roads, it is necessary to do traffic study. This is an essential element that must be a prerequisite to any project for the construction or development of transport infrastructure. It renders it possible to determine different types of traffic and classes of traffic, appropriate models of traffic used, preliminary study on existing traffic analysis, traffic stream parameters as well as classifying vehicles according to their various criteria.

1.2.1. Different types of traffic

There are various classifications of traffic, which are based in nature of formation. These include; normal, diverted, induced, and total traffic (B40, 1977).

- **Normal traffic:** It is an existing traffic on the old development without considering the new project.
- **Diverted Traffic:** It is the traffic directed towards the new developed road and borrowing, without investment, other roads having the same destination, the diversion of traffic is only a transfer between the different means of reaching the same destination.
- **Induced traffic:**
 - This is the traffic that results from:
 - New movements of people who take place and which due to the poor quality of the old road, improvements were not carried out previously or were carried out to other destinations.
 - An increase in production and sales due to the ease provided by the new road development.
- **Total traffic:** The traffic on the new development which is the sum of the induced and deviated traffic.

1.2.2. Different classes of traffic

The traffic classes are defined by the average daily traffic of heavy goods vehicles (payload greater than 5 T) travelling on the roadway (LCPC-SETRA, 1994) (Table 1.1).

Table 1.1. Different classes of traffic

CLASS	Label	Label
Class t6	0 to 10	PL/j
Class t5	10 to 25	PL/j
Class t4	45 to 50	PL/j
Class t3	50 to 100	PL/j
Class t3	100 to 150	PL/j
Class T3	50 to 150	PL/j
Class T2	150 to 300	PL/j
Class T1	300 to 750	PL/j
Class T0	750 to 2 000	PL/j

We thus obtain these traffic classes defining two main categories of roads (Figure 1.1);

- Low-traffic roads grouping together all classes from t6 to t3 +,
- Medium and heavy traffic roads grouping all classes from T3 to T0 (Fédéric, 2015).

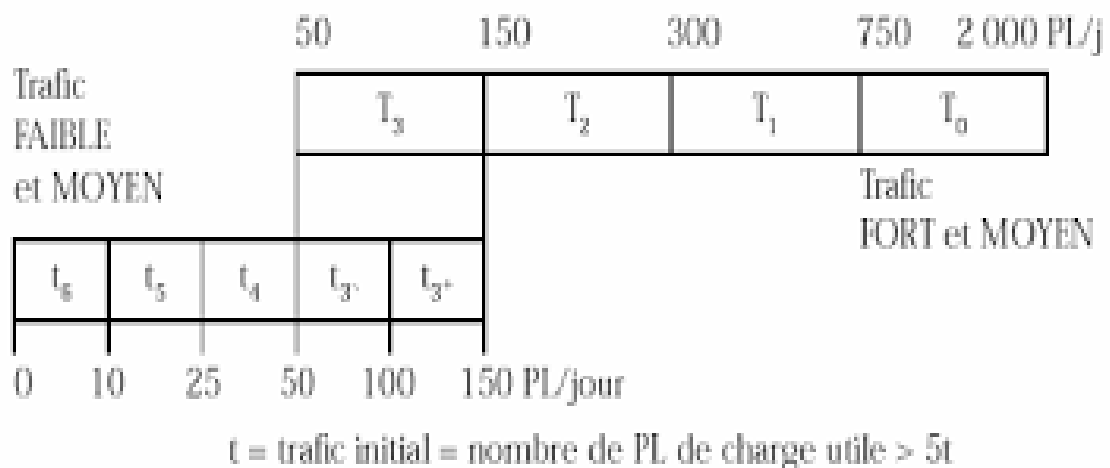


Figure 1.1 : Traffic classification (SETRA, 2000).

1.2.3. Presentation of traffic models

In the study of traffic projections, the first operation consists in defining a certain number of traffic flows which constitute homogeneous sets, in terms of development or allocation (B40, 1977).

The various methods used to estimate traffic in the future are:

a) Extension of the past development

The method consists of extrapolating globally over the coming years, the evolution of traffic observed in the past. We usually establish a model exponential type growth.

b) Correlation between traffic and economic parameters

It consists of looking in the past for a correlation between the level of traffic on the one hand and certain macroeconomic indicators:

- Gross national product (GNP).
- Fuel products, on the other hand, if it is believed that this correlation will remain to be verified in the rate of traffic growth, but this method requires the use of a simulation model, which is beyond the scope of our study.

c) Gravity model

It is necessary for the resolution of problems concerning current traffic in the near future, but it lends itself poorly to projection.

d) Growth factor model

This type of model allows us to project an origin - destination matrix. The most used method is that of FRATAR which takes into account the following factors:

- The rate of motorization of light vehicles and their use.
- The number of jobs.
- The population of the area.

This method requires precise statistics and a thorough research of the area to be studied.

1.2.4. Existing traffic analysis and Traffic counting methods

Traffic study is an important step in the development of a road project and consists of characterising the traffic conditions of road users (volume, composition, traffic conditions, saturation, origin and destination). Moreover, this is carried out using different traffic measurements methods such as counting and surveys that usually begin with the collection of data.

Traffic counting method is the essential element of the traffic study, and it is further classified into manual and automatic counts (B40, 1977).

a) Manual counts

They are carried out by investigators or surveyors who record the composition of the traffic to supplement the indicators provided by the automatic counts. Manual counts make it possible to know the percentage of heavy goods vehicles and public transport. Traffic is expressed as an annual daily average (ADR).

b) Automatic counts

They are carried out using a recording device comprising a pneumatic detection carried out by a rubber tube stretched across the roadway. A distinction is made between those which are permanent and those which are temporary:

- **Permanent counts:** are carried out at certain points chosen for their representativeness on the most important roads: motorway network, national road network and the province road with the most traffic.
- **Temporary counts:** carried out once a year for one month during the period when traffic is intense on the remains of the road networks using rotating counting stations.

1.2.5. Classification of vehicles

Automobiles can be classified according to various criteria: size, weight, type of use, shape of their bodywork, engine, type of transmission, level of equipment, level of customization or transformation. Obviously, each automobile model has a specific trade name to distinguish it from others.

In the field of road traffic, specialists are much more interested in the following three criteria:

- The total height of the vehicle or rolling assembly.
- The number of axles on the ground of the vehicle or the rolling assembly
- And most importantly, gross vehicle weight rating (GVWR) (for rolling assemblies, only the GVWR of the towing vehicle is considered.

We distinguish for types of vehicles namely: (Fédéric, 2015)

a) Light vehicles

Light vehicles or rolling assemblies with a GVWR less than 3.5 tonnes and a total height less than or equal to 2 meters (Figure 1.2).

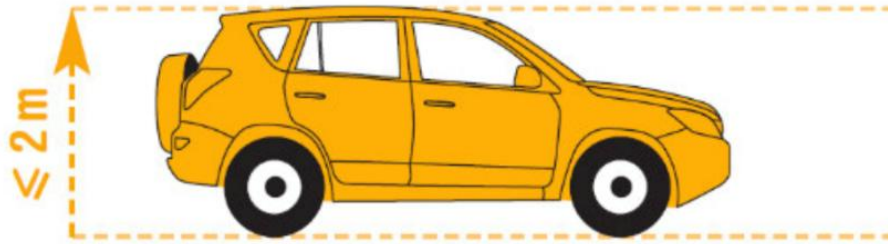


Figure 1.2. Light vehicles.

b) Intermediate vehicles

Vehicles or rolling assemblies whose GVWR is less than or equal to 3.5 tonnes and whose total height is strictly included (Figure 1.3).



Figure 1.3. Intermediate vehicles.

c) Heavy-duty vehicles

Heavy goods vehicles are also divided into two categories:

- **Heavy goods vehicles and coaches with 2 axles**

Vehicles with 2 axles, the total height of which is greater than or equal to 3 meters or whose GVWR is greater than 3.5 tonnes (Figure 1.4).

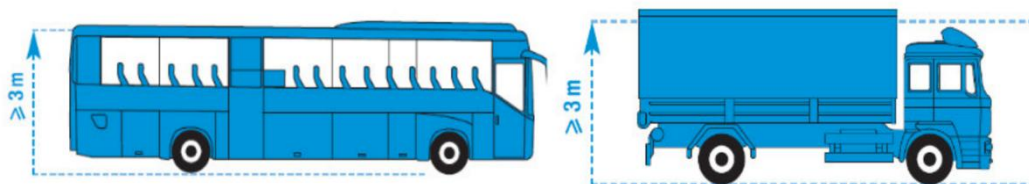


Figure 1.4. Heavy goods vehicles and coaches with 2 axles.

- **Heavy goods vehicles and coaches with 3 axles and more**

Vehicle or combinations of vehicles with more than 2 axles, the total height of which is greater than or equal to 3 meters or whose GVWR is greater than 3.5 tonnes (Figure 1.5).

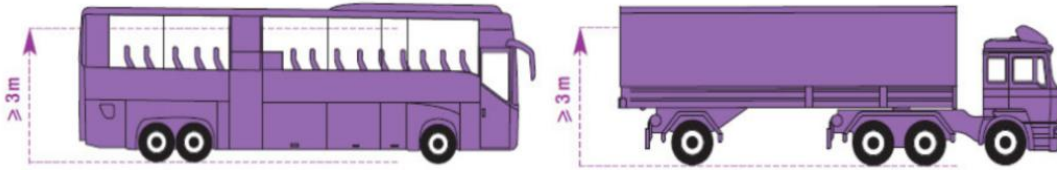


Figure 1.5. Heavy goods vehicles and coaches with 3 axles.

1.2.6. Traffic stream parameters

According to Mathew and Krishna Rao (2006), the traffic stream includes a combination of driver and vehicle behavior. The driver or human behavior being non-uniform, traffic stream is also non-uniform in nature. It is influenced not only by the individual characteristics of both vehicle and human but also by the way a group of such units interacts with each other. Thus a flow of traffic through a street of defined characteristics will vary both by location and time corresponding to the changes in the human behavior.

Thus the traffic stream itself is having some parameters on which the characteristics can be predicted. The parameters can be mainly classified as: measurements of quantity, which includes density and flow of traffic and measurements of quality which includes speed. The traffic stream parameters can be macroscopic which characterizes the traffic as a whole or microscopic which studies the behavior of individual vehicle in the stream with respect to each other.

As far as the macroscopic characteristics are concerned, they can be grouped as measurement of quantity or quality as described above, i.e. flow, density, and speed while the microscopic characteristics include the measures of separation (i.e. the headway or separation between vehicles which can be either time or space headway). The fundamental stream characteristics are speed, flow, and density and are discussed below.

1.2.6.1. Speed

Speed is considered as a quality measurement of travel as the drivers and passengers will be concerned more about the speed of the journey than the design aspects of the traffic. It is defined as the rate of motion in distance per unit of time. Mathematically speed or velocity v is given by Eq. 1:

$$v = \frac{d}{t} \quad (1)$$

where: v is the speed of the vehicle in m/s, d is distance travelled in m in time t seconds. Speed of different vehicles will vary with respect to time and space. To represent these variations, several types of speed can be defined. Important among them are spot speed, running speed, journey speed, time mean speed and space mean speed.

1.2.6.2. Flow

There are practically two ways of counting the number of vehicles on a road. One is flow or volume, which is defined as the number of vehicles that pass a point on a highway or a given lane or direction of a highway during a specific time interval. The measurement is carried out by counting the number of vehicles, n_t , passing a particular point in one lane in a defined period t . Then the flow q expressed in vehicles/hour is given by Eq. 2.

$$q = \frac{n_t}{t} \quad (2)$$

Flow is expressed in planning and design field taking a day as the measurement of time.

- **Variation of volume**

The variation of volume with time, i.e. month to month, day to day, hour to hour and within a hour is also as important as volume calculation. Volume variations can also be observed from season to season. Volume will be above average in a pleasant motoring month of summer, but will be more pronounced in rural than in urban area. But this is the most consistent of all the variations and affects the traffic stream characteristics the least. Weekdays, Saturdays and Sundays will also face difference in pattern. But comparing day with day, patterns for routes of a similar nature often show a marked similarity, which is useful in enabling predictions to be made. The most significant variation is from hour to hour. The peak hour observed during mornings and evenings of weekdays, which is usually 8 to 10 per cent of total daily flow or 2 to 3 times the average hourly volume. These trips are mainly the work trips, which are relatively stable with time and more or less constant from day to day.

- **Types of volume measurements**

Since there is considerable variation in the volume of traffic, several types of measurements of volume are commonly adopted which will average these variations into a single volume count to be used in many design purposes.

- **Average Annual Daily Traffic (AADT)** : The average 24-hour traffic volume at a given location over a full 365-day year, i.e. the total number of vehicles passing the site in a year divided by 365.
- **Average Annual Weekday Traffic (AAWT)** : The average 24-hour traffic volume occurring on week- days over a full year. It is computed by dividing the total weekday traffic volume for the year by 260.
- **Average Daily Traffic (ADT)** : An average 24-hour traffic volume at a given location for some period of time less than a year. It may be measured for six months, a season, a month, a week, or as little as two days. An ADT is a valid number only for the period over which it was measured.
- **Average Weekday Traffic (AWT)** : An average 24-hour traffic volume occurring on weekdays for some period of time less than one year, such as for a month or a season.

The relationship between AAWT and AWT is analogous to that between AADT and ADT. Volume in general is measured using different ways like manual counting, detector/sensor counting, moving-car observer method, etc. Mainly the volume study establishes the importance of a particular route with respect to the other routes, the distribution of traffic on road, and the fluctuations in flow. These eventually determine the design of a highway and the related facilities. Thus, the volume is treated as the most important of all the parameters of traffic stream.

1.2.6.3. Density

Density is defined as the number of vehicles occupying a given length of highway or lane and is generally expressed as vehicles per km (Figure 1.6). One can photograph a length of road x , count the number of vehicles, n_x , in one lane of the road at that point of time and derive the density k as Eq. 3.

$$k = \frac{n_x}{x} \quad (3)$$

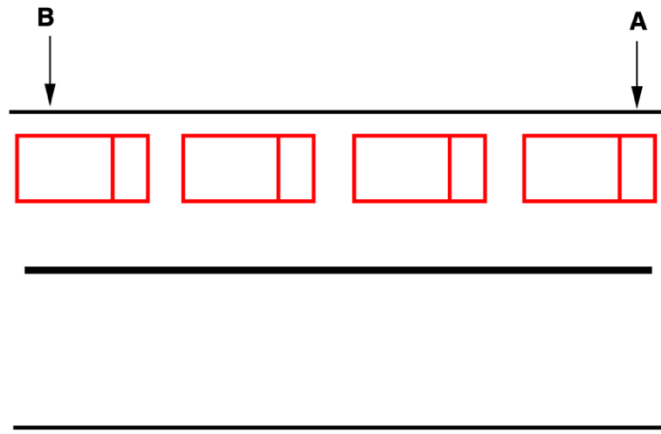


Figure 1.6. Illustration of density [Mathew and Krishna Rao \(2006\)](#).

This is illustrated in figure 30:1. From the figure, the density is the number of vehicles between the point A and B divided by the distance between A and B. Density is also equally important as flow but from a different angle as it is the measure most directly related to traffic demand. Again it measures the proximity of vehicles in the stream which in turn affects the freedom to manoeuvre and comfortable driving.

1.3. The different types of pavement structures

Depending on the mechanical functioning of the road, there are generally three different types of structures ([Jean-Michel, 2017](#)):

- Flexible pavements;
- Semi-rigid pavements;
- Rigid pavements.

1.3.1. Flexible pavements

Flexible pavements are those which have low or negligible flexural strength and are rather flexible in their structural action under applied loads. In these pavements, the deformation of the lower layers is reflected on to the road surface. Thus, if the lower layers or soil subgrade is undulated, a similar failure manifest on pavement surface ([Figure 1.7](#)). A typical flexible pavement consists of four components;

- Soil subgrade
- Sub-base course
- Base course
- Surface course

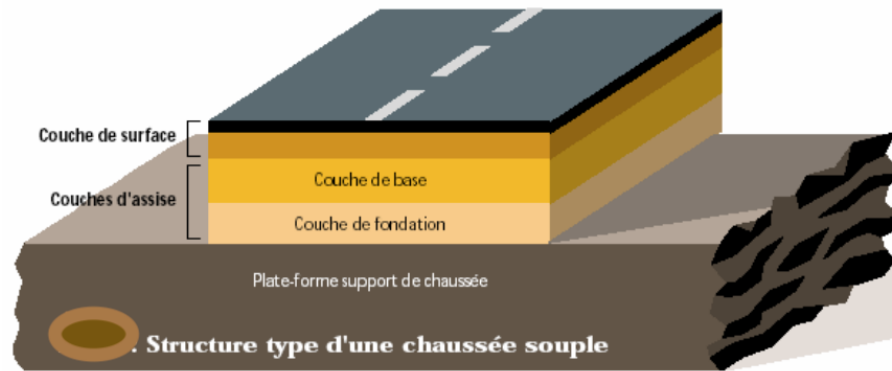


Figure 1.7. Typical structure of a flexible pavement (Jean-Michel, 2017).

The flexible pavement layers transmit the vertical or compressive stresses to the lower layers by grain-to-grain transfer through the points of contact in the granular structure. A well compacted granular structure consisting of strong graded aggregate (interlocked aggregate structure with or without binder materials) can transfer the compressive stresses through a wider area and thus forms a good flexible pavement layer. The load spreading ability of this layer therefore depends on the type of materials and the mix design factors. Bituminous concrete is one of the best flexible pavement layer materials. Other materials which fall under the group are, all granular materials with or without bituminous binder, granular base and sub-base course materials like the Water Bound Macadam, crushed aggregate, gravel, soil-aggregate mixes etc.

The vertical compressive stress is maximum on the pavement surface directly under the wheel load and is equal to the contact pressure the wheel. Due to the ability to distribute the stresses to a larger area in the shape of a truncated cone, the stresses get decreased at the lower layers. Therefore, by taking full advantage of the stress distribution characteristics of the flexible pavement, the layer system concept was developed. According to this, the flexible pavement may be constructed in a number of layer and top layer has to be the strongest as the highest compressive stresses are to be sustained by this layer, in addition to the wear and tear due to the traffic. The lower layers have to take up only lesser magnitudes of stresses and there is no direct wearing action due to traffic loads, therefore inferior materials with lower cost can be used in the lower layers. The lowest layer is the prepared surface consisting of the local soil itself, called the subgrade. An example of a flexible pavement structure is shown in Fig. 7; this consists of a wearing surface at the top, below which is the base course followed by the sub-base course and the lowest layer consists of the soil subgrade which has the lowest stability among the four typical flexible pavement components. Each of the flexible pavement layers above the subgrade, viz sub-base, base course and the surface course may consist of one or more number of layers of the same or slightly different materials and specifications.

Flexible pavements are commonly designed using empirical design charts or equations taking into account some of the design factors. There are also semi-empirical and theoretical design methods.

1.3.2. Semi-rigid pavements

When bonded materials like the pozzolanic concrete (lime-fly ash-aggregate mix), lean concrete or soil-cement are used in the base course or sub-base course layer the pavement layer has considerably higher flexural strength than the common flexible pavement layers (Figure 1.8). However, these bonded materials do not possess as much flexural strength as the cement concrete pavements. Therefore, when this intermediate class of materials are used in the base or sub-base course layer of the pavements, they are called semi-rigid pavements. This category of semi-rigid pavements is either designed as flexible pavements with some correction factors to find the thickness requirements based on experience, or by using a new design approach. These semi-rigid pavement materials have low resistance to impact and abrasion and therefore are usually provided with flexible pavement surface course.

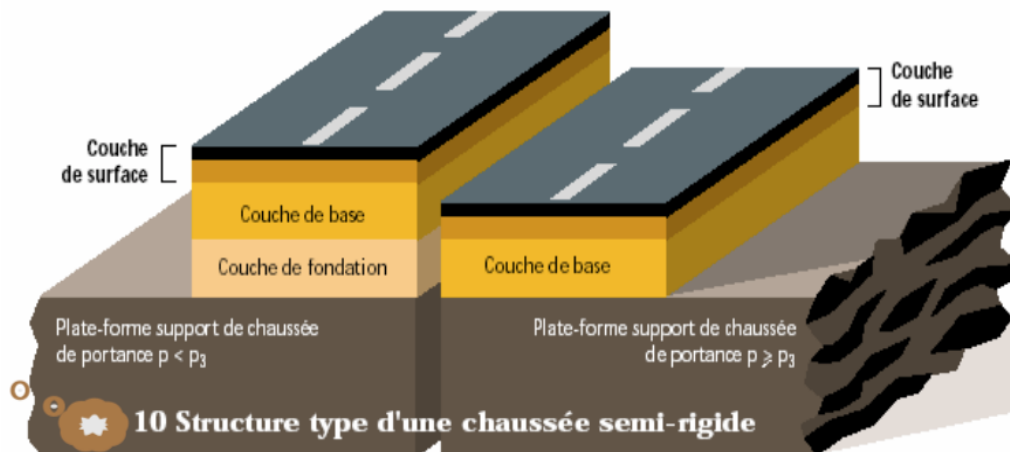


Figure 1.8. Typical structure of a semi-rigid pavement (Jean-Michel, 2017).

1.3.3. Rigid pavements

Rigid pavements are those which possess note-worthy flexural strength or flexural rigidity. The stresses are not transferred from grain to grain to the lower layers as in the case of flexible pavements. The rigid pavements are made of Portland cement concrete—either plain, reinforced or prestressed. The plain cement concrete slabs are expected to take up about $40\text{kg}/\text{cm}^2$ flexural stress (Figure 1.9). The rigid pavement has the slab action and is capable of transmitting the wheel load stress through a wider area below. The main point of the difference in the structural behaviour of rigid pavements as compared to the flexible pavement is that the critical condition of stress in the rigid pavement is the maximum flexural stress occurring in the slab due to the wheel load and the temperature changes whereas in the flexible pavement, it is the distribution of compressive

stresses. As the rigid pavement slab has tensile strength, tensile stresses are developed due to the bending of the slab under wheel load and temperature variations. Thus, the types of stresses developed and their distribution within the cement concrete slab are quite different. The rigid pavement does not get deformed to the shape of the lower surface as it can bridge the minor variation of lower layers.

The cement concrete pavement slab can very well serve as a wearing surface as well as effective base course. Therefore, usually the rigid pavement structure consists of a cement concrete slab, below which a granular base or sub-base-course may be provided. Though the cement concrete slab can also be laid directly over the soil subgrade, this is not preferred particularly when the subgrade, consists of fine-grained soil. Providing a good base or sub-base course layer under the cement concrete slab, increases the pavement life considerably and therefore works out more economical in the long run. The rigid pavements are usually designed and the stresses are analysed using the elastic theory, assuming the pavement as an elastic plate resting over an elastic or viscous foundation.

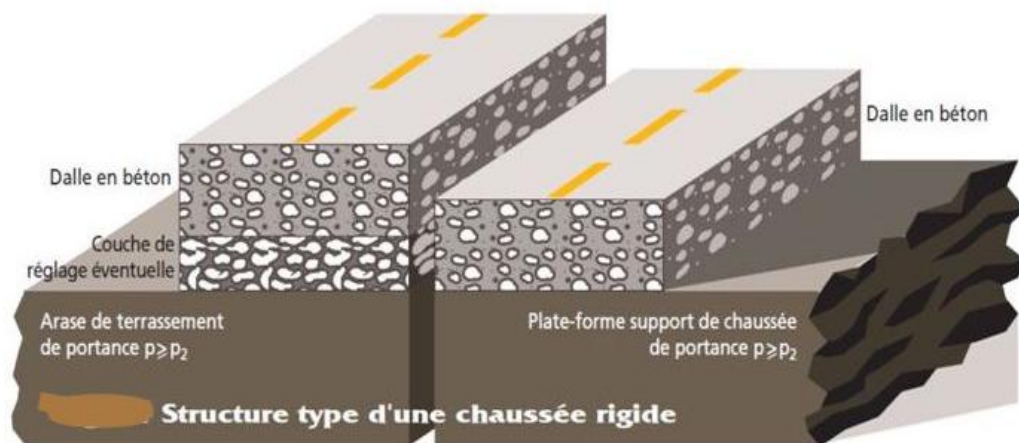


Figure 1.9. Typical structure of a rigid pavement (Jean-Michel, 2017).

1.4. Materials used in the construction of road pavements

Road construction is a highly technical venture that requires a range of distinct materials to ensure the motorways are durable and well able to support heavy loads and traffic. These materials range from natural soils, aggregates (derived from rocks), binders such as lime, asphalt, concrete, and assorted products used as admixtures for improved quality of roads (Mugdha, 2000).

1.4.1. Soil

Soil naturally tops the list of materials used in the construction of roads. It is the eventual point which supports the complete structure of the road. Indeed, soil is the primary material for the

foundation, subgrade, or the pavement in the case of low traffic rural roads. It provides the essential flat base that offers the vital support for the road structure.

A process known as compaction, where soil particles are pressed together to reduce pore space between them, is usually carried out on site to give the soil at the base some higher resistance and greater stability. Being a natural material, soils have different qualities that need to be studied carefully before building a road. Soils with more clay and silt particles, for example, are prone to erosion and contraction if they come into contact with water. Such soils require special treatment to avoid poor workmanship.

1.4.2. Aggregate

Stone aggregate, also known as mineral aggregate, is easily the most important component of road construction materials. It is made by breaking up naturally occurring rocks to form coarse aggregate (like gravel) or fine aggregate (like sand). Aggregates are used for granular bases, sub-bases, as part of bituminous mixes and cement concrete. They are also used as the primary material for relatively cheaper road, known as water-bound macadam. Like soil, aggregates must be tested by a road engineer to ascertain that they are strong enough and durable for a specific project. These properties are influenced by their origin, mineral components and the nature of bond between the components.

1.4.3. Asphalt and bitumen

Asphalt and bitumen are often mistaken as being one and the same thing. However, while asphalt is a mixture of aggregates, binder and filler, used for constructing roads and their associated furniture, bitumen is actually the semi-solid binder that holds asphalt together. Bitumen, which is also known as mineral tar, is obtained through unfinished distillation of crude petroleum. It contains 87% carbon, 11% hydrogen and 2% oxygen. On the other hand, asphalt is manufactured in a factory that heats, dries and mixes aggregate, bitumen and sand into a composite mix. The material is then applied on site using a paving machine at a nominated or required thickness, depending on the type of project. When used for road construction, asphalt comes in the form of a composite material known as asphalt concrete. This material consists of 70% asphalt and 30% aggregate particles. Asphalt is 100% recyclable, which makes it a highly popular road construction material.

1.4.4. Concrete

Concrete offers a lot of flexibility and ease of construction – making it an important road construction material. It is created by mixing cement, coarse aggregate, fine aggregate, water, and

chemical admixtures (which make up 25-40% of concrete). In addition to reducing costs, concrete is popular among road builders due to its ability to extend the service life of a road. It can also be used to raise the bearing capacity of existing pavement layers. A well-made concrete mixture sets and hardens because of the binding property of cement. It forms a mixture with slimmest void space. On curing with water, it provides a strong, steady and long-lasting pavement for a road – resisting repetitive impact from heavy commercial vehicles.

1.4.5. Composite pavement

This is a type of pavement that uses both asphalt and concrete to form a ‘super’ pavement. Composite pavements can potentially become a cheaper alternative to traditional pavements thanks to their ability to provide higher levels of performance and durability, both structurally and functionally. The downside of concrete is that it is susceptible to problems such as reflective cracking and rutting in the surface layer. However, these potential hitches can be resolved by applying a premium asphalt surface or through some other (costly) mitigation techniques.

1.5. Conclusion

In this chapter we have exposed: traffic analysis, different types of traffic, traffic presentation model, different classes of traffic and generality on the classification of vehicles. In addition, we saw traffic stream parameters, the different types of the pavements and materials used in road construction. There are 3 types pavements, flexible, rigid and semi-rigid respectively in which they could be made up of different layers, the support soil, subbase, base layer, foundation layer and surface layer depending on the type of pavement chosen. Furthermore, for construction these pavements, materials that are more durable, economic and environmentally suitable are used and these are soil, aggregate (derived from rocks), concrete, composite pavement, asphalt and bitumen. This also depends on the type of pavement chosen.

Therefore, a detailed bibliographical summary will be developed in the following chapter in order to learn about the synthesis of road pavement simulation models for a better and safe pavement choice.

Chapter 2

Summary of road pavement simulation models

2.1. Introduction

In this chapter, an overview of road pavement simulation models including behaviour models and their types is highlighted. Several road pavements models such as [Westergaard Bilayer \(1926\)](#), [Hogg's Bilayer \(1938\)](#), [Burmister Model \(1943\)](#), [Jeuffroy Model \(1955\)](#) and [Boussinesq \(1885\)](#) have been proposed over the years and we therefore discuss their operation and choice of each model.

2.2. Road pavement simulation models

Road pavements are permanently subjected to mechanical and thermal stresses combined with chemical phenomena (that is, aging of materials). These various stresses participate more or less quickly in the degradation of commonly observed road upper layers, in general deterioration of the pavement, and surface cracks ([LAVOC, EPF Lausanne Suisse](#)). The models discussed below allow the evaluation of the level of stress on a pavement structure. Furthermore, the model chosen should represent the performance of the pavement structures studied as closely as possible because pavements are designed for a certain lifespan which differs from one region (or country) to another.

2.2.1. Behaviour Models

As shown in [Figure 2.1](#), a behaviour model is a mathematical law developed on the basis of theoretical or empirical considerations (based on observation), making it possible to predict the evolution over time of an index characterizing the state of a degradation ([Selvaraj, 2012](#)).

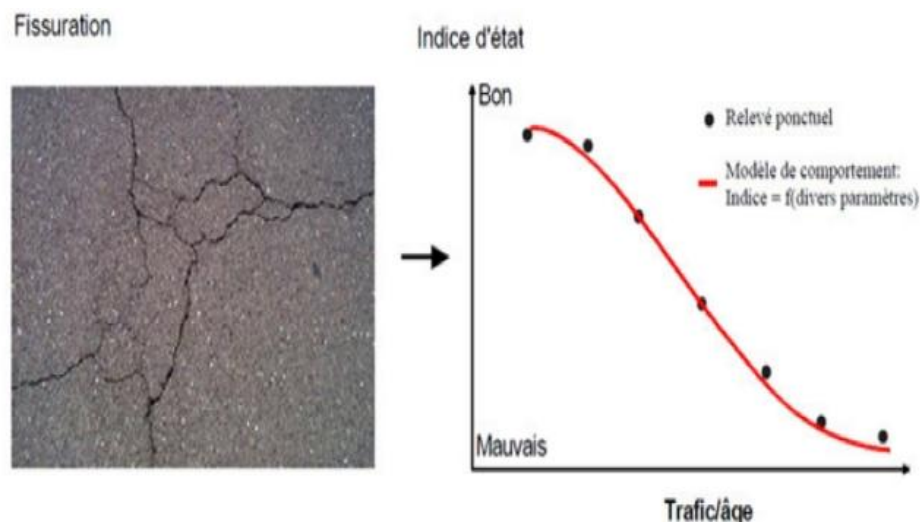


Figure 2.1. An example of a degradation behaviour model.

The evolution of degradation can be schematized by a trend grouping together the points of the readings of the degradation of a typical pavement taken at different periods. This evolution can be divided into 3 phases, namely (Figure 2.2):

- **An initiation phase** representing the period between the construction of the coating and the first appearance of degradation on the surface thereof. The time of the first onset of degradation depends on the quality of the original materials and workmanship of the superstructure, mechanical and / or thermal loads, and the ability of the structure to withstand these various loads
- **A propagation phase** representing the period during which a degradation, after having appeared on the surface of the roadway, will develop according to its own law of evolution, this one being able to be linear, exponential or other.
- **A stabilization phase** representing the period from which degradation tends to stabilize. This phase is not the object to modelling. It is beyond a critical threshold, or even beyond the admissible safety threshold and, therefore, will have already required the performance of maintenance work.

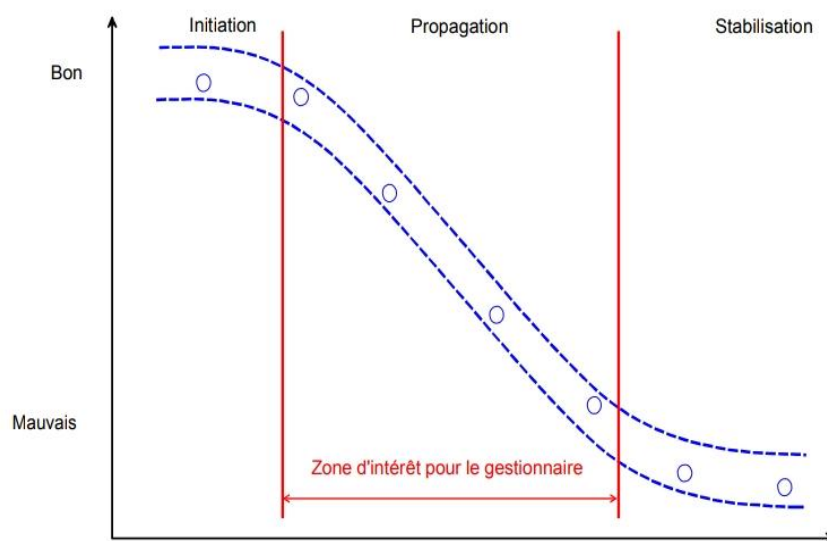


Figure 2.2. Example of the evolution of a degradation

Among the 3 phases, the propagation phase represents the area of interest for the manager who must decide and plan maintenance interventions.

2.2.2. Types of Behaviour Models

Depending on the type of approach used to develop behaviour models, three types of models can be considered (Figure 2.3).

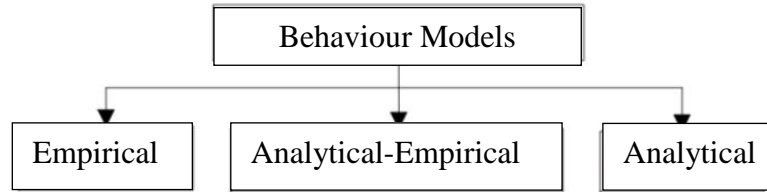


Figure 2.3. Types of behavioural models (LAVOC, EPF Lausanne Suisse).

2.2.2.1. Empirical Models

Empirical models are models based on the analysis of the observation of deterioration of pavements and in particular their evolution.

These models come from 4 possible options according to: (Selvaraj, 2012).

- Observation of a network (photo method).
- Monitoring of the evolution of the network (video method)
- Monitoring of in situ test boards
- Accelerated tests (ALT: Accelerating, Landing Test) (Figure 2.4).



Figure 2.4. Fatigue rides at EPFL and EPFZ

The in-situ test boards are pavement sections chosen in certain places of the network, subjected to traffic loads and real climatic conditions. While these data describe the actual development of pavement degradation, they present two major drawbacks for the development of behavioural laws. The first is that the development of degradation on standard sections of the road network takes place relatively slowly. It is therefore necessary that the observations used for the establishment of behaviour models cover a period of several years. On the other hand, the development of degradation can only be observed until the usual level of intervention is reached.

These two disadvantages do not apply to data obtained using accelerated testing. Through the very rapid application of mechanical loading cycles, the development of degradation is also accelerated. In addition, degradation can be observed up to the total destruction of the road, since the safety of users and the structural integrity of the road are not decisive.

On the other hand, the accelerated test has the defect of not integrating the effect of aging, in particular that of bituminous binders. Similarly, climatic stresses are not or that poorly simulated.

2.2.2.2. Establishment of Empirical Model

Depending on the amount and type of data available, two empirical methods can be used to develop new behavioural models. These methods, presented below, are the "photo" and the "video" methods. [12]

a) Photo Method

Photo models are obtained by analysing real data observed over an entire network, assembled in a "Condition = f(Time)" diagram. This means that the observed Condition Values are classified according to the age of the pavement at the time of the measurement.

They are referred to as "photo" type data because it is like taking photos at certain points in the network and superimposing them according to the age of the pavement. This also expresses the "static" aspect of the data.

Principle: In order to establish "photo" type development models, the following steps should be taken (Figures 2.5 and 2.6):

- Carry out a survey of the state of deterioration that you wish to model on the entire network to be managed. For each data item, it is necessary to determine the age of the surface at the time of the survey.
- Gather all the data relating to a degradation in a diagram giving the state of the degradation as a function of time.
- Determine the parameters that influence the evolution of the degradation under consideration (traffic load, type of surfacing, layer thickness, climatic conditions, etc.).
- Filter the data according to the influencing parameters.
- Determine the appropriate regression for the various data groups. This regression then represents the constitutive law, applicable to pavements having the same characteristics.

Advantages: Performing a single set of measurements, Fast **and** Economical.

Disadvantages: Data filtering does not reflect a real evolution but a trend and does not take into account the history of the pavement.

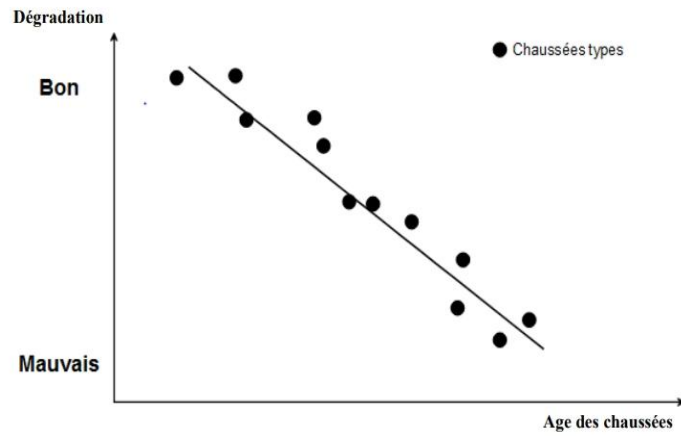


Figure 2.5. Typical representation of a photo method

The points from the figure 2.5 correspond to the state of degradation considered for pavements of a defined type, of different ages and which are subjected to the same order of stresses.

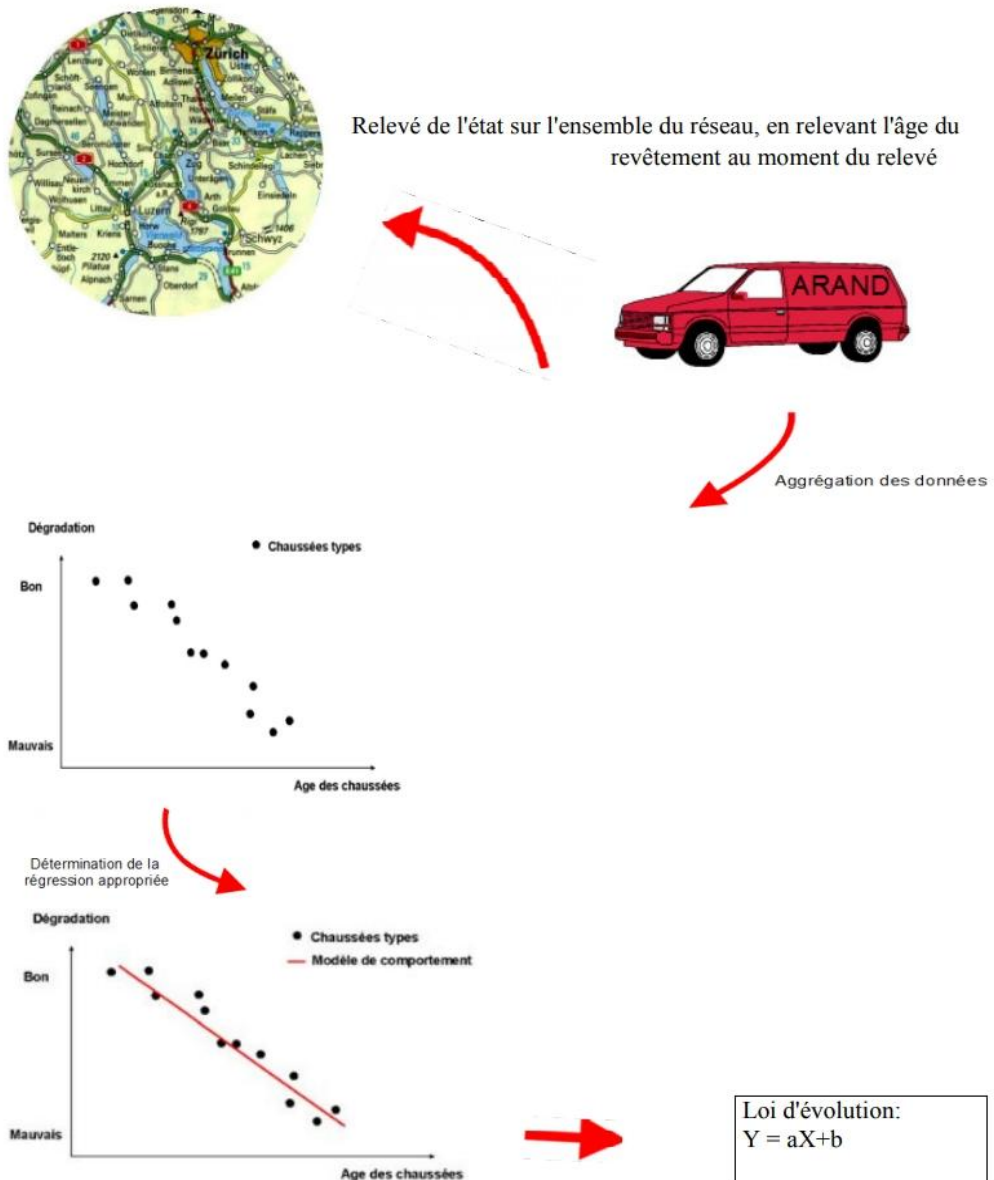


Figure 2.6 Description of the photo method

b) Video method

The video type models are obtained by following the evolution of the deterioration on given sections of the network.

They are called "video" type because the information is obtained as if a video had been fixed on a section of pavement during a given period, and the evolution of the deteriorations was analysed using the film. This notion also expresses the evolutionary aspect of the data.

Principle: To establish evolution models of the "video" type, the following steps must be carried out (Figure 2.7 and 2.8):

- Select representative sections of the network.
- Record over several years the state of degradation that we want to analyse.
- Represent the data in a diagram giving the state of degradation as a function of time.
- Determine the appropriate regression for the data.

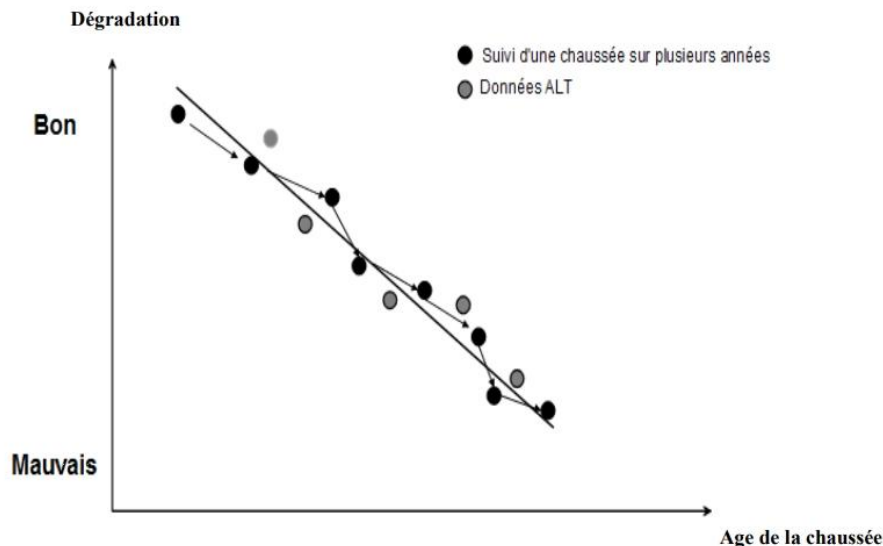


Figure 2.7. Typical representation of a video method

Advantages: Represents the actual evolution of a given pavement, takes into account the structure's past or history, simple to carry out and accuracy of the result.

Disadvantages: Requires several rounds of surveys/readings and time consuming (several years)

Note: In order to reduce the time required to develop video-type laws, it is possible to use data from test boards subjected to a fatigue ride. These make it possible to simulate the traffic flow in an accelerated manner, and therefore allow the behaviour of the structure to be observed in a short time. This data is called ALT (Accelerating, loading test) data.

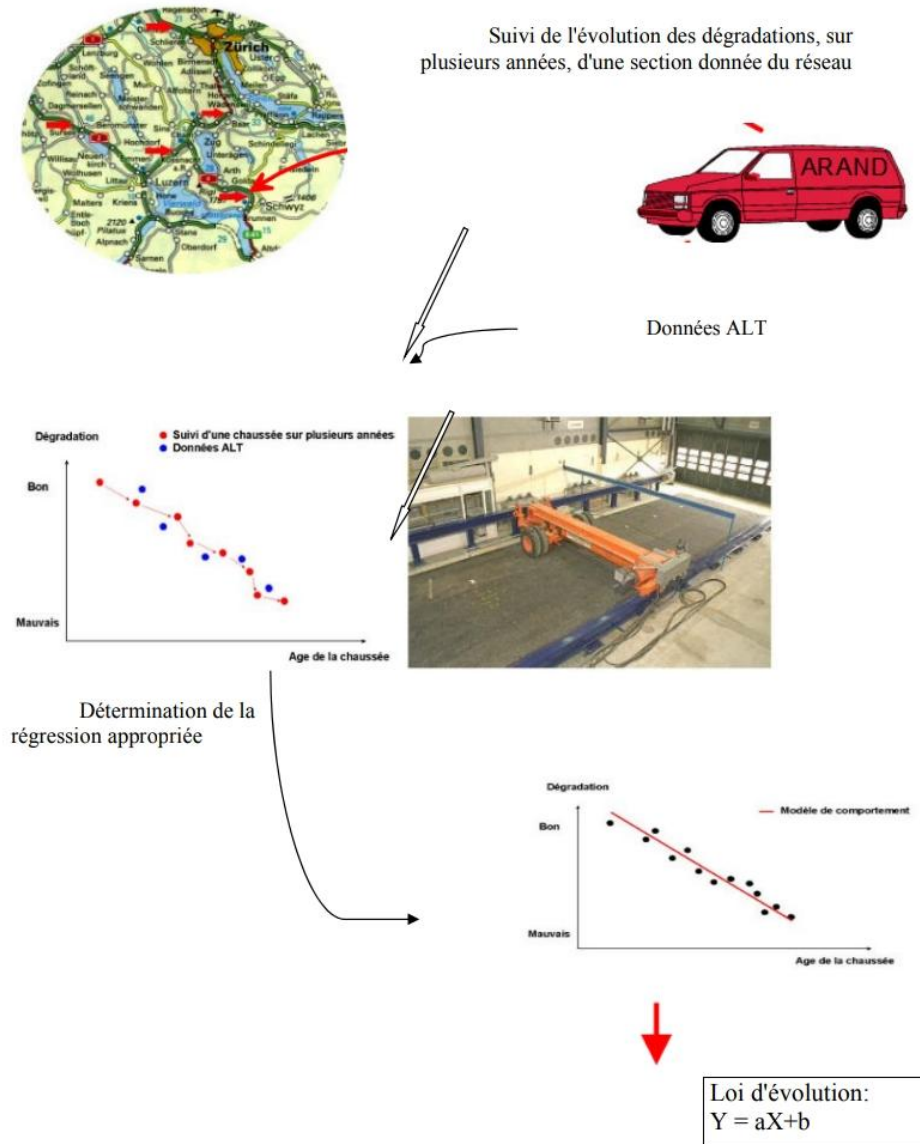


Figure 2.8. Description of the video method

- **Monitoring of in situ test beds**

The in-situ test beds are selected pavement sections at certain locations in the network, subjected to actual traffic loads and climatic conditions. While these data describe the actual development of pavement degradation, they have two major drawbacks for the development of behavioural laws.

The first is that the development of deterioration on standard sections of the road network occurs relatively slowly. It is therefore necessary that the observations used for the establishment of behaviour models cover a period of several years.

On the other hand, the development of degradation can only be observed until the usual level of intervention is reached.

- **Accelerated tests**

The development of degradation is accelerated by the very rapid application of mechanical loading cycles. In addition, the degradation can be observed up to the total destruction of the pavement, since the safety of users and the structural integrity of the pavement are not a determining factor. On the other hand, the accelerated test has the defect of not integrating the effect of aging, particularly that of bituminous binders. Likewise, climatic stresses are not simulated or are only poorly simulated.

2.2.2.3. Analytical-Empirical Models

Analytical-empirical models are based partly on behaviour laws of materials, but also on the observation of the evolution of pavement degradation. These models combine the advantages of analytical and empirical models while reducing the disadvantages of both (Selvaraj, 2012).

2.2.3. Analytical Models

Analytical models are based on the application of theoretical laws of material behaviour. As pavement structures are a multi-layer system of hydrocarbon materials, these models require the determination of a considerable number of parameters. These models have the advantage of being able to simulate the behaviour of any type of bituminous structure for defined stress conditions (load, temperature). However, these models are difficult to apply due to the difficulty of setting or matching the theoretical stresses with the real stresses to which the pavement is subjected.

In recent years, fundamental research has been moving towards such approaches, but this development requires a considerable investment of time and money for the manager of a road network.

2.2.3.1. Boussinesq Model (1885)

The soil is considered as a semi-infinite elastic mass. It is further assumed that the pavement body made of granular material is not very different from the supporting soil (Triaw, 2006). The tyre load applied to the pavement generates a depth-dependent stress. The aim is to find out at what depth of the subsoil the vertical stress has been sufficiently diffused not to exceed the allowable stress. The shape of the stress diagram at different depths is shown in Figure 2.9. The stress expression Eq 1:

$$\sigma = q_0 \left[1 - \frac{z^3}{(a^2 + z^2)^{\frac{3}{2}}} \right]$$

where: **q₀**: pressure applied by the tyre,

a: radius of action of the load,

z: depth

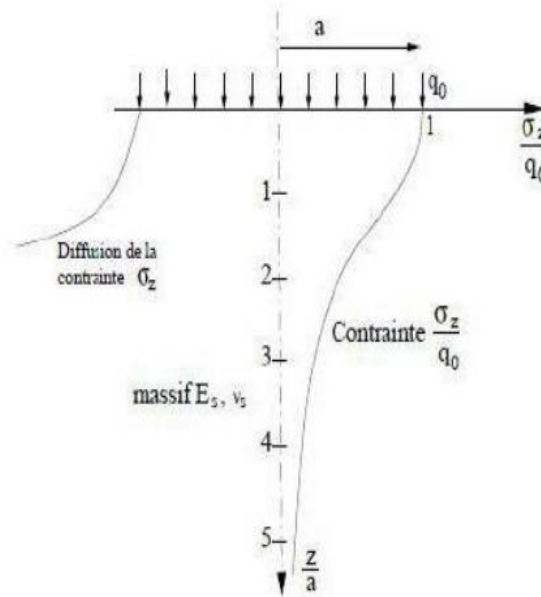


Figure 2.9. Diagram of Boussinesq Model.

It remains to determine the allowable soil stress σ and the depth (thickness of the pavement body) for which the vertical stress σz on the supporting soil does not exceed the allowable soil stress.

The application of this model to the study of cracking in pavement structures has the following inconveniences:

- This model cannot take into account discontinuities;
- The area of application is limited (only for cases where the pavement body is not too different from the natural ground);
- It cannot model multi-layer structures.

2.2.3.2. Westergaard Bilayer Model (1926)

This model gives the stresses and strains of a system consisting of a plate resting on a soil that is assimilated to a set of vertical springs with no horizontal connections, commonly known as a

Winkler foundation, whose vertical displacement at a point is proportional to the vertical pressure at that point.

This implies that the soil reacts elastically and only in the vertical direction. However, the soil does not behave like an elastic mass: it undergoes permanent deformations. The reaction of the soil is therefore not strictly vertical: the stresses are dispersed in depth and shear stresses cannot be excluded.

N.B All specialists now recognise that Westergaard's model overestimates the stresses.

Example:

The vertical displacement w at a point of contact between the layer and the mass is then proportional to the vertical pressure σ_{zz} at that point, i.e. $\sigma_{zz} = kw$ (Figure 2.10) where k is called the foundation reaction modulus and is a function of the latter (Shighiga, 2007).

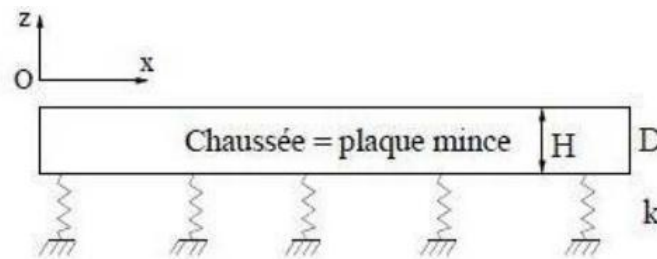


Figure 2.10. Diagram of Westergaard Model

2.2.3.3. Hogg's Bilayer Model (1938)

It gives the stresses and strains of a plate resting on a semi-undefined elastic mass of the Boussinesq type (Figure 2.11).

The pavement is represented by a thin plate ($E_1; \nu_1$) and rests on an infinite Boussinesq-like mass ($E_S; \nu_S$). With the assumption that the pavement slides perfectly on its support, there are only two main unknowns of the problem to be determined: u_z and σ_{zz} at the pavement-soil interface. The two continuity relations for these two unknowns are provided on the one hand by the thin plate equations, on the other hand by the Boussinesq equations of a semi-infinite elastic mass.

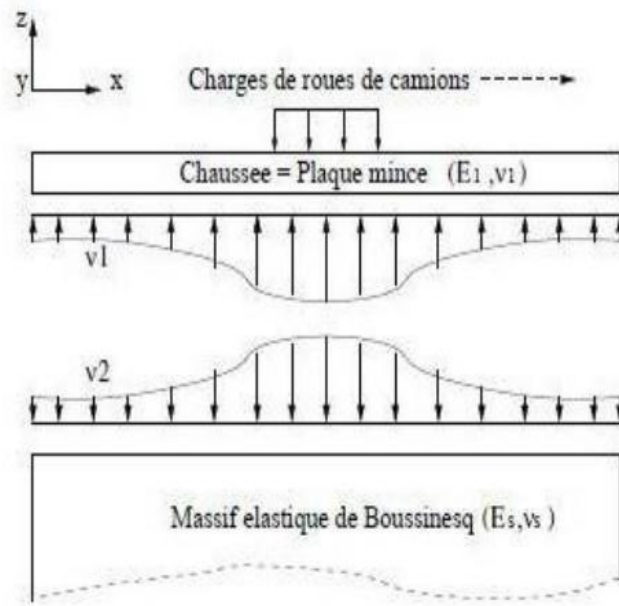


Figure 2.11. Diagram of Hogg's Model.

This model still has the following inconveniences:

- Shear stresses are not taken into account at the pavement-soil interface, which greatly influences the results.
- It cannot represent a complex type multilayer pavement complex.

2.2.3.4. Burmister Model (1943)

It approaches and treats the general problem of a structure with n layers resting on a semi-undefined elastic mass according to (Sadok, 2015). The main features of the model are the following:

- The layers are treated as elastic structures (and not plates),
- The interfaces between layers can be glued or peeled,
- The case of complex loads can be treated by adding the effects of elementary loads,
- Its main limitation is that the layers are infinite in plan, as in the case of Hogg's model.
- In the case of concrete slabs, it is particularly necessary to supplement it with a finite element model to assess the consequences of the loads at the edge or at the slab angle.

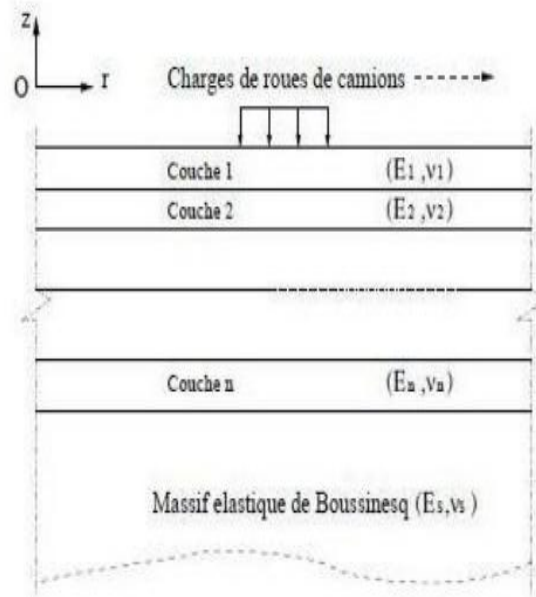


Figure 1.12. Diagram of Burmister Model.

2.2.3.5. Jeuffroy Model (1955)

This model is a combination of the Hogg and Burmister models (Sadok, 2015). It consists of a thin plate resting without friction on an elastic Burmister layer (Figure 2.13). The floor is a semi-infinite solid. With this combination, the model allows the introduction of vertical discontinuities in the first pavement layer (concrete slab pavement). The second layer is treated as an elastic solid.

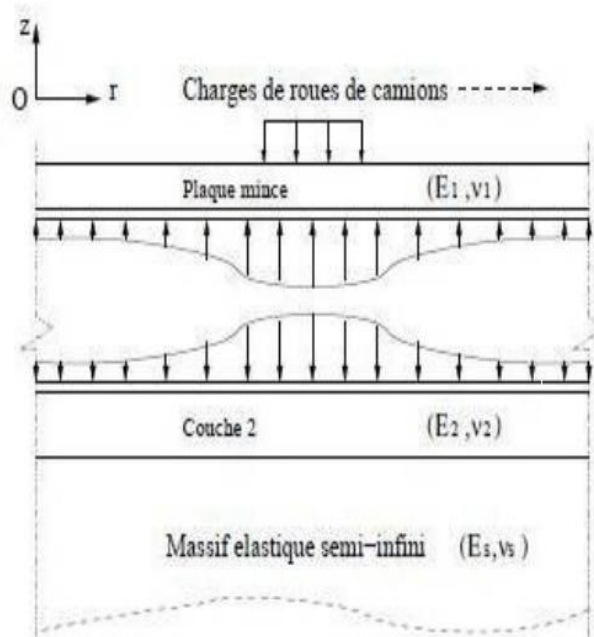


Figure 2.13. Diagram of Jeuffroy Model.

A road network has a wide variety of combinations of structure types and material types whose composition, application and age will influence pavement behaviour. In addition, not all sections of a network are subject to the same stresses.

Traffic loads and local climatic conditions as well as the geometric situation may differ. The ideal model would be one that takes into account all these parameters that affect the considered deterioration. However, such a model proves to be of rare complexity.

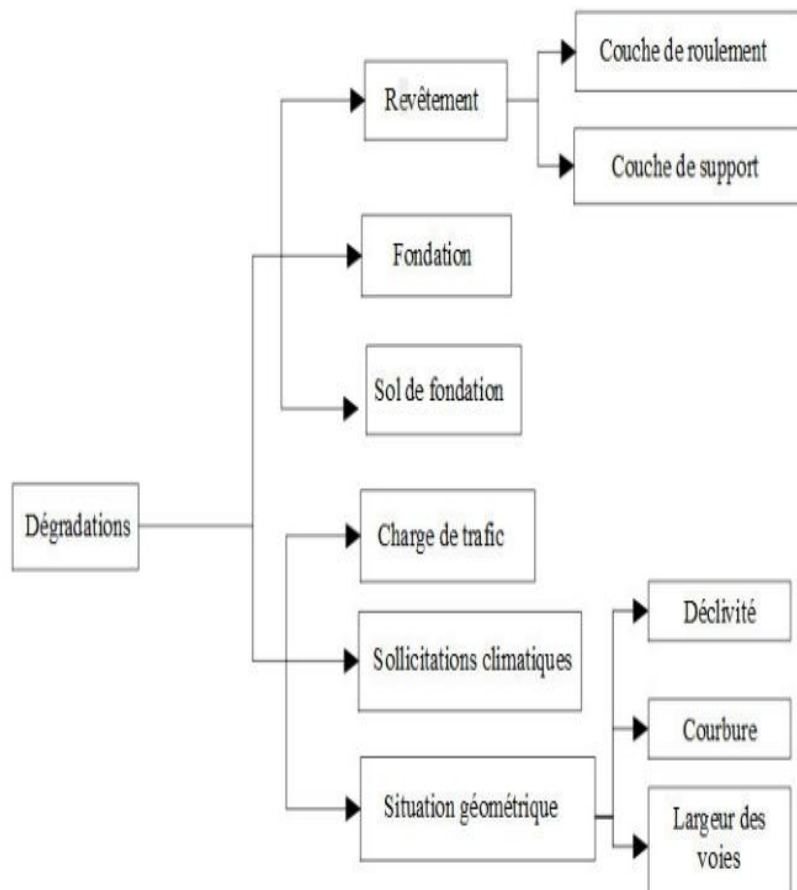


Figure 2.14. Parameters influencing the appearance and evolution of degradation

2.3. Conclusion

A large number of bibliographic research presented above represents the study of simulation models of pavements developed (in particular for behaviour models) on the basis of theoretical or empirical considerations (based on observation), allowing to predict the evolution over time of an index characterizing the state of a degradation divided into 3 phases, (initiation phase, propagation and stabilization). Among the 3 phases, the propagation phase represents the zone of interest to the manager who must decide and plan maintenance interventions. Moreover, the bibliographical review allowed us to know the importance of behaviour models according to their type of approach (empirical, analytical and analytical-empirical) and the other models (Westergaard, Boussinesq, Hogg and Jeuffroy) have in elaborations with the roadway.

Chapter 3
Presentation of
PLAXIS Software

3.1. Introduction

PLAXIS is a reference finite element software for geotechnical engineering, the development of which started in 1987 at the initiative of the Dutch Ministry of Public Works and Hydrology. Its initial aim was to create a 2D finite element code that could be easily used to analyse the effect of a river dike on soft clays in the Netherlands. Within a few years, PLAXIS was extended to many other areas of geotechnical engineering. In 1998, the first version of PLAXIS for Windows was developed. During the same period a 3D version of the software was developed. After a few years of development, the 3D PLAXIS Tunnel program was released in 2001. PLAXIS 2D is thus a two-dimensional program specially designed to perform deformation and stability analyses for different types of geotechnical applications. Real situations can be represented by a plane (plane deformation) or axisymmetric model. The general algorithm of the PLAXIS code consists of solving a system of non-linear algebra equations in an iterative process to determine the values of displacements at the different nodes of the mesh, the stress field and the ground failure states.

3.2. PLAXIS-2D code simulation

The program uses a convenient graphical interface that allows users to quickly generate a geometric model and finite element mesh based on the vertical section of the structure to be studied.

3.2.1. Plaxis calculation code

The use of complex behaviour laws in finite element models for engineering is delicate. It requires heavy specific studies for determination of the parameters, which are beyond the scope of engineering projects. The integration of such laws in finite element codes is difficult. The cost of these calculations is generally significant and few codes are currently operational ([Levasseur, 2007](#)).

The approach followed in the development of PLAXIS is to provide the user with a finite element code that is both robust and user-friendly, making it possible to deal with real geotechnical problems, within a reasonable period of time using a soil behaviour model whose parameters can be determined from a normal geotechnical survey. Different behaviour models, more or less sophisticated, have been implemented in Plaxis; linear elastic, Mohr-Coulomb, soil models with hardening or specific soft soils, etc.

The PLAXIS code from the company Plaxis B.V is a software package now commonly used in engineering offices. Designed by numerical geotechnicians at the University of Delft in the Netherlands in the 1980s, the Plaxis finite element code is a practical tool for geotechnical analysis

and testing. Although the code was originally developed to analyse dykes and soft soils, its scope of application now extends to a wide range of geotechnical problems. It allows the analysis of elastic, elasto-plastic, elasto-viscoelastic problems in 2D or 3D and in large displacements. Very reliable numerically. The Plaxis code user manual provides a detailed description of the software. The set of default options (boundary conditions) makes data entry easy and fast (Brinkgreve, 2003).

Finally, the simplified options (stress initiation, pore pressures) allow you to get straight to the point (predicting the behaviour of a structure).

3.2.2. Default options and approximate solutions

The system of the default options and specific approximate solutions is intended to save the operator time, to avoid having to make annoying choices, and to improve the user-friendliness of the software. This system is inseparable from the tree menu processing. These options take into account the experience of digitisers in this field. The default options start with the mesh: if only the broad lines of the mesh are important, the details of the elements, optimally arranged from a numerical point of view, will be entirely generated by the software from a small number of nodes. The same applies to displacement boundary conditions: if they are standard (zero displacement vector at the base of the studied domain and zero horizontal displacement vector on its lateral faces), the application can be carried out automatically (by default) from the menu with immediate control of the results on the screen. The application of the initial stresses due to the weight of the earth can be carried out exactly by activating the loading multiplier for the dead weight. On the other hand, if, as is often the case in geotechnical engineering, a given K_0 state is known or can be estimated, it can be specified directly. In this case, the structure is often slightly unbalanced (incompatibility between K_0 and other mechanical characteristics). The menu then allows, with a fictitious zero loading, to re-equilibrate the solid, then to reset the displacement field to zero so as to take as new origin the state of the material after the application of gravity. The K_0 option is particularly interesting (and realistic) in this case of a heterogeneous model with an almost horizontal free surface.

3.2.3. Plaxis sub-programs

The PLAXIS user interface consists of four subroutines (Input, Calculations, Output and Curves):

3.2.3.1. The data input program (Input)

The program contains everything necessary to create and modify a geometric model, to generate the corresponding finite element mesh and to generate the initial conditions (Figure 3.1).

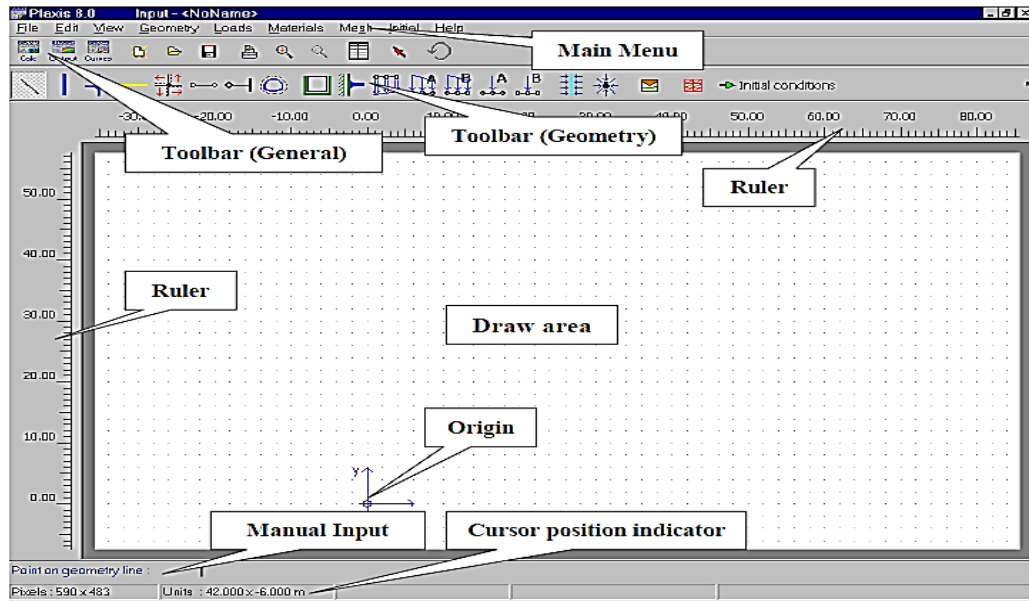


Figure 3.1. Main window of the Input program (geometric creation).

3.2.3.2. The calculation program (Calculations)

This program contains all the elements to define and start a calculation by the finite element method. At the beginning of the calculation program, the user has to choose the project for which the calculations will be defined (Figure 3.2).

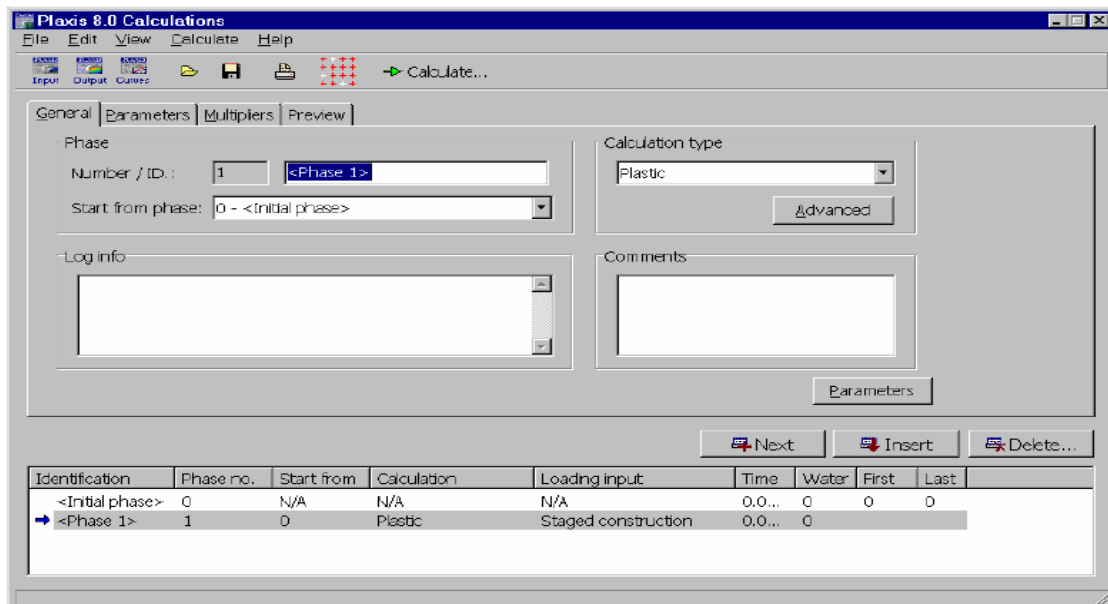


Figure 3.2. Main window of the calculation program.

The current step and iteration values indicate the current calculation step and iteration number respectively. The maximum steps value indicates the number of the last possible step for the current

calculation phase according to the additional step parameter (Figure 3.3). The maximum iterations value corresponds to the maximum iteration parameter of the iterative procedure settings.

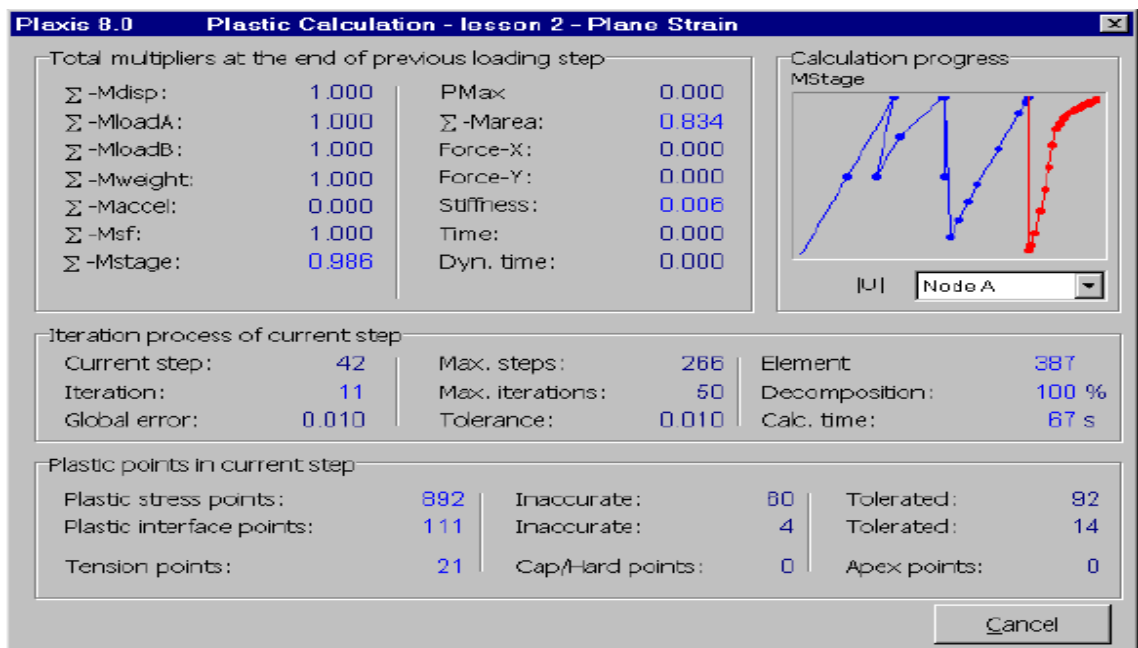


Figure 3.3. Calculation window.

The main results of a finite element calculation are displacements at nodes and the stresses at the stress points. In addition, when a finite element model includes structural elements, forces are calculated in these elements. A wide range of tools is offered by PLAXIS to display the results of a finite analysis.

3.2.3.3. The output programmes

This program contains all the elements that allow to see the results of the generated data and finite element calculations. At the beginning of the results program, the user has to choose the model and the appropriate calculation phase or step number for which the results will be displayed (Figure 3.4).



Figure 3.4. Toolbar of the main window of the Output program.

3.2.3.4. The programme curves

This program contains everything necessary to generate load-displacement curves, stress paths and stress-strain curves. The realisation of a model with PLAXIS is generally translated by the following steps (Figure 3.5):

- Use of the "Plaxis Input" pre-processor, for the generation of data (mesh, data set and initial constraints).
- Launching of the finite element calculation code "PLAXIS Calculate", to carry out the numerical resolution of the problem studied.
- Use of the "Plaxis Output" post-processor, for the interpretation of results on a graphic screen.
- Use of the post-processor "PLAXIS Curve", for the interpretation of the curves (consolidation curve, stress path, etc.).



Figure 3.5. Toolbar in the main window of the curve's program.

3.2.4. The modelling approach with PLAXIS

We present here the process and main stages of a calculation under PLAXIS.

3.2.4.1. Geometry

The first step in Plaxis is the definition of the geometry. A number of properties are available:

- The geometric lines that are there to draw the organisation of the ground.
- The << Plates >> tool allows to draw and define slender structures that have tensile and compressive strength. This tool is mainly used to model walls, beams, shells, plates and rigid areas (mainly elements with a strong extension along the axis perpendicular to the modelling plane (here z)).
- << Anchor >> which is used to model the connections between the elements. These are springs, which are used to model cofferdams or more precisely the connection between the different elements of a cofferdam.
- The << Geogrid >> tool is used to draw slender structures with compressive or tensile strength but which have no bending strength. This tool is generally used to model geogrids and anchors.

On Plaxis, there is also a tunnel tool that allows the modelling of a tunnel taking into account the factors that concern this type of structure.

3.2.4.2. Boundary conditions

Once the geometry has been defined, the boundary conditions must be entered, i.e. the displacements and stresses imposed on the external boundaries of the geometry. If no boundary conditions are set on a section, the software defaults to the assumption that the element is not subject to any external forces and is free to move in all directions.

The boundary conditions that can be imposed are those that impose a displacement in a given direction or those that impose a force in a given direction. A wide range of boundary conditions can be created with several tools (distributed force, point force, embedding, sliding, etc.).

3.2.4.3. Definition of material parameters

Then, it is advisable to define the various properties of the various materials according to its type (ground and interface, plate, anchoring, geogrid, etc.....), the model of behaviour and the various parameters making it possible to define it. For soils, in addition to the definition of mechanical characteristics, their interfaces with other types of elements can be parameters, it is also necessary to define the hydraulic behaviour of the soil (draining, non-draining or non-porous).

3.2.4.4. Mesh Size

The mesh is generated automatically, which is a strong point of Plaxis. The operator can set the fineness of the mesh between different options (very coarse, coarse, medium, fine, very fine), the operator can also decide to mesh more finely a certain region of the ground or/and the neighbourhood of a feature thanks to the refine options in the mesh menu.

Once the mesh has been created, the initial soil conditions must be set. This procedure generally passes by the definition of a coefficient of grounds at rest.

3.2.4.5. The initial conditions

The definition of the initial conditions is done in two distinct steps First, when the initial conditions window opens, only the ground is activated. The operator activates the constructive elements (displacements and/or imposed constraints, anchorage, plate) which correspond to the initial moment. It deactivates the soil elements which do not correspond to this initial moment.

A << Switch button >> gives access to two different windows each representing the geometry of the model:

- The first, which is called "initial pore pressure", makes it possible to define an initial groundwater level (if necessary), and to generate the corresponding pore pressures;

- The second window is used to generate the initial stresses inside the structure (self-weight and pressure).

3.2.4.6. Calculation phase

After having carried out the whole of these parameter settings one can reach the calculations by the push button "calculation". The "input" interface of << Plaxis >> closes and gives way to a new interface: "calculation". A phase 0 is already calculated, this phase corresponds to the initial state of the structure. This interface allows defining the phasing of the construction modelling.

New calculation phases can be created based on an existing phase. For each phase, the geometry can be modified through the same interface that was used to define the initial conditions. Changes can therefore only be made by activating or deactivating elements. The level of the water table can be modified, as well as certain properties of the materials, elements other than the soil (modification of input parameters, impermeability and/or non-consolidation of certain walls). The level of intensity and the position of the boundary conditions of the displacement and stress loads can also be modified.

However, no new element can be created at this level whether it is a load, a displacement, a boundary condition or an anchor plate etc....

Other types of phases can be created other than simple activation or deactivation of elements (Exp. consolidation phase). A number of types of calculation can be simulated (consolidation, determination of the safety factor, plastic deformation, dynamic study). Once the study phase is completed, characteristic points can be placed.

The Plaxis result curves will be calculated at these points. After pressing << calculate >> the calculations will start. Once finished, the results can be viewed by pressing << output >>.

3.2.4.7. Visualisation of Results

The PLAXIS code contains several tools to visualise and analyse soil results either in deformations (deformed mesh, total displacements and deformations) or in stresses (effective and total stresses, plastic points, pore pressures).

3.3. Behavioural laws in PLAXIS

The objective of soil modelling is to determine a behavioural model that allows the study of the evolution of its physical and mechanical characteristics. The model should be able to represent as much as possible all the essential aspects of the behaviour revealed by the laboratory and in situ tests. The model is thus a complete description of the soil behaviour. Most materials have an elastoplastic behaviour, which is characterised by the occurrence of reversible elastic deformations

and irreversible elastic and plastic deformations. On the load surface, two cases of behaviour are possible: the load surface does not change, we speak of law perfectly plastic elastic, this is the case of the Mohr-Coulomb model; the surface of load evolves during the loading, one speaks about elastoplastic model with hardening of which the Hardening Soil Model (HSM) by Plaxis is part (Levasseur, 2007). In Plaxis, there are several types of models; we define in the following two elastoplastic models as the most used for both drained and undrained soil where HSM can be used for treated soil.

3.3.1. Mohr-Coulomb's model

The Mohr-Coulomb model is a model often used to represent shear failure in soft soils and rocks. This law is characterized by an isotropic linear elasticity of Hooke, a surface of load and a plastic potential. The flow rules are not associated. Within the fracture surface, the behaviour of the material is assumed to be linear elastic isotropic or anisotropic. On the fracture surface, the behaviour is considered to be perfectly plastic (Figure 3.6).

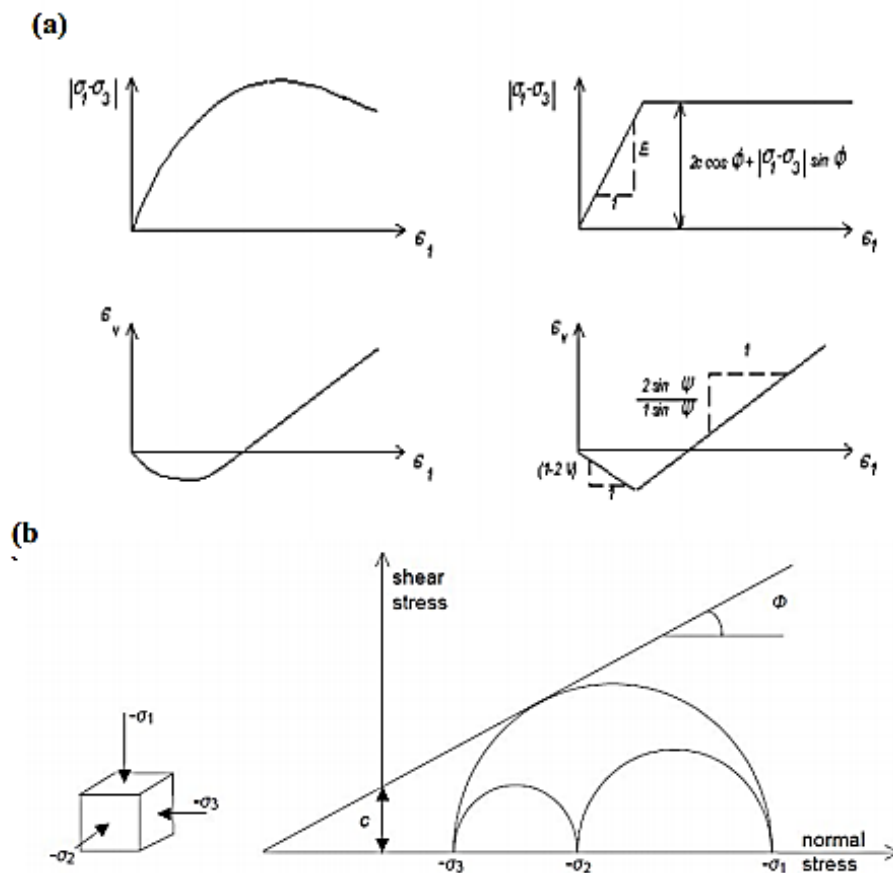


Figure 3.6. Modelling of a triaxial compression test with the Mohr Coulomb model (a) and representation of the stresses in the Mohr plane (b).

The Mohr-Coulomb model requires five fundamental parameters:

- Two elastic parameters: The Young's modulus E and the Poisson's ratio ν ;
- Two parameters relating to the conditions at failure: the cohesion c and the angle of friction angle ϕ ;
- A parameter relating to the plastic flow rule, the angle of dilatancy ψ . These parameters are easily identifiable from laboratory tests, oedometer or triaxial tests, as shown in [Figure 3.6](#) above.

Several studies have been carried out on the influence of various factors on this parameter ([Mestat, 2002](#)). The value of the friction angle ϕ is commonly between 15° and 45° . Values less than or equal to 30° are typical clays, while higher values, between 25° and 45° , characterize sands. For a given compactness, the angle of friction is practically independent of the water content of the soil, but it increases with the average grain diameter. The angle of friction also depends on the shape and surface condition of the grains.

The three-dimensional Coulomb criterion assumes that the intermediate stress does not occur. The shape of the criterion is that of an irregular pyramid built around the trisector ([Figure 3.7](#)) on the irregular Mohr-Coulomb hexagon.

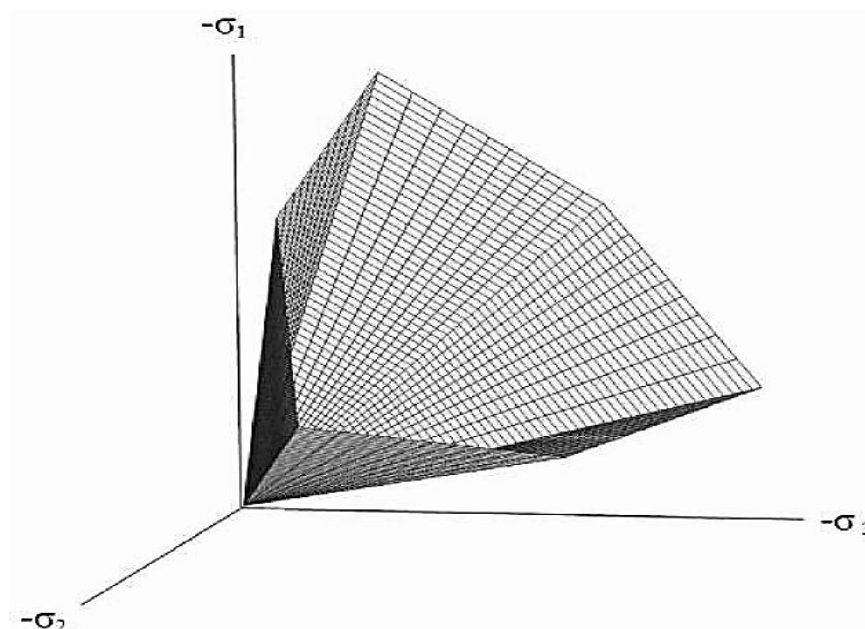


Figure 3.7. Mohr-Coulomb pyramid plotted for $c=0$.

The model requires the determination of five parameters ([Figure 3.8](#)). The first two are E and ν (elasticity parameters). The other two are c and ϕ , respectively.

These are classic geotechnical parameters, often provided by laboratory tests, but necessary for deformation or stability calculations.

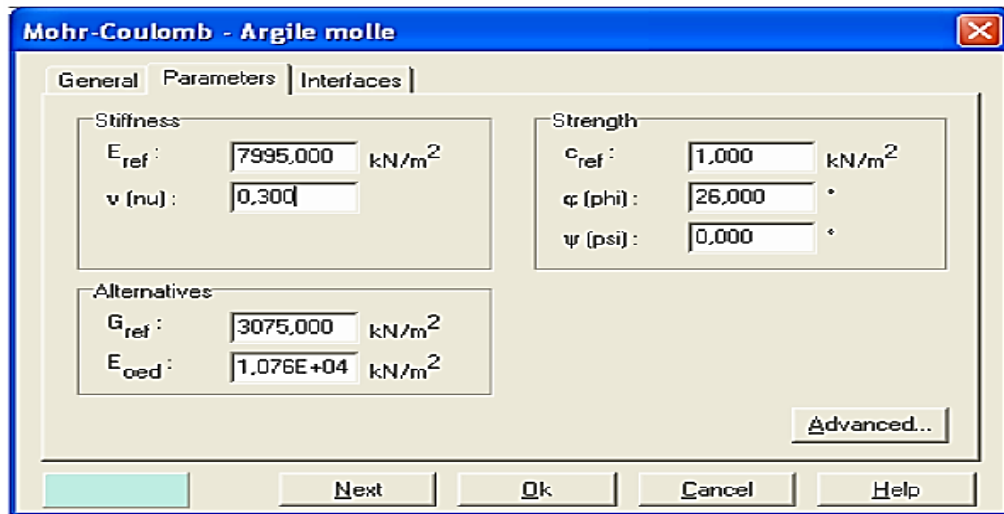


Figure 3.8. Mohr-Coulomb window settings

3.3.1.1. Young's Modulus

The choice of a deformation modulus is one of the most difficult problems in geotechnical engineering. The modulus of deformation varies with the strain and with the average stress. In the Mohr-Coulomb model, the modulus is constant. It seems unrealistic to consider a tangent modulus at the origin (which corresponded to the measured **G max** in dynamic tests or in very low deformations). This module requires special tests. It is advisable to take an average module, for example the one corresponding to a level of 50% of the failure deviator (Figure 3.9).

The user must remain aware of the importance of the choice of the module he/she will be taking into account. This is not surprising, and the same issue is found in any classic foundation calculation, for example;

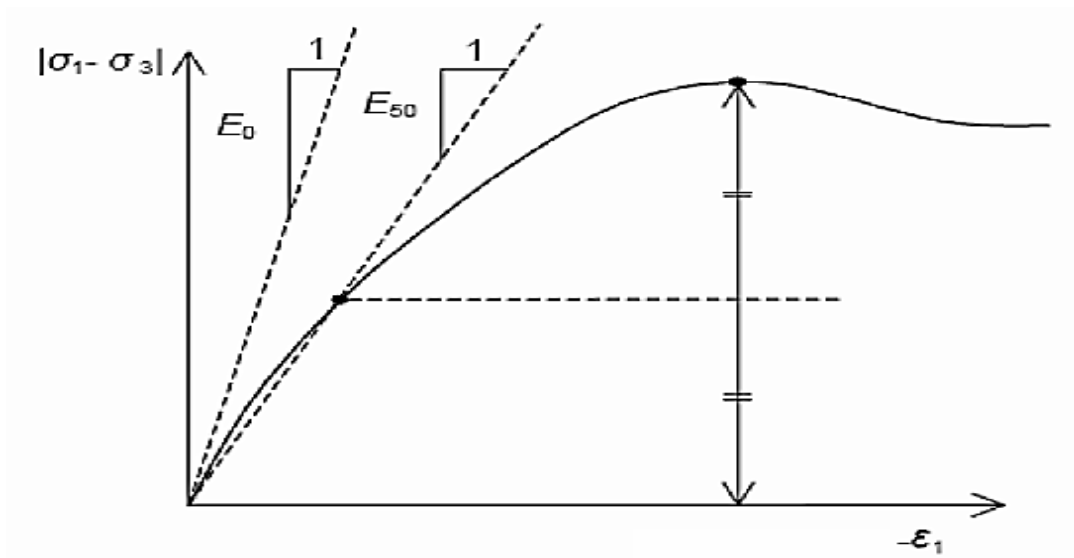


Figure 3.9. Definition of modulus at 50% failure

In the advanced parameters dialog box, we can also enter a gradient giving the variation of the modulus with the depth.

3.3.1.2. Poisson's ratio

A value of 0.2 to 0.4 for the Poisson's ratio is recommended. This is realistic for the application of dead weight (K0 procedure or gravity loading). For some problems, especially in landfills, lower values can be used. For incompressible soils, the Poisson's ratio approaches 0.5, but this value is not usable.

3.3.1.3. Friction Angle

PLAXIS does not take into account a variation of the friction angle with the average stress. The friction angle to be entered is either the peak friction angle or the bearing friction angle. It should be noted that friction angles greater than 35° can considerably increase the calculation time. It can be advised to start calculations with reasonable friction angle values, even if it means increase thereafter. This value of 35° is compatible with the friction angles ϕ (at constant volume, at the bearing). The angle of friction can be determined from the intrinsic curve of the Mohr-Coulomb model (Figure 3.6).

3.3.1.4. Cohesion

The pulverulent soils have practically no cohesion, $0 < c < \text{a few kilo Pascals}$. We speak of capillary cohesion or cementation in place. Coherent soils have cohesion of between a few kilo-pascals and several hundred kilo-Pascals.

It may be useful to assign, even to purely frictional materials, a very low cohesion (0.2 to 1 KPa) for numerical purposes.

3.3.1.5. The angle of dilatancy

The angle of dilatancy ψ is generally between 0 and 15. Loose sands and clays have very low dilatancy values, barely a few degrees or even zero. In general, the angle of friction is almost always greater than the angle of dilatancy. The value of ψ can be simply determined from the slope of dilatancy observed in the triaxial tests (Figure 3.7). There is also a simple empirical relationship, generally well verified for dense sands, between the angle of dilatancy and the angle of internal friction as shown in Eqs 1 and 2:

$$\Psi = \varphi - 30 \text{ for } \varphi > 30^\circ \quad (1)$$

$$\Psi = 0^\circ \text{ for } \varphi < 30^\circ \quad (2)$$

The case $\Psi < 0^\circ$ corresponds to very loose sands (often called metastable or static liquefaction). The value $\Psi = 0^\circ$ corresponds to a perfectly plastic elastic material, where there is no expansion when the material reaches plasticity. This is often the case for clays or for low or medium density sands under fairly high stress (Figure 3.10).

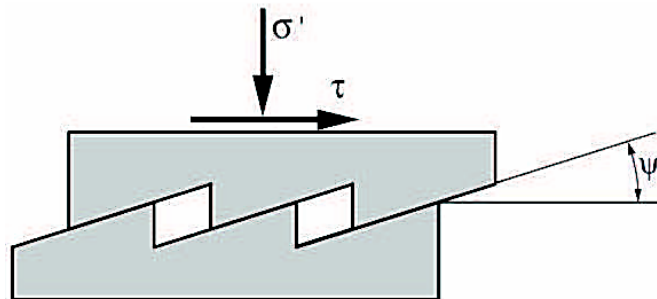


Figure 3.10. Angle of Dilatancy (Ψ).

3.3.1.6. Tensile stresses

The Mohr-Coulomb pyramid allows tensile stresses (Figure 3.7). These are often unrealistic for soils and it is possible to cut these tensile stresses (cut-off tension) or to reduce them (Tensile strength).

3.3.1.7. Advanced settings

Advanced settings include increasing stiffness and increasing cohesion with depth, as well as suppressing **drag/pulls**. The latter option is used by default but can be disabled here, if desired (Figure 3.11).

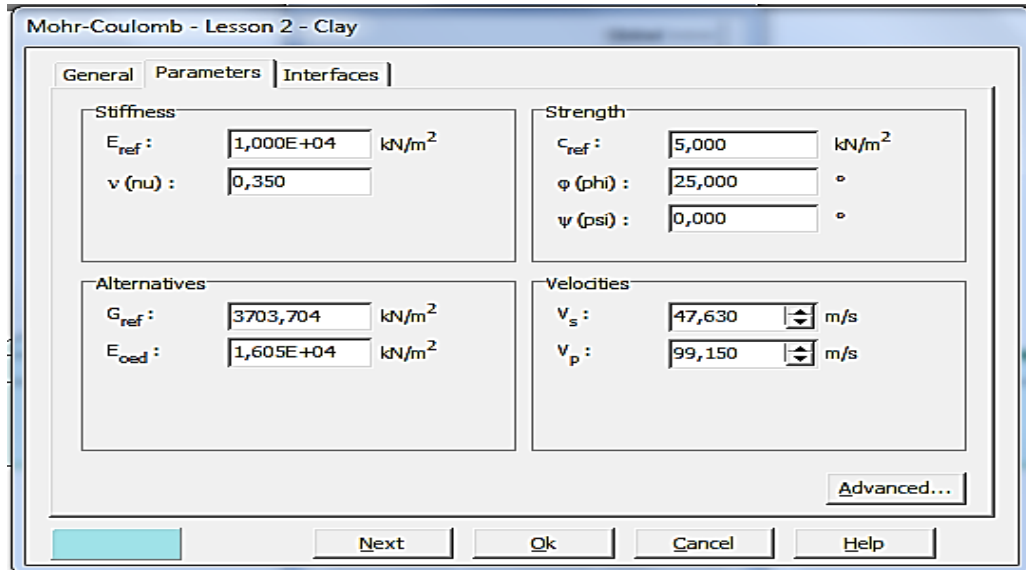


Figure 3.11. Mohr-Coulomb advanced window settings.

3.3.2. Hardening Soil Model (H.S.M)

An elastoplastic behavioural law with strain hardening such as the HSM model makes it possible to take better account of the irreversible deformations that are observed in the soil even far from failure (Nova, 2005). This concept is derived from the behaviour of hardened metals, the level of plasticity of which increases with the intensity of the plastic deformations undergone.

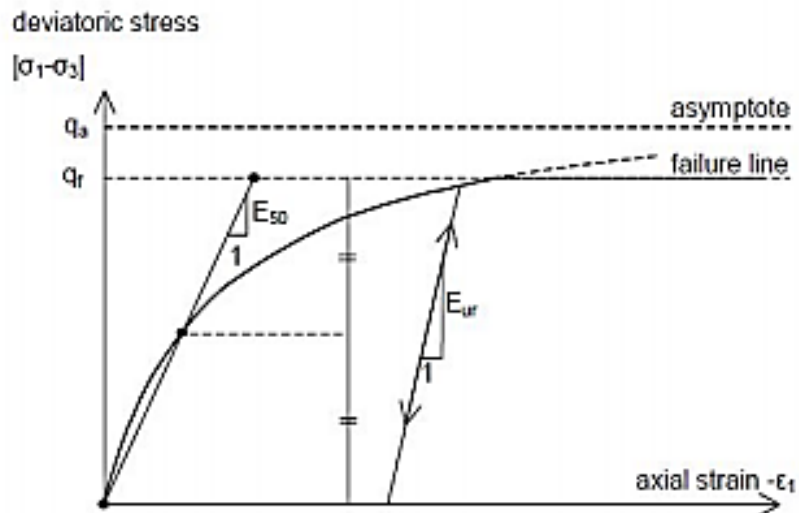


Figure 3.12. Representation of the hyperbolic relation managing the hardening of the HSM model.

The implementation of this model in the Plaxis computer code is presented by (Schanz and al. 1999). Note however that the Hardening Soil model is an advanced constitutive soil model based on the Duncan & Chang model (Duncan and Chang, 1970) but modified to take into account the plasticity of the soil. The plasticity can be of two types: related to shearing or to compression.

The axial strain and the stress deviator are related in the Hardening Soil model by a hyperbolic function as shown (Figure 3.12). The shear stiffness is used to model irreversible deformations due to primary deviatoric loading. The compressive stiffness is used to model irreversible plastic deformations due to primary oedometer and isotropic compression respectively.

The HSM model therefore mainly requires the following eight parameters, which as for the Mohr-Coulomb model are identifiable from oedometer or triaxial tests as illustrated (Figures 3.13):

- A deviatorial plastic strain modulus, E_{50}^{ref} , for a reference pressure p^{ref} ;
- A modulus of plastic deformation in oedometer compression, E_{oed}^{ref} , for a reference pressure p^{ref} ;
- A modulus and a Poisson's ratio in elastic discharge / recharge, E_{ur}^{ref} and ν_{ur} for a reference pressure p^{ref} ;
- A factor \mathbf{M} allowing to link stress and strain according to a power law; Three Mohr-Coulomb plasticity parameters; a cohesion c , the angle of friction φ and the angle of dilatancy ψ .

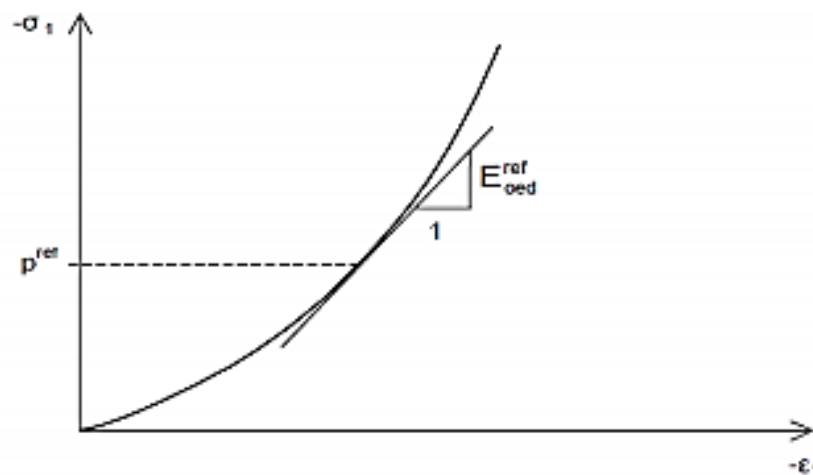


Figure 3.13 Definition of the parameter E from the results of an oedometer test.

From a qualitative point of view, this type of model based on the theory of plasticity with hardening is able to take into account the major aspects of soil behaviour and to reproduce with sufficient accuracy the evolution observed in experimental tests (Nova, 2005). It can then be considered as a second order approximation of the real behaviour of a soil. The choice of the behavioural model depends on the problem at hand: underpinning, embankment settlement, landslide, foundation on sloping ground, tunnel: which behavioural model should be used for which geotechnical problem? The question is not simple because there is no "universal" model. The HSM parameters are shown in Figure 3.14.

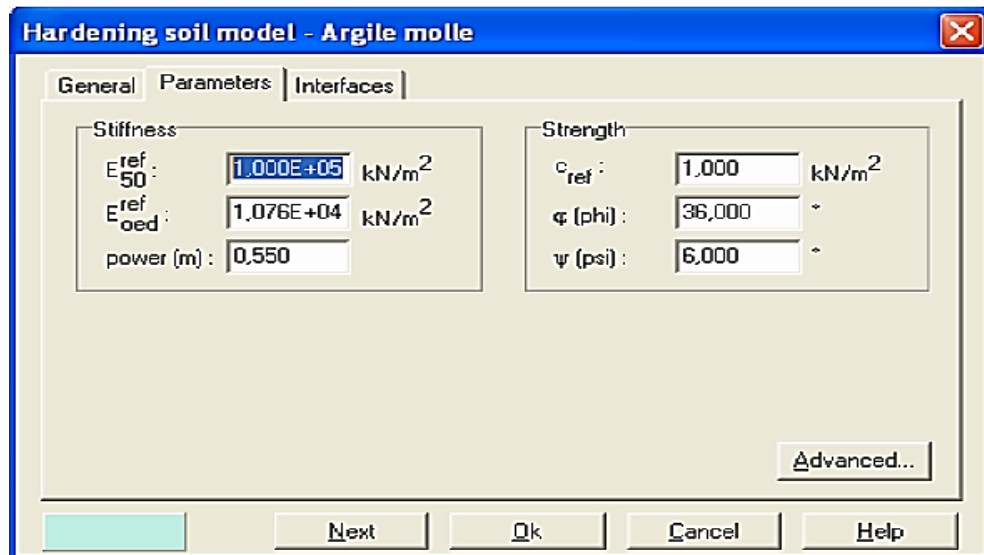


Figure 3.14. Hardening Soil Model window settings

Parameters of Mohr-Coulomb law;

C	: cohesion (effective)	[kN/m ²].
Φ	: effective friction angle	[°].
Ψ	: angle of dilatancy	[°].

Stiffness parameters;

E_{50}^{ref}	: secant modulus in a triaxial test	[kN/m ²].
E_{oed}^{ref}	: tangent modulus in an oedometer test	[kN/m ²].
m	: Power (about 0.58 for sands)	[-].

3.4. Conclusion

Numerical modelling of a geotechnical structure, carried out using a finite element calculation code, is a simplified approach to the geometrical and geo-mechanical reality of the structure. The models available in the Plaxis 2D code were briefly described and the choice of the model of behaviour depends on the problem posed. Therefore, in the next chapter we will study the response from PLAXIS Software by numerical modelling of a lime-stabilised road pavement through a collection of data from a completed project.

Chapter 4

**Presentation of study area,
Numerical modelling, Results and
Interpretation**

4.1. Introductions

This chapter first presents a summary of the study area, soil used and its characterisation, in addition, presenting the analysis and interpretation of the results obtained from PLAXIS software by numerical modelling of a lime-stabilized road pavement using collection of data from a completed project ([Case of the Harchoun motorway section, W. Chlef](#)).

4.2. Presentation of study area

The soil that was used in this numerical modelling study is a red clay soil obtained from 5m depth in the Harchoun area. It will be used as a subbase layer in a project of East-West Highway located approximately 25km east of the city of Chlef ([Figure 4.1](#)) ([Harichane et al. 2009](#)).



Figure 4.1. Sampling of red clay soil from a depth of 5m in the region of Harchoun, Algeria.

4.3. Identification and characterization of soil used

[Table 4.1](#) shows the different chemical-mineralogical and physico-mechanical characteristics of the fine red soil used in the highway project as well as its geotechnical classification ([Harichane et al. 2011](#)). These characteristics were determined according to American standards ([ASTM, 2000](#)).

Table 4.1. Physico-mechanical and chemico-mineralogical properties of red soil used as a subbase soil.

Properties name	Chemical formula	Soil used
Chemico-mineralogical properties of soils		RS
Calcium oxide (%)	CaO	2.23
Alumina (%)	Al ₂ O ₃	19.01
Silica (%)	SiO ₂	57.02
pH	-	9.05
Calcite (%)	CaCO ₃	4.0
Quartz (%)	SiO ₂	30
Illite (%)	2K ₂ O.Al ₂ O ₃ .24SiO ₂ .2H ₂ O	24.0
Kaolinite (%)	Al ₂ Si ₂ O ₅ (OH) ₄	16.0
Montmorillonite (%)	Al ₂ ((Si ₄ Al)O ₁₀)(OH) ₂ .H ₂ O	-
Physico-mechanical properties of soils		
Specific Gravity (-)		2.84
Passing 80 µm sieve (%)		97.5
Liquid Limit (LL, %)		46.5
Plastic Limit (PL, %)		22.7
Classification System (USCS), (-)		CL
Unconfined Compressive Strength (UCS, KPa)		510

4.4. Geotechnical parameters used

PLAXIS software is selected for analysis as it combines a better representation of the geometry of the structure of different layers of the soil through the parameters of the behaviour model, and also to verify the behaviour of the pavement body after application of loads (passage of traffic). Two models were used for the calculation with the geotechnical data which are summarized in [Table 4.2](#). Moreover, the time required to reach displacement measured in case of consolidation are 5 and 200 days as short- and long-term calculation, respectively. However, the residual pore pressure used is equal to 1km/m².

4.5. Geometric models

The geometric models chosen for pavement modelling are shown in [Figures 4.2 and 4.3](#). In the present study, two different geometrical models (Model-A and Model-B) have been suggested in order to assess the effect of three different parameters namely: (1) physical parameter (Min (200kPa) and Max (600kPa) loads were applied to simulate the traffic circulation) ([LCPC-SETRA, 2000](#)), (2) mechanical parameter (subbase layer with and without treatment by adding 8% lime as an additive ([Gadouri, 2017](#)) and (3) geometrical parameter (0.9m thickness was used for untreated subbase layer and both 0.3m and 0.6m thicknesses ([LCPC-SETRA, 2000](#)) were used for lime-treated subbase layer, respectively) on the behaviour of the road structure.

Chapter 4: Presentation of study area, Numerical Modelling, Results and Interpretation

Table 4.2. Geotechnical and geometrical parameters.

Materials	Base layer	Foundation layer	Subbase layer for 60 days curing time		Subgrade Soil (Natural soil)	Applied load	
			Untreated Soil (Model-A)	Treated with 8% lime (Model-B)		Min-A (kPa)	Max-B (kPa)
Thickness[m]	0.2	0.2	0.9	0.3 and 0.6m	3	200 Applied on 20cm larger (LCPC-SETRA 1994)	600 Applied on 60cm larger (LCPC-SETRA 1994)
Young's modulus [E] (KN/m ²)	2,5. 10 ⁵	3. 10 ⁵	1,4. 10 ⁵	21. 10 ⁵	1,4. 10 ⁵		
Poisson's ratio [ν]	0.35	0.35	0.35	0.33	0.35		
Density [γ] (KN/m ³)	21.3	22	22	18.2	20		
Cohesion [C] (KN/m ²)	30	20	81.8 (Gadouri and al. 2017)	239 (Gadouri and al. 2017)	20		
Friction Angle [φ] (Degree)	43	44	36.3 (Gadouri and al. 2017)	47.3 (Gadouri and al. 2017)	36		
Dilatancy Angle [Ψ] (Degree)	13	14	6	8	6		

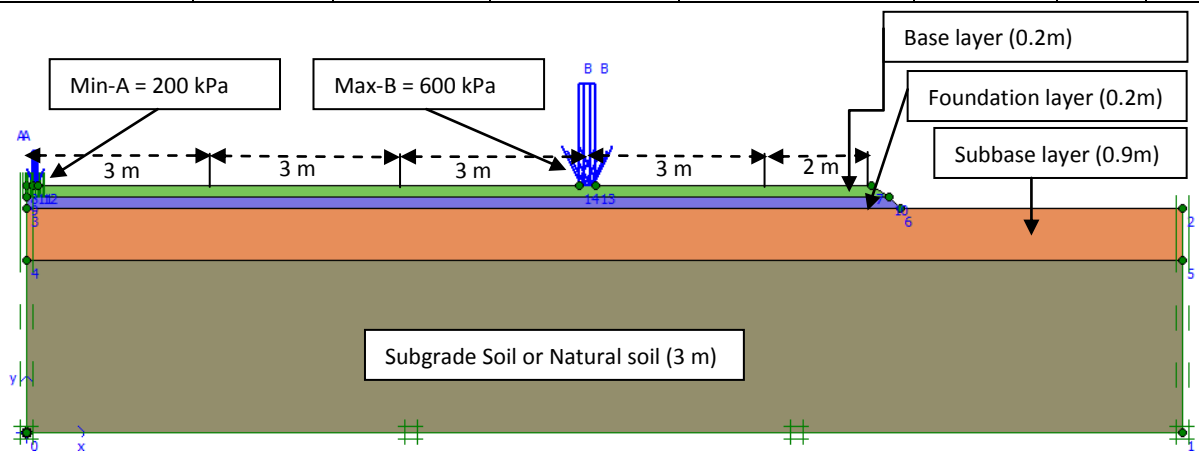


Figure 4.2. Model-A suggested for subbase layer without treatment.

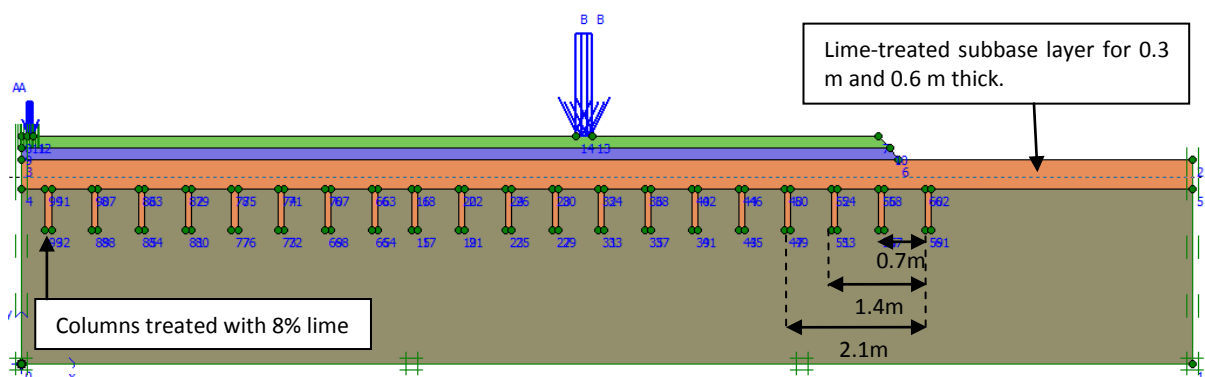


Figure 4.3. Model-B suggested for subbase layer treated with 8% lime based on columns treated with the same lime content.

In addition, a total of 20 columns of lime-treated soil (70 cm high and 10 cm larger) were introduced in the subgrade soil in order to decrease the eventual deformations in the subbase soil. Thus, the treated columns are incorporated into the subbase soil with different spacing distance of 0.7, 1.4 and 2.1 m which corresponds to 20, 10 and 7 columns, respectively (Narasimha and Rajasekaran 1994).

4.6. Numerical Modelling

4.6.1. Mesh generation

The plane-strain model was chosen for both models (A and B). The elements used for the mesh are triangular elements with 15 nodes. This gives us a finer distribution of nodes (Figures 4.4 and 4.5), which implies that the results will be more accurate compared to the mesh with 6 nodes. However, using 15-node elements takes more time to calculate.

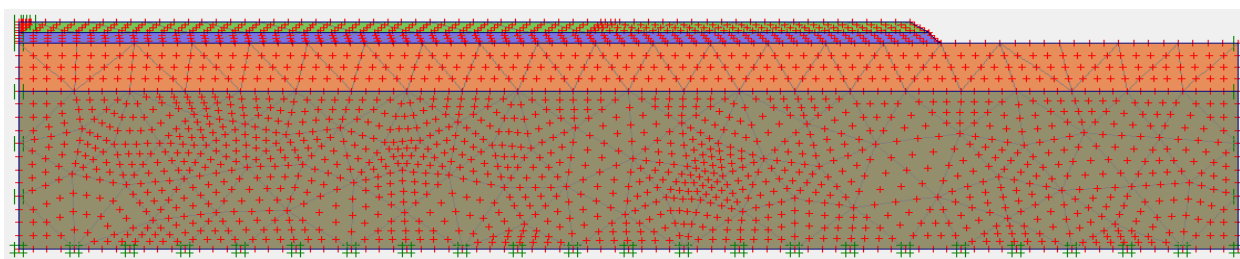


Figure 4.4. Mesh generation for Model-A.

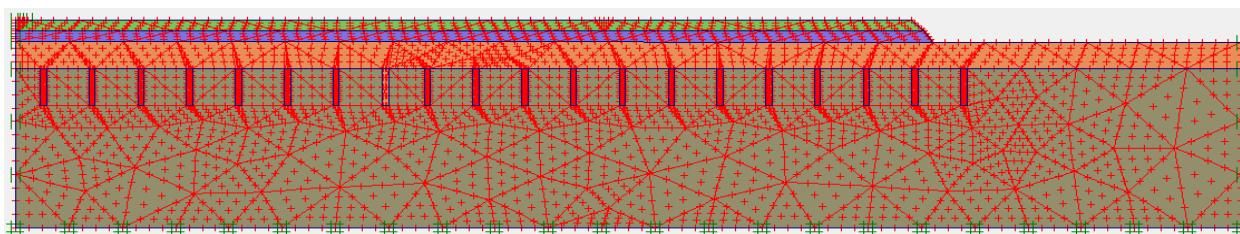


Figure 4.5. Mesh generation for Model-B.

The general information (types of geometry models used, types of elements used, number of elements, number of nodes, number of stress points and average element size) obtained from the mesh generation step for both models (A and B) are illustrated in Table 4.3.

Table 4.3. General information from mesh generation.

General information	Types of geometry models used	Types of elements used	Number of elements	Number of nodes	Number of stress points	Average element size
Model-A	Plane-Strain	15-Nodes	365	3089	5011	$281.70 \cdot 10^{-3}$
Model-B	Plane-Strain	15-Nodes	489	4035	5868	$400.38 \cdot 10^{-3}$

4.6.2. Boundary conditions

The boundary conditions in a problem are often complex, and they naturally condition the quality and accuracy of the modelling. The groundwater level was taken at 3m depth for both selected models (A and B).

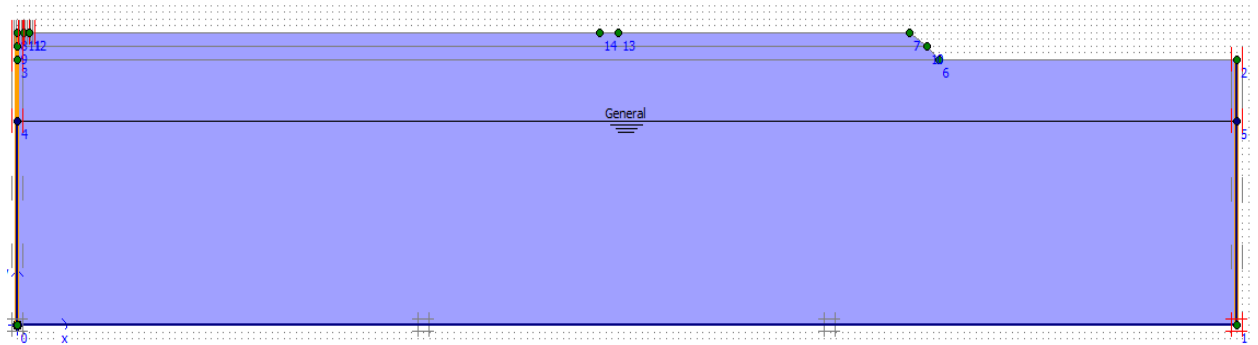


Figure 4.6. Boundary conditions for Model-A.

However, the mechanical boundary conditions are those based on the mechanical equilibrium equations (either kinematic or static), in this case, the displacements are imposed as zero along the OX axis on the left and right of the model, zero along the OX and OZ axes on the bottom of the supporting soil (Figures 4.6 and 4.7).

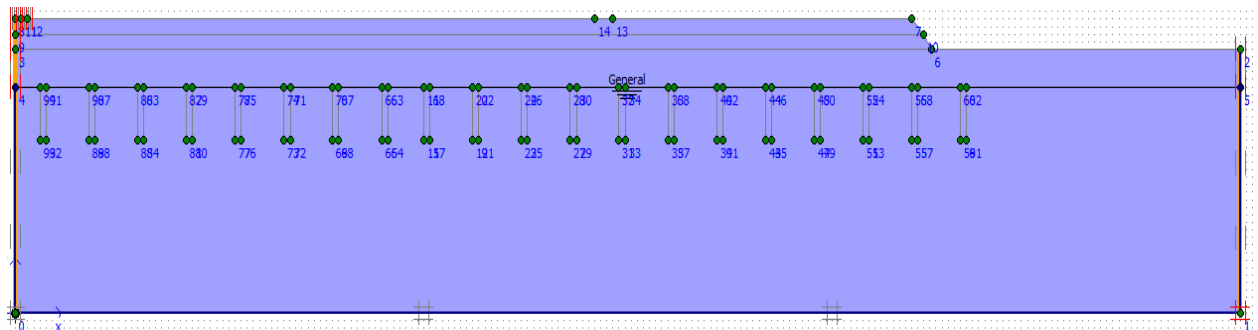


Figure 4.7. Boundary conditions for Model-B.

4.6.3. Pore pressure generation

As said in the above section, the groundwater level was taken at 3m depth for both selected models (A and B). This allows us to generate the pore pressure which is an important parameter for obtaining the effective stress in the next step (Figures 4.8 and 4.9). The extreme pore pressures for both models (A and B) are 22.5kN/m² and 35.7kN/m², respectively.

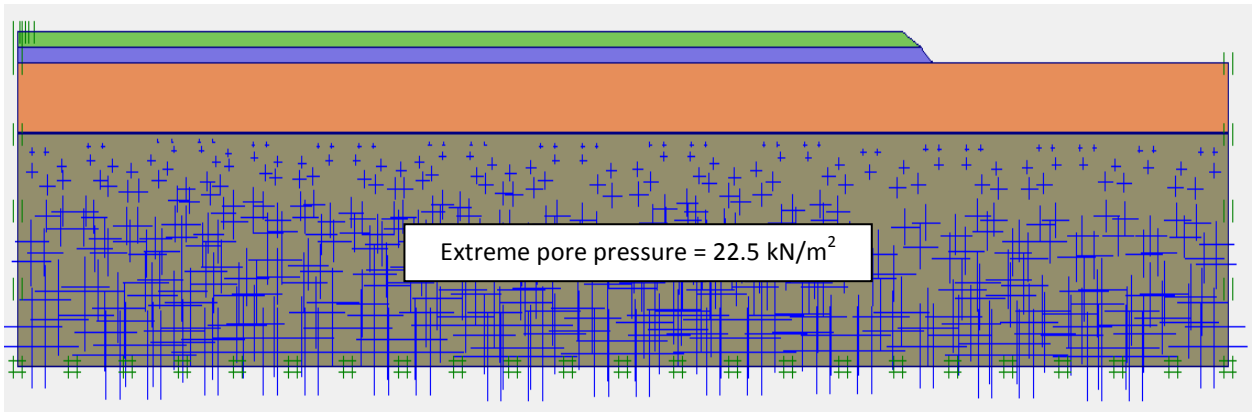


Figure 4.8. Pore pressure generation for Model-A.

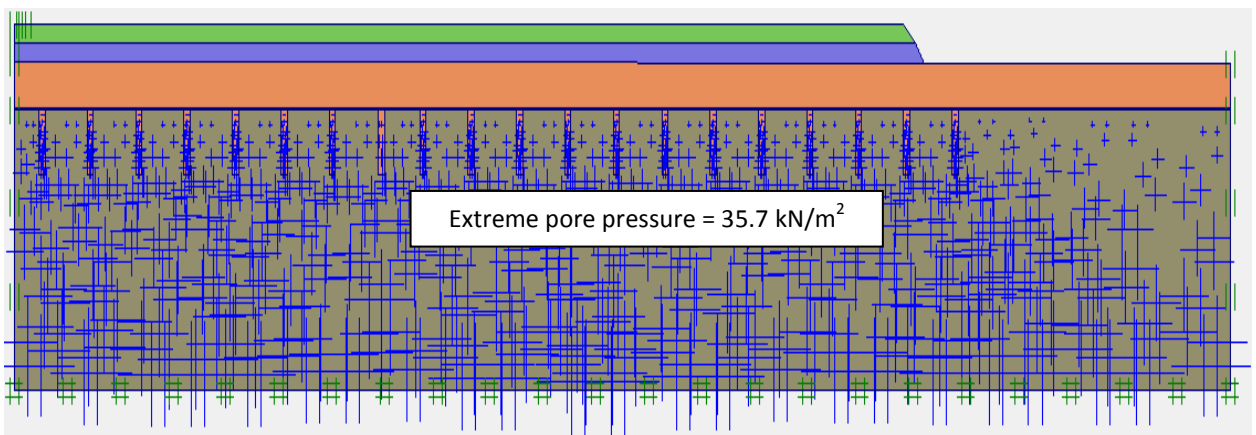


Figure 4.9. Pore pressure generation for Model-B.

4.6.4. Effective stress generation

The effective stress is the result of the groundwater activation obtained from pore pressure generation. This is an important parameter for controlling the consolidation of different layers of road structure (Figures 4.10 and 4.11). The extreme effective principal stresses for both models (A and B) are 46.7kN/m^2 and 62.5kN/m^2 , respectively.

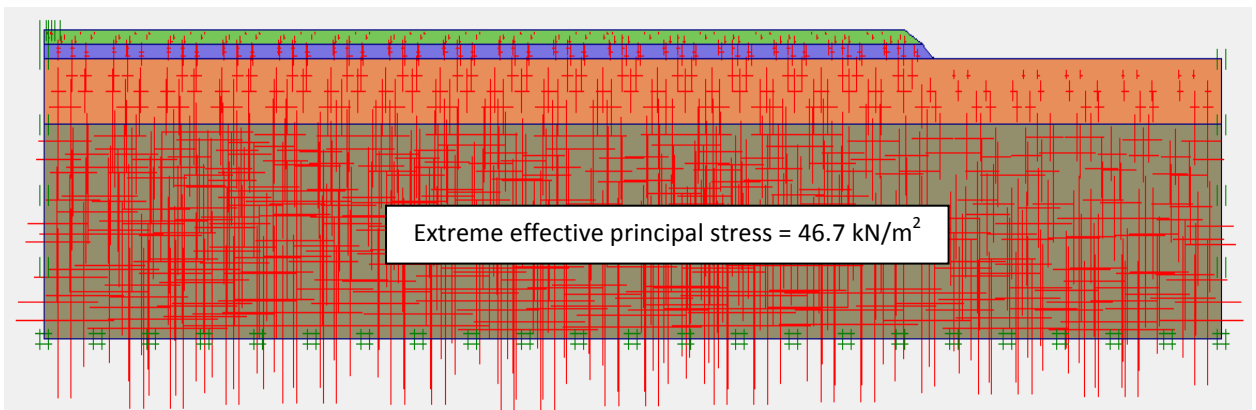


Figure 4.10. Effective stress generation for Model-A.

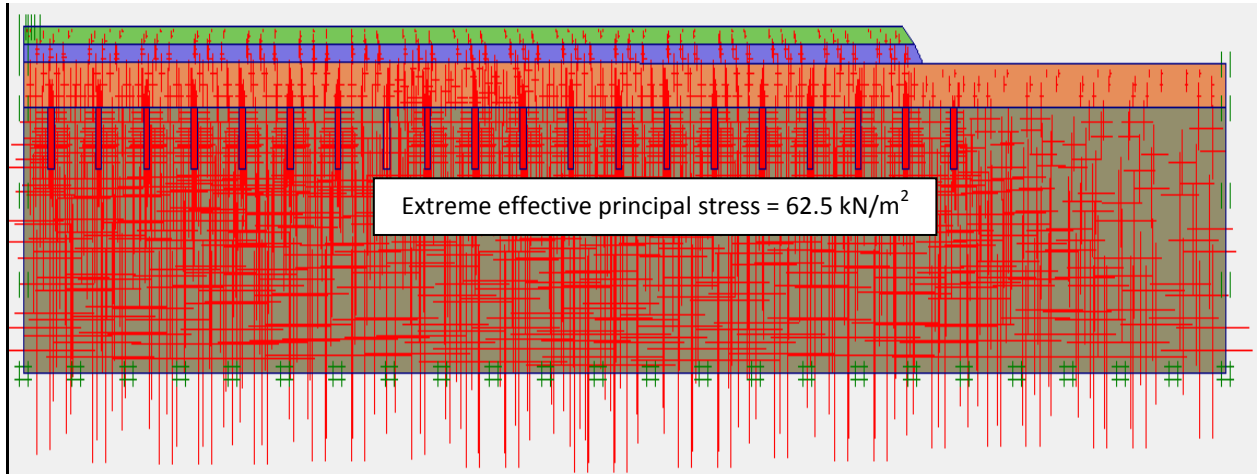


Figure 4.11. Effective stress generation for Model-B.

4.7. Results and discussion

4.7.1. Case of the untreated subbase layer “Model-A”

Different calculation phases (14 phases) were created in order to evaluate the overall safety coefficients (F_s) of the Model-A proposed for the two loads Min (200 kPa) and Max (600 kPa) applied on the road surface studied (Figure 4.12). All the layers constituting the roadway were subjected to a consolidation calculation with and without overload coming from the circulation of vehicles. The subbase layer has a thickness of 0.9 m in the present case.

4.7.1.1. Extreme total displacement in the untreated subbase layer

It should be noted that the minor load (200 kPa) was applied just on the left side of the road (3rd position) because it is occupied by light vehicles. However, heavy vehicles generally occupy the 1st position of the road (right side) where the major load (600 kPa) was applied. As shown in figures 4.13 and 4.14, the application of the two loads of 200 kPa and 600 kPa caused displacements of $100 \cdot 10^{-3}$ m (10 cm) and $180.3 \cdot 10^{-3}$ m (18 cm), respectively.

Chapter 4: Presentation of study area, Numerical Modelling, Results and Interpretation

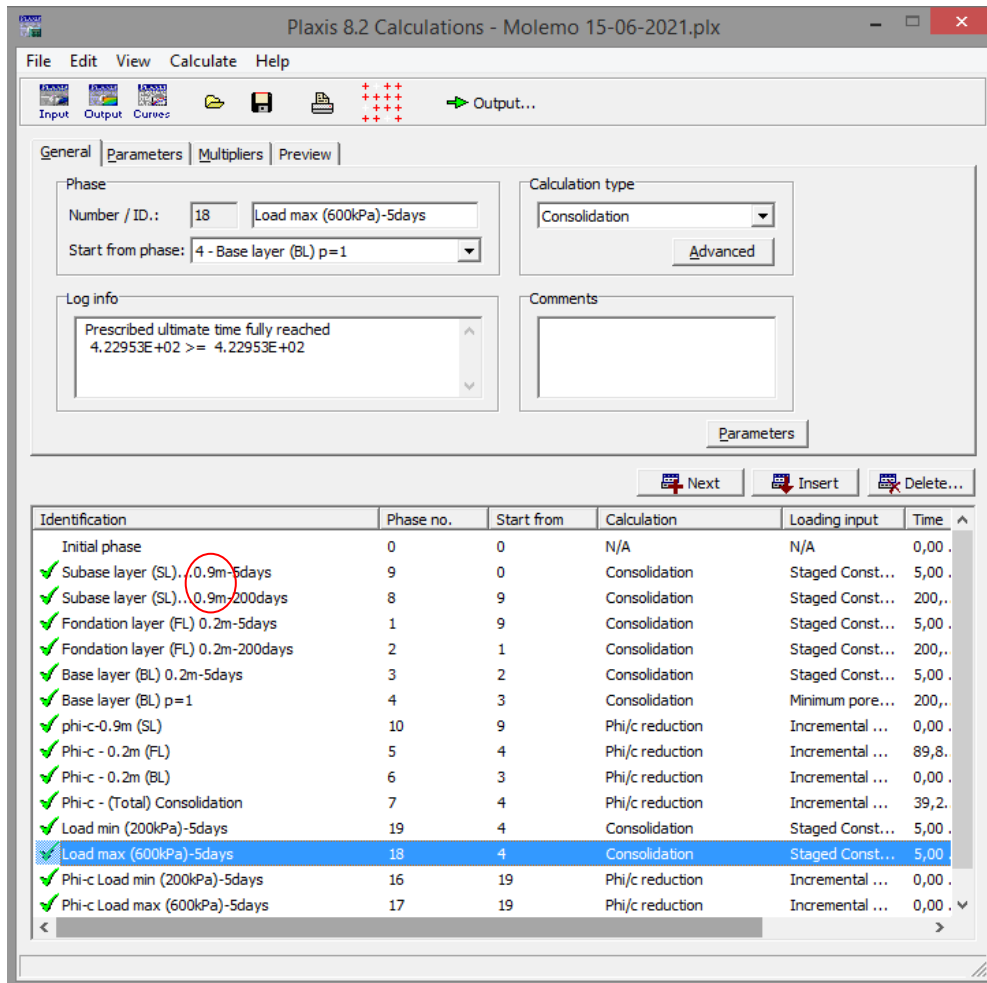


Figure 4.12. Different calculation phases made for the untreated subbase layer by the application of Min (200kPa) and Max (600kPa) loads (Model-A).

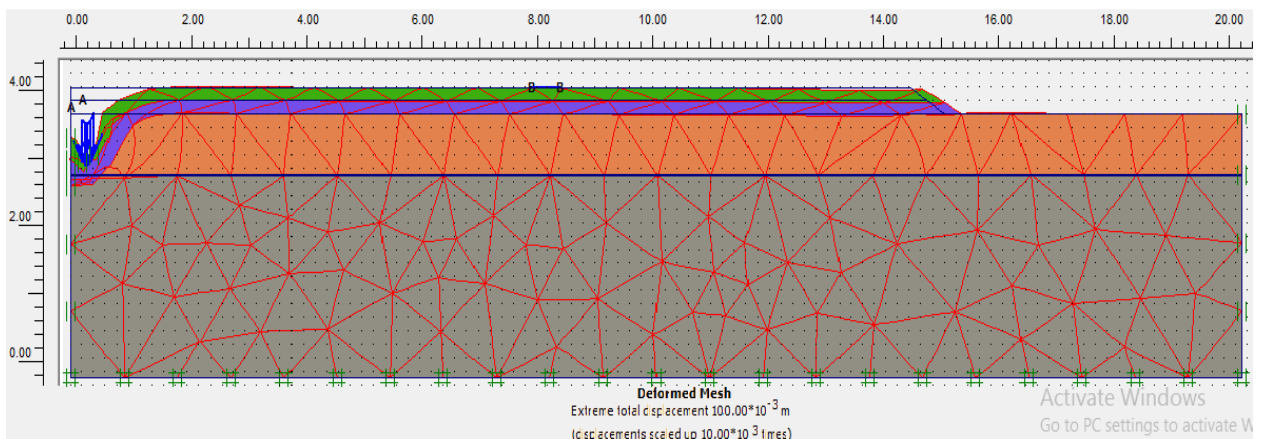


Figure 4.13. Extreme total displacement of the untreated subbase layer obtained from the application of Min-load (200kPa) (Model-A).

These displacements (or deformations) can be considered inadmissible, which necessitate the treatment of the subbase layer with mineral additives or reinforcement with lime-treated columns soil as a combination treatment. The geo-textile reinforcement of the subbase layer is also one of the existent solutions not used in the present study.

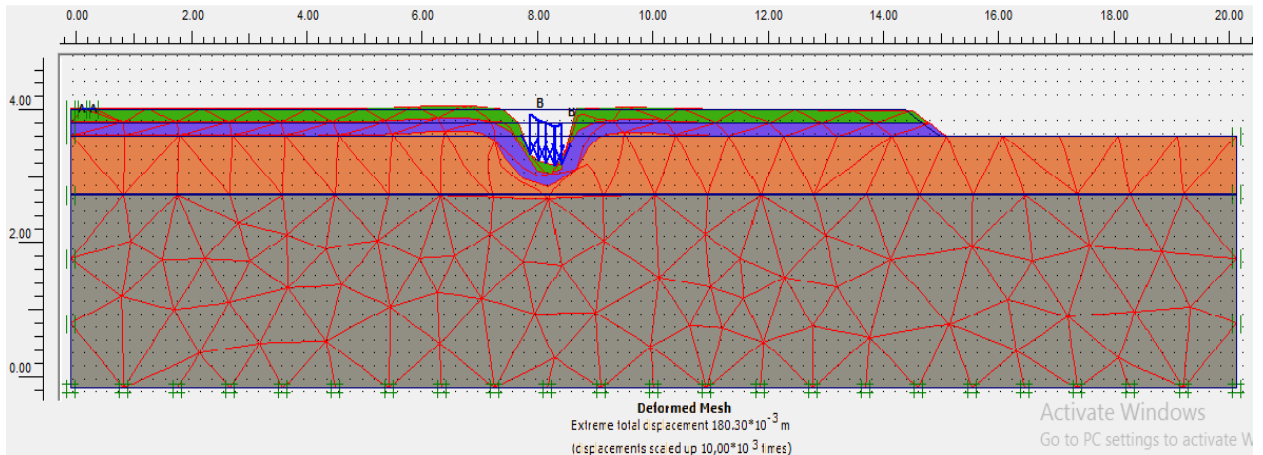


Figure 4.14. Extreme total displacement made on the untreated subbase layer obtained from the application of Max-load (600kPa) (Model-A).

4.7.1.2. Coefficient security obtained with Min and Max loads for Model-A

Partial safety coefficients of less than "1" were obtained for the various layers constituting the roadway after a short (5 days) and long term (200 days) calculation.

Consequently, overall safety coefficients less than '1' were also recorded of $F_s = 0.68$ and $F_s = 0.32$ which correspond to the application of 200 kPa and 600 kPa, respectively (Figures 4.15 and 4.16). These two values are insufficient to support the different loads for both short- and long-term calculation.

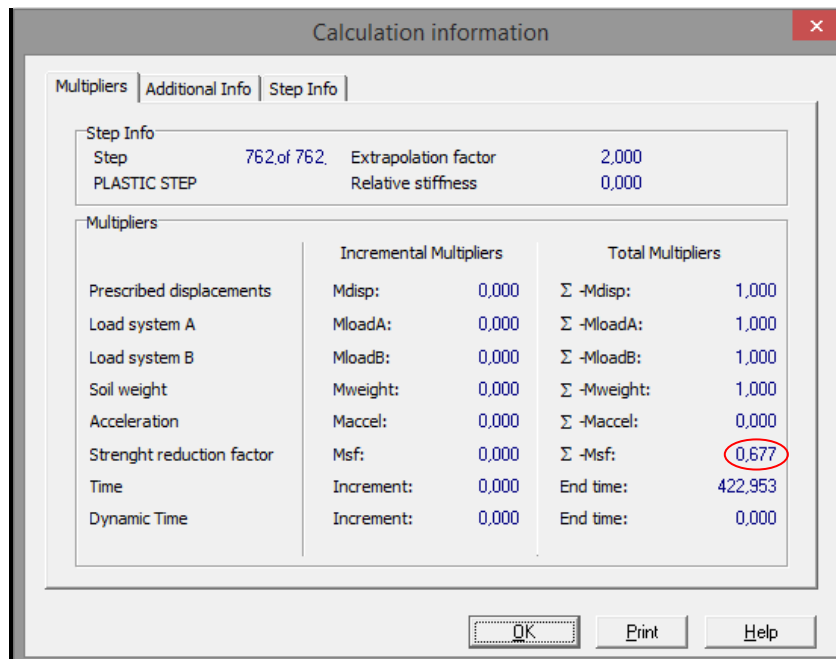


Figure 4.15. Coefficient security obtained by the application of Min-load (200 kPa) for Model-A.

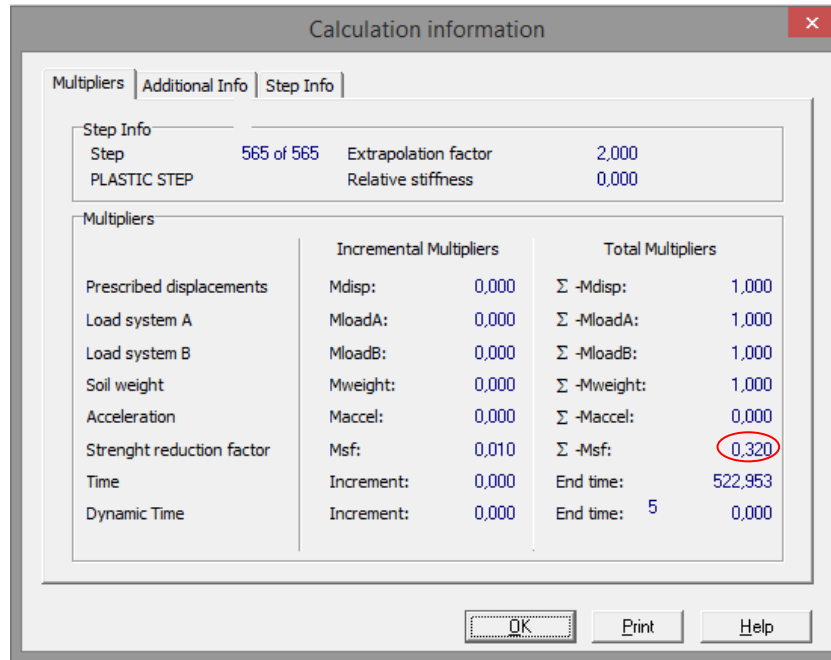


Figure 4.16. Coefficient security obtained by the application of Max-load (600 kPa) for Model-A.

4.7.2. Case of the treated subbase layer “Model-B”

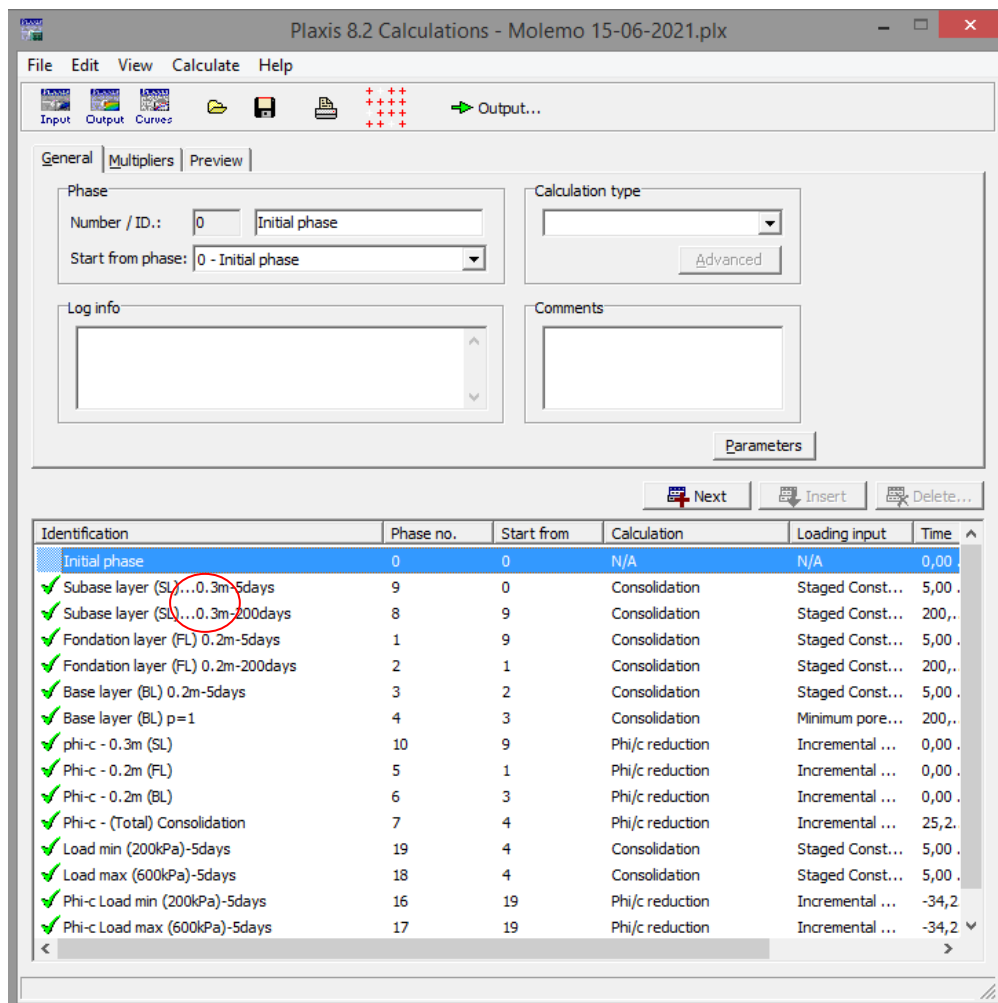


Figure 4.17. Different calculation phases made for lime-treated subbase layer (0.3 m thick) by the application of Min (200kPa) and Max (600kPa) loads (Model-B).

In the same way, different calculation phases (14 phases) were created in order to evaluate the overall safety coefficients (Fs) of the Model-B proposed for the two loads Min (200 kPa) and Max (600 kPa) applied on the road surface studied after its stabilization with 8% lime based on different lime-treated columns soil spaced by 0.7, 1.4 and 2.1 m. However, the response of the subbase layer treated with 8% lime was studied for two different thicknesses 0.3 and 0.6 m based on lime-treated columns soil (Figures 4.17 and 4.18). Indeed, all the layers constituting the roadway were subjected to a consolidation calculation with and without overload coming from the circulation of vehicles.

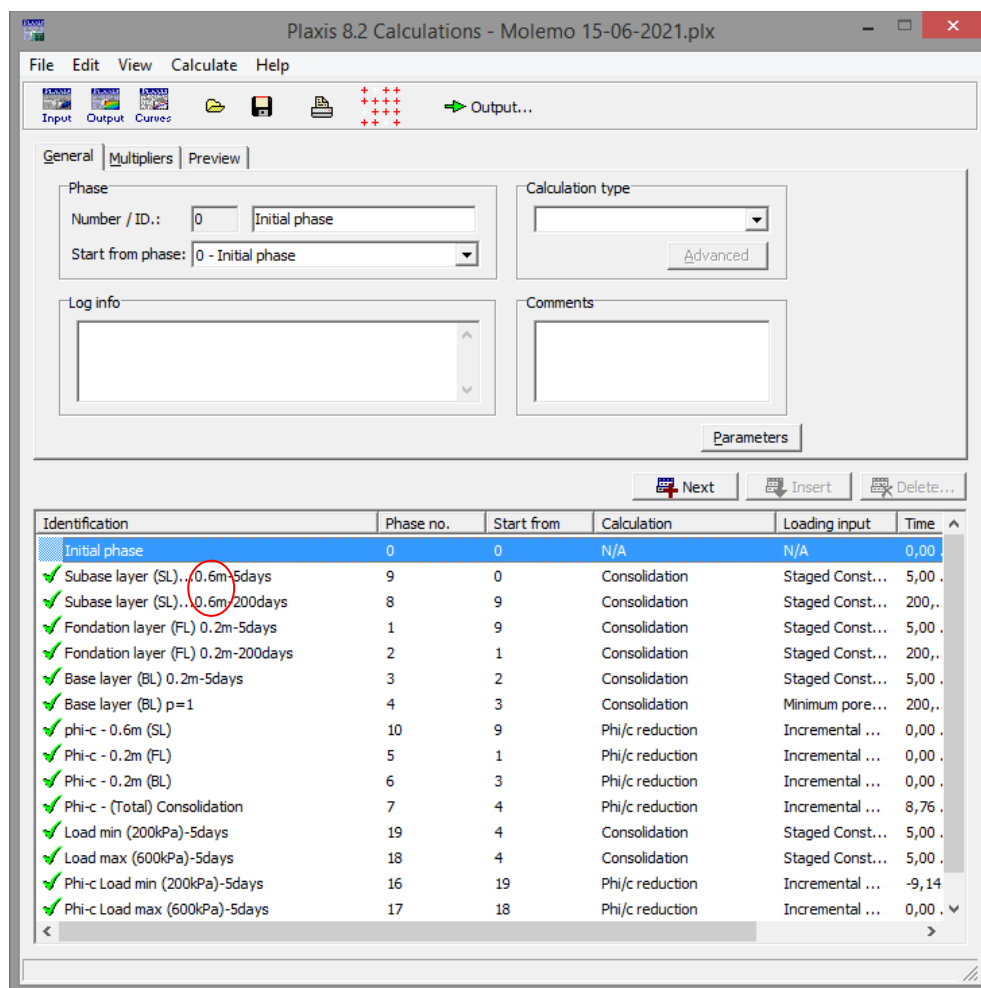


Figure 4.18. Different calculation phases made for lime-treated subbase layer (0.6 m thick) by the application of Min (200kPa) and Max (600kPa) loads (Model-B).

4.7.2.1. Extreme total displacement in the untreated subbase layer

With the same way, the minor load (200 kPa) was applied just on the left side of the road (3rd position) because it is occupied by light vehicles. However, heavy vehicles generally occupy the 1st position of the road (right side) where the major load (600 kPa) was applied.

4.7.2.1.1. Extreme total displacement for lime-treated subbase layer without treated columns

In the case where lime-treated columns are absent; the lime-treated subbase layer with 0.3m thickness shows that the application of the two loads of 200 kPa and 600 kPa caused displacements of $71 \cdot 10^{-3}$ m and $132.1 \cdot 10^{-3}$ m, respectively (Figures 4.19 and 4.20). However, the application of the same loads (200 kPa and 600 kPa) caused displacements of $51.9 \cdot 10^{-3}$ m and $97.7 \cdot 10^{-3}$ m while increasing the lime-treated subbase layer up to 0.6m thickness (Figures 4.21 and 4.22).

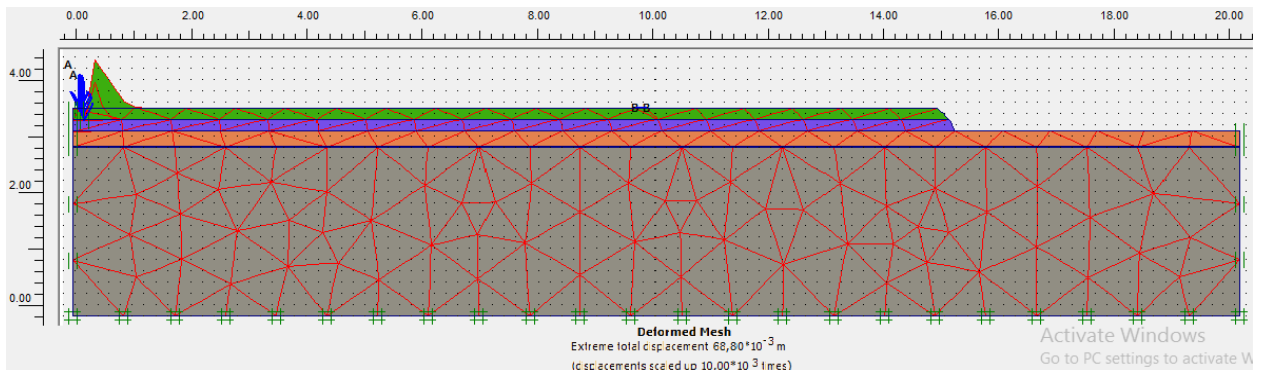


Figure 4.19. Extreme total displacement of lime-treated subbase layer (0.3 m thick) caused by the application of Min-load (200kPa) (Model-B).

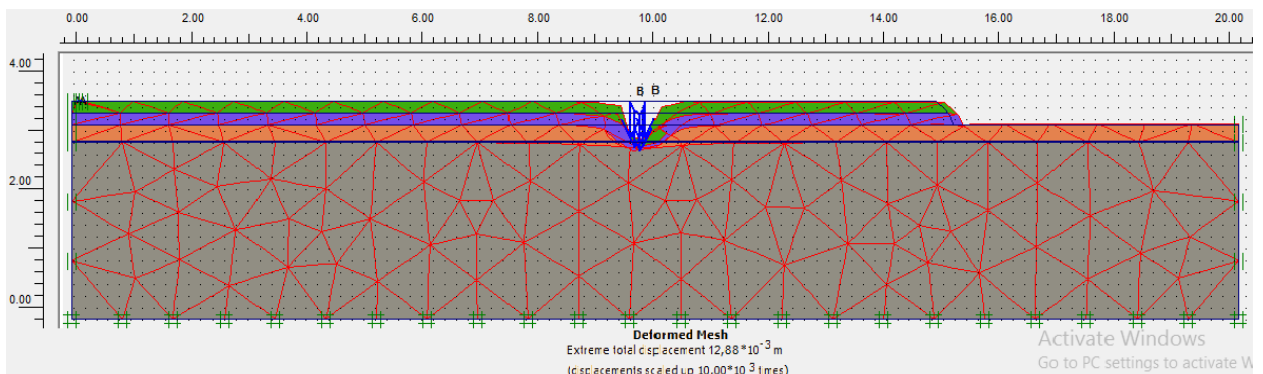


Figure 4.20. Extreme total displacement of lime-treated subbase layer (0.3 m thick) caused by the application of Min-load (600kPa) (Model-B).

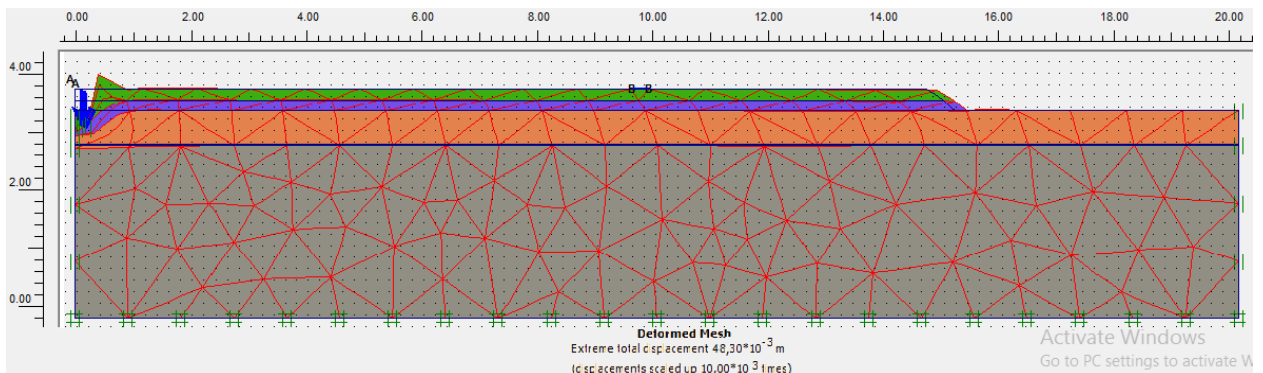


Figure 4.21. Extreme total displacement of lime-treated subbase layer (0.6 m thick) caused by the application of Max-load (200kPa) (Model-B).

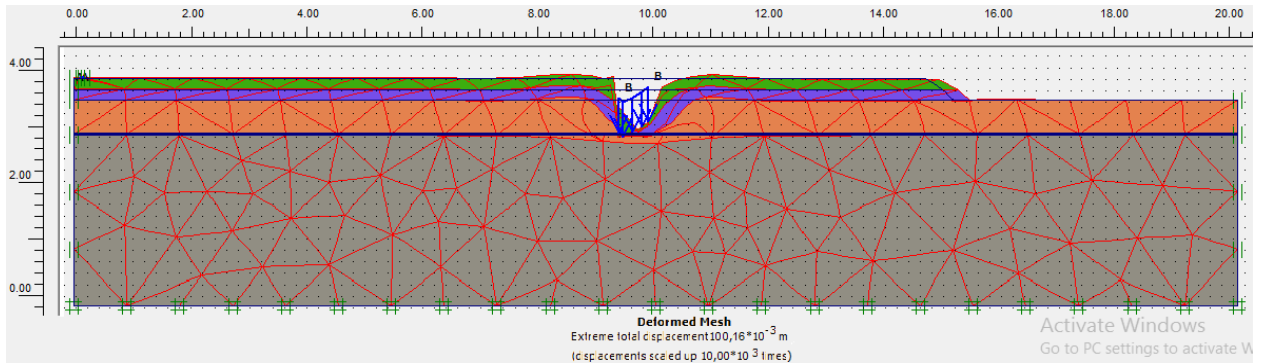


Figure 4.22. Extreme total displacement of lime-treated subbase layer (0.6 m thick) caused by the application of Max-load (600kPa) (Model-B).

4.7.2.1.2. Extreme total displacement for lime-treated subbase layer based on lime-treated columns

- **Case of lime-treated subbase layer with 0.3 m thickness based on lime-treated columns**

In the case of the presence of lime-treated columns, the subbase layer with 0.3m thickness shows that the application of 200 kPa on the road surface caused displacements of $21.2 \cdot 10^{-3}$ m, $36.8 \cdot 10^{-3}$ m and $60.1 \cdot 10^{-3}$ m respectively with the spaced columns distance of 0.7, 1.4 and 2.1 m (Figures 4.23, 4.24 and 4.25). However, with the same thickness, the application of 600 kPa on the road surface caused displacements of $34.2 \cdot 10^{-3}$ m, $55.9 \cdot 10^{-3}$ m and $83.4 \cdot 10^{-3}$ m with the same spaced columns distance (Figures 4.26, 4.27 and 4.28).

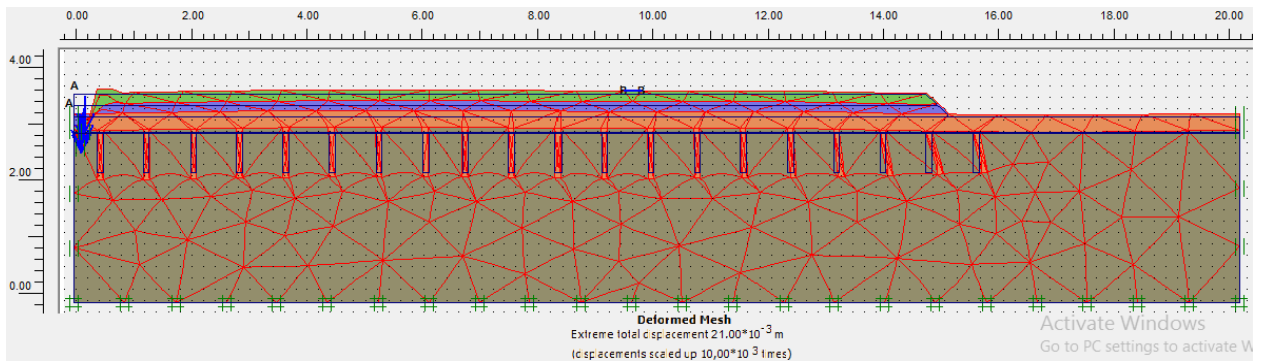


Figure 4.23. Extreme total displacement of lime-treated subbase layer (0.3 m thick) made by the application of Min-load (200kPa) based on lime-treated columns spaced by 0.7 m (Model-B).

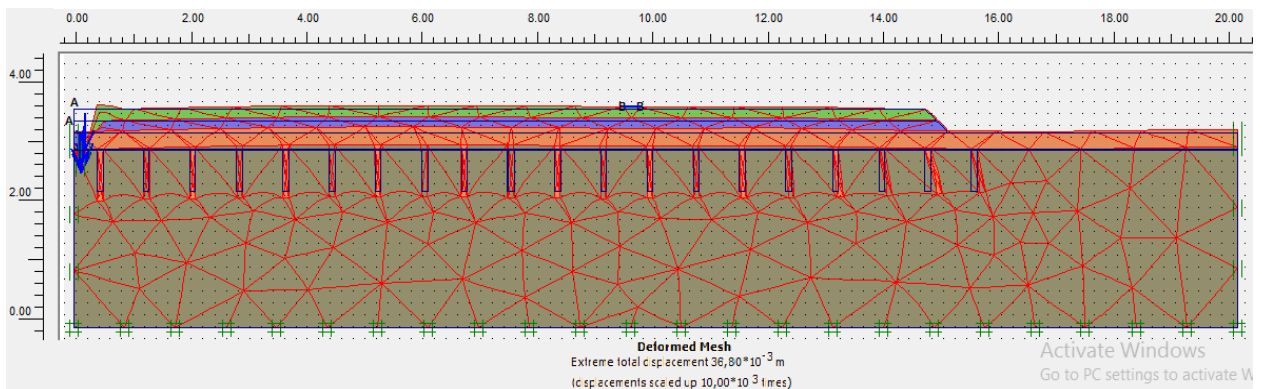


Figure 4.24. Extreme total displacement of lime-treated subbase layer (0.3 m thick) made by the application of Min-load (200kPa) based on lime-treated columns spaced by 1.4 m (Model-B).

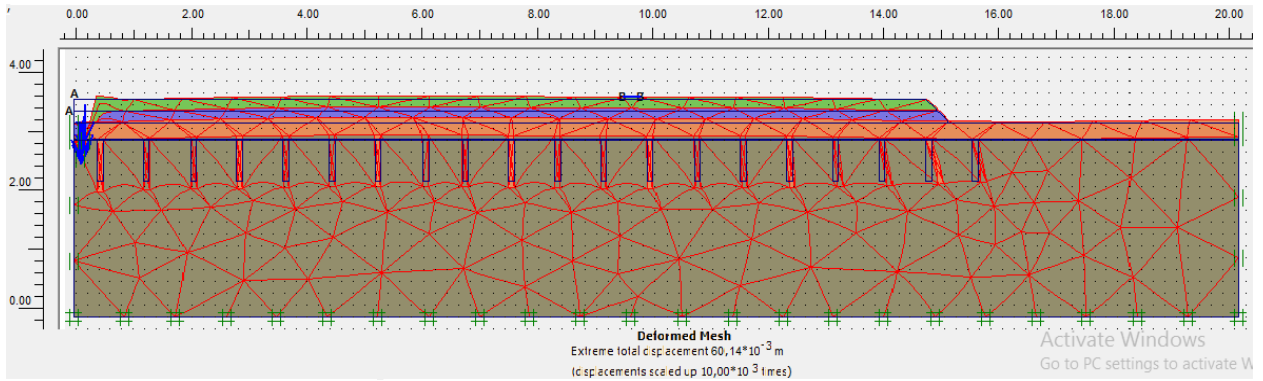


Figure 4.25. Extreme total displacement of lime-treated subbase layer (0.3 m thick) made by the application of Min-load (200kPa) based on lime-treated columns spaced by 2.1 m (Model-B).

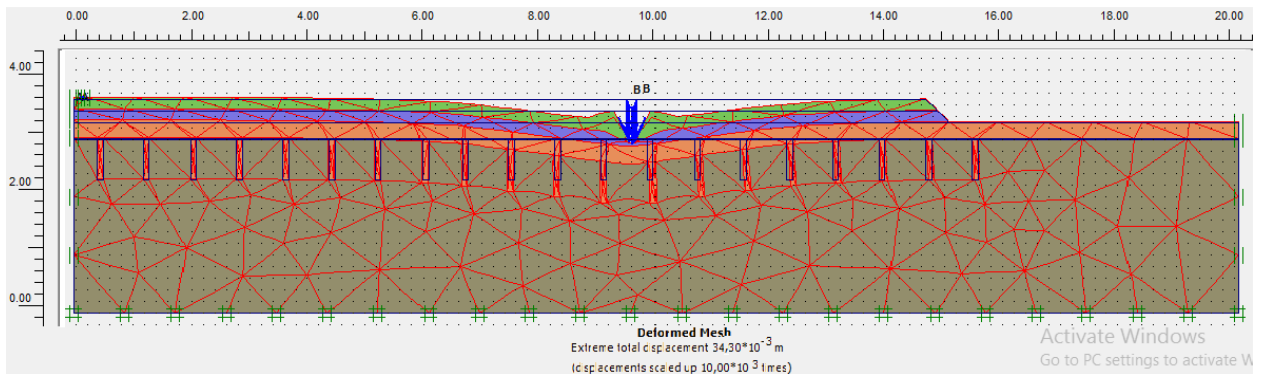


Figure 4.26. Extreme total displacement of lime-treated subbase layer (0.3 m thick) made by the application of Max-load (600kPa) based on lime-treated columns spaced by 0.7 m (Model-B).

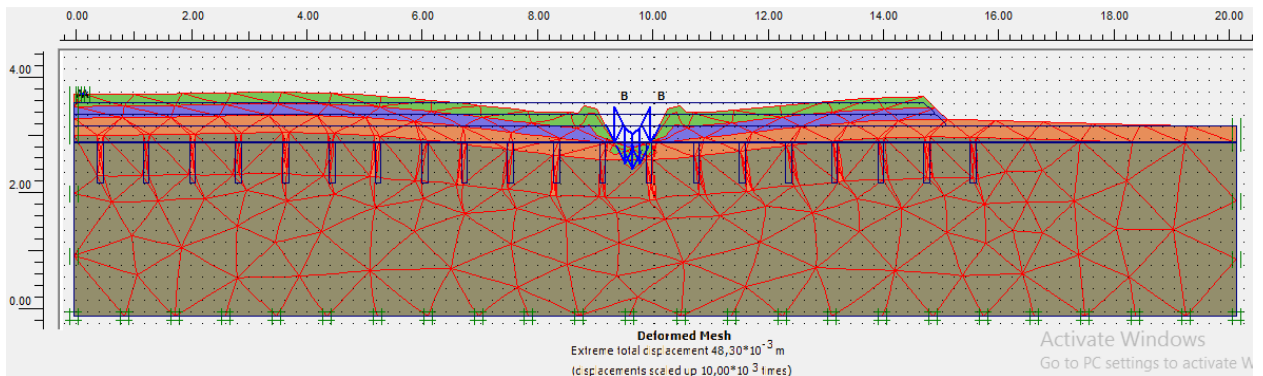


Figure 4.27. Extreme total displacement of lime-treated subbase layer (0.3 m thick) made by the application of Max-load (600kPa) based on lime-treated columns spaced by 1.4 m (Model-B).

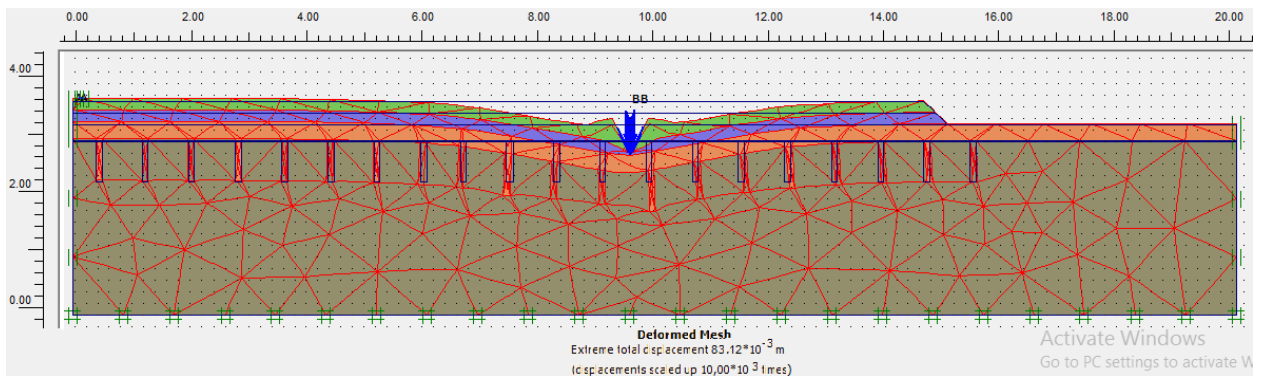


Figure 4.28. Extreme total displacement of lime-treated subbase layer (0.3 m thick) made by the application of Max-load (600kPa) based on lime-treated columns spaced by 2.1 m (Model-B).

- **Case of lime-treated subbase layer with 0.6 m thickness based on lime-treated columns**

According to Figures 4.29, 4.30 and 4.31, it can be seen that the application of 200 kPa on the road surface caused displacements of $3.01 \cdot 10^{-3}$ m, $11 \cdot 10^{-3}$ m and $22.3 \cdot 10^{-3}$ m respectively with the spaced columns distance of 0.7, 1.4 and 2.1 m if the subbase layer thickness is equal to 0.6m. Nevertheless, with the same thickness (0.6m), the application of 600 kPa on the road surface caused displacements of $8.04 \cdot 10^{-3}$ m, $16.9 \cdot 10^{-3}$ m and $27.1 \cdot 10^{-3}$ m respectively with the same spaced columns distance (Figures 4.32, 4.33 and 4.34). These displacements (or deformations) can be considered admissible to compare to the untreated subbase layer for Model-A.

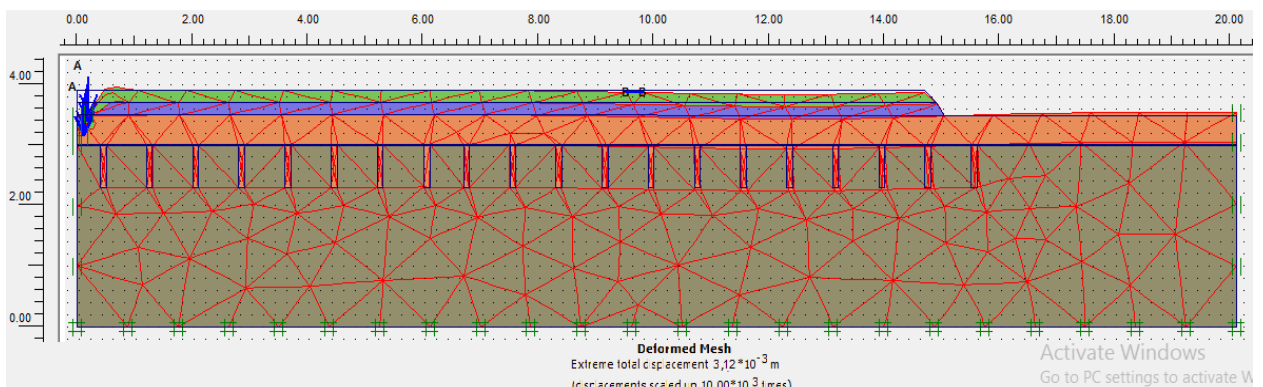


Figure 4.29. Extreme total displacement of lime-treated subbase layer (0.6 m thick) made by the application of Min-load (200kPa) based on lime-treated columns spaced by 0.7 m (Model-B).

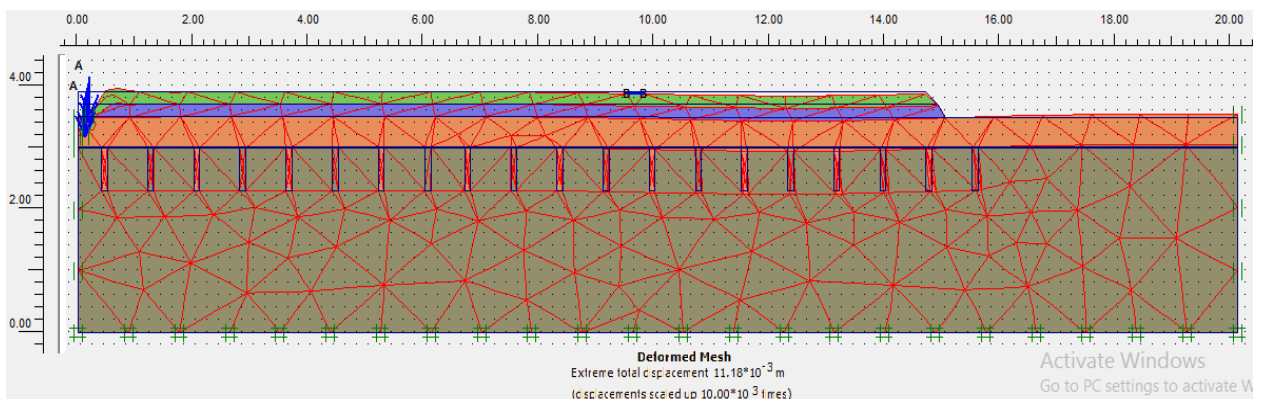


Figure 4.30. Extreme total displacement of lime-treated subbase layer (0.6 m thick) made by the application of Min-load (200kPa) based on lime-treated columns spaced by 1.4 m (Model-B).

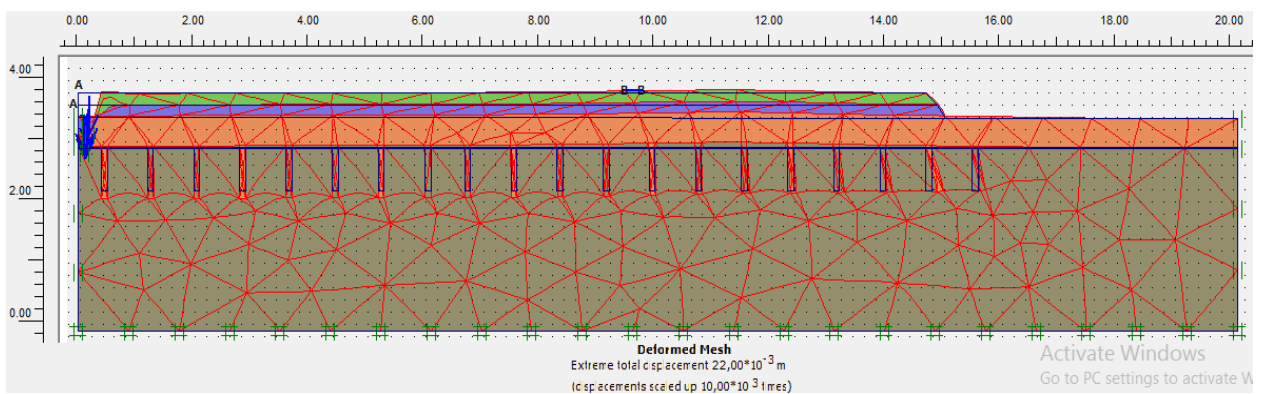


Figure 4.31. Extreme total displacement of lime-treated subbase layer (0.6 m thick) made by the application of Min-load (200kPa) based on lime-treated columns spaced by 2.1 m (Model-B).

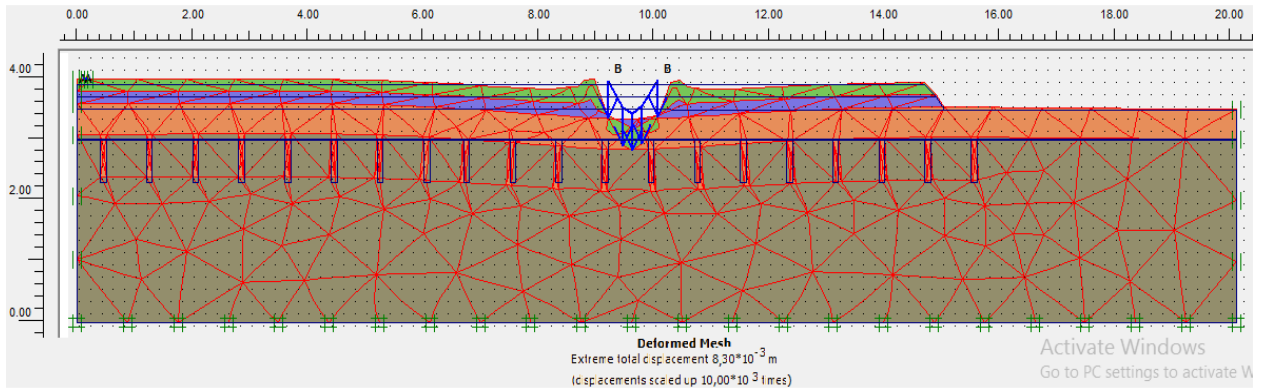


Figure 4.32. Extreme total displacement of lime-treated subbase layer (0.6 m thick) made by the application of Max-load (600kPa) based on lime-treated columns spaced by 0.7 m (Model-B).

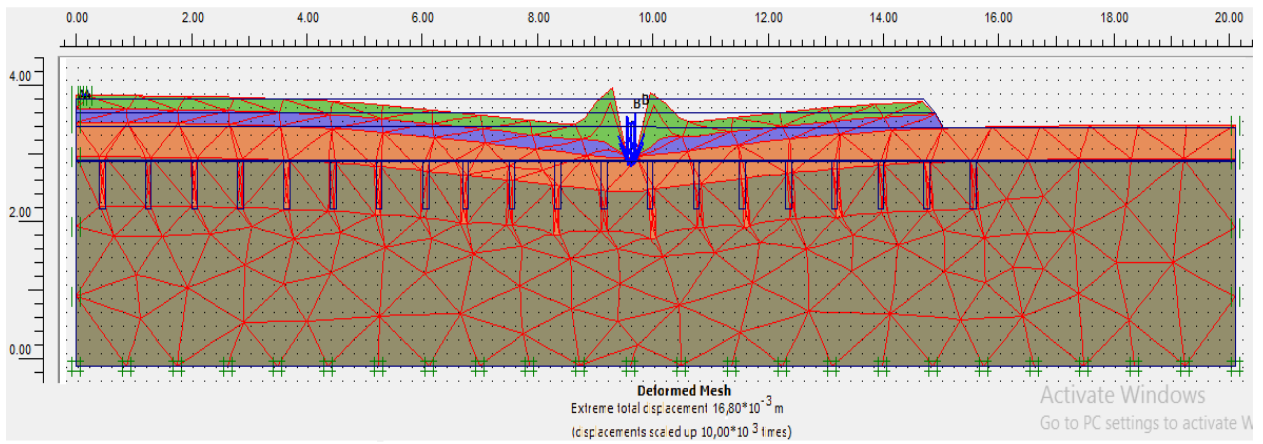


Figure 4.33. Extreme total displacement of lime-treated subbase layer (0.6 m thick) made by the application of Max-load (600kPa) based on lime-treated columns spaced by 1.4 m (Model-B).

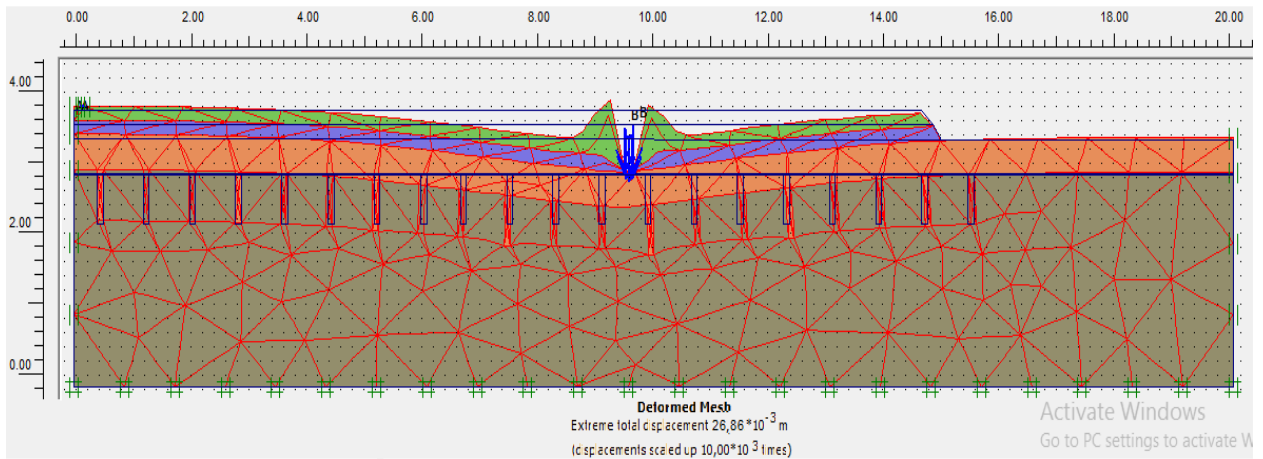


Figure 4.34. Extreme total displacement of lime-treated subbase layer (0.6 m thick) made by the application of Max-load (600kPa) based on lime-treated columns spaced by 2.1 m (Model-B).

4.7.2.2. Coefficient security obtained with Min and Max loads for Model-A

Displacements values and partial safety coefficients for untreated subbase layer, lime treated subbase layer without lime-treated columns, and lime treated subbase layer with lime-treated columns are depicted in [Tables 4.4, 4.5 and 4.6](#), below respectively.

Table 4.4. Displacements for untreated subbase layer.

Loads (kPa)	Displacement (ds) (cm)	Safety Coefficient (Fs)
200	10	0.68
600	18	0.32

Table 4.5. Displacement for lime-treated subbase layer without lime-treated columns.

Loads (kPa)	Displacement (ds) (cm) and safety coefficient (Fs)	
	0.3 m thickness	0.6 m thickness
200	ds = 6.9 Fs = 0.81	ds = 4.8 Fs = 0.83
600	ds = 13 Fs = 0.45	ds = 10 Fs = 0.65

Table 4.6. Displacement for lime-treated subbase layer with different spacing distance of lime-treated columns soil (LTCS).

Loads (kPa)	Displacement (ds) (cm) and safety coefficient (Fs)					
	Subbase layer with 0,3m thickness			Subbase layer with 0,6m thickness		
	0,7m of space	1,4m of space	2,1m of space	0,7m of space	1,4m of space	2,1m of space
200	ds = 2.1 Fs = 1.25	ds = 3.7 Fs = 1.07	ds = 6 Fs = 0.98	ds = 0.3 Fs = 2.5	ds = 1.1 Fs = 1.98	ds = 2.2 Fs = 1.32
600	ds = 3.4 Fs = 1.05	ds = 4.8 Fs = 0.91	ds = 8.3 Fs = 0.88	ds = 0.2 Fs = 2.6	ds = 1.7 Fs = 1.7	ds = 2.7 Fs = 1.2

We base on the above two [Tables 4.4](#) and [4.5](#) to draw the [Figure 4.35](#) in order to make a comparison between the results of untreated subbase layer (USL) known as “control soil or reference soil” and those of the same layer treated with 8% lime with different thicknesses (0.3 and 0.6m).

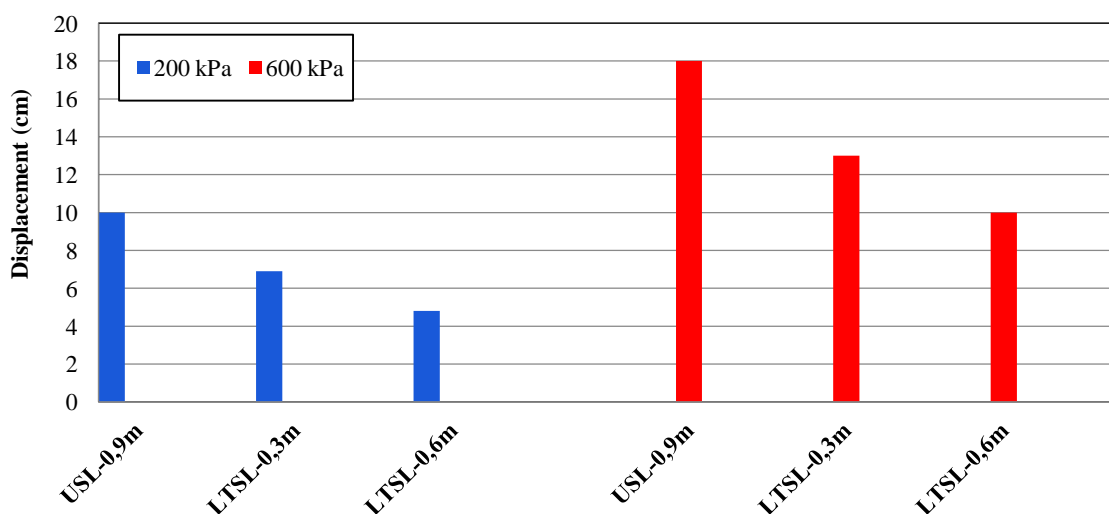


Figure 4.35. Effects of different applied loads on the untreated and lime-treated subbase layer with different thicknesses.

Figure 4.35 represents the variation of displacement in relation to the load applied. It can be seen that displacement increases with increasing load. However, for both loads, displacement decreases with increasing subbase thickness. Therefore, these results are considered non-admissible.

From the graph above, the low displacements were found for the treated subbase layer with 0.6m thickness but despite this, we cannot inherit it for our pavement construction. We base on the above two tables 4.5 and 4.6 to draw the figures 4.36 and 4.37 to make a comparison between the results of lime-treated subbase layer (LTSL) known as “control soil or reference soil” and those of the same layer treated with 8% lime with different thicknesses (0.3 and 0.6m) which is based on various spacing treated-columns.

Figures 4.36 and 4.37 depict the effects of both different applied loads (200 and 600kPa) and lime-treated columns under different spacing (0.7, 1.4 and 2.1) on the behaviour of lime-treated subbase layer with 0.3 and 0.6 m thickness, respectively. In the case of lime-treated subbase layer with 0.3m of thickness, it is obvious to observe that whatever the applied load and whatever the spacing value between lime-treated columns, the displacements are very low compared to those of the same layer stabilized with lime-treated columns (Figure 4.36).

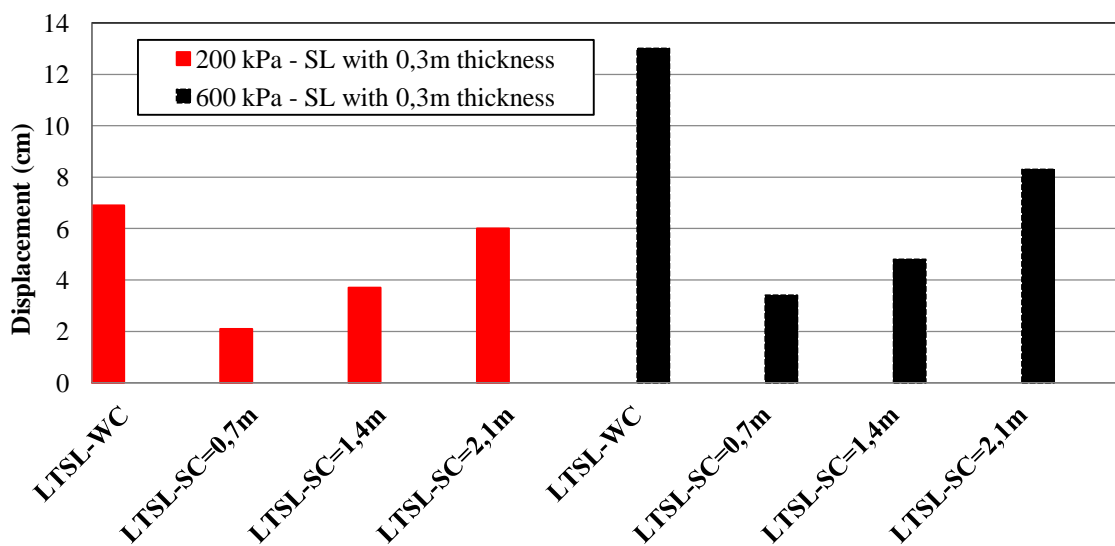


Figure 4.36. Effects of both different applied loads and lime-treated columns under different spacing on the behaviour of lime-treated subbase layer with 0.3m thickness (LTSL-WC: lime-treated subbase layer without treated columns; LTSL-SC: lime-treated subbase layer based on lime-treated columns under different spacing).

However, for the same layer with 0.6m of thickness submitted to the same loads in the presence of the same lime-treated columns, it is quite clear to see that the same behavior was recorded compared to lime-treated subbase layer with 0.3m of thickness but with high reduction in displacement values (Figure 4.37).

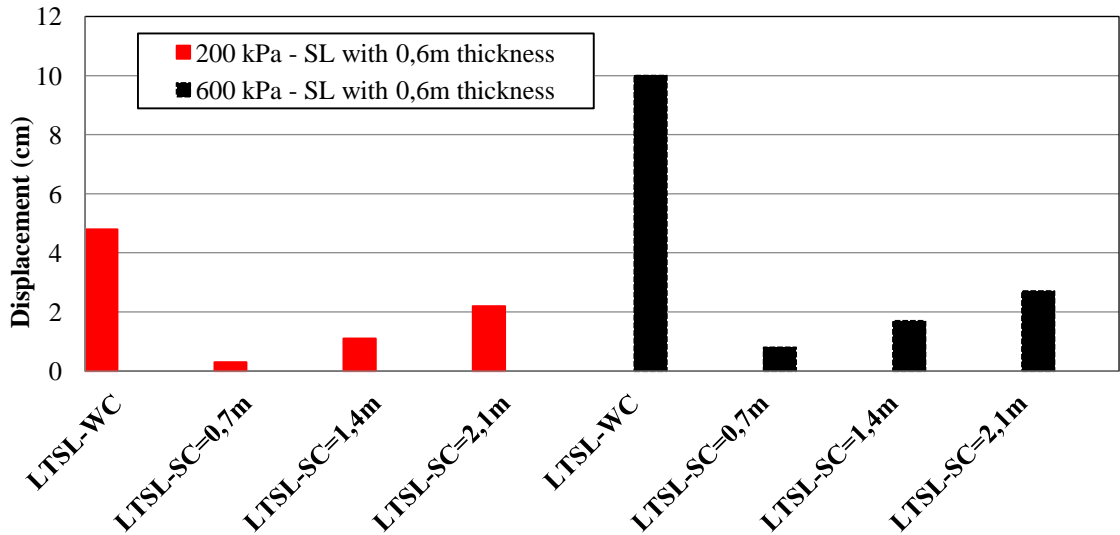


Figure 4.37. Effects of both different applied loads and lime-treated columns under different spacing on the behaviour of lime-treated subbase layer with 0.6m thickness (LTSL-WC: lime-treated subbase layer without treated columns; LTSL-SC: lime-treated subbase layer based on lime-treated columns under different spacing).

For the case of lime-treated subbase layer with 0.3 m of thickness, all the displacements are greater than the limit value (3cm) mentioned in (LCPC-SETRA, 1994) except the case when this one was based on columns spaced by 0.7m in the presence of 200 kPa load. In contrast, for lime-treated subbase layer with 0.6 m of thickness, without exception, all the displacements are lower than the limit value. This leaves us with only three possible cases where we can choose one of them considered as the most economic solution and consequently the sufficient security, which corresponds to the case of lime-treated subbase layer with 0.6 m of thickness and columns spaced by 2.1m.

4.8. Conclusion

Two models have been studied for a road pavement and based on the above results; the following conclusions can be drawn:

- The displacement of the untreated subbase layer is noted that the minor load (200 kPa) was applied just on the left side (3rd position) because it is occupied by light vehicles.
- Heavy goods vehicles generally occupying the 1st position of the road (right side) where the major load (600 kPa) has been applied.
- In the untreated soil (model A) applied for two loads min (200kPa) and max (600kPa) can cause unacceptable displacements or deformations; for that it requires a treatment.
- Model B can withstand both loads and not cause considerable deformation.
- In the case of a 0.3 m thick lime-treated subbase layer, it is obvious to observe that whatever the load applied and whatever the value of the spacing between the treated

columns with lime, the displacements are very low compared to those of the same stabilized layer with columns treated with lime.

- The untreated subbase layer (0.9m) and those of the same layer treated with lime at 8% with differences in thickness (0.3m and 0.6m), displacement increases with increasing load. However, for both loads, displacement decreases with increasing thickness of the subbase.

**General
Conclusions and
Recommendations**

1. General conclusions

This thesis is part of the study of the numerical modelling of a roadway stabilized with lime against road traffic. This work has the advantages of studying the response, by numerical modelling, of a roadway stabilized with lime. Indeed, the collection of data from the literature or taken into account from a road project completed through the use of PLAXIS code.

Firstly, a methodology was followed for the collection of data, road traffic, the different types of road structures, materials used in the construction of road pavements and synthesis of road pavement simulation developed. Secondly, experimental studies were made concerning the presentation of the PLAXIS software, presentation of the project or of the data and case studies (digital modelling by the PLAXIS code). And then lastly, analysis and interpretation of the results obtained with the PLAXIS software were made, by numerical modelling of a lime-stabilized pavement from the collection of data of a completed project (case of the Harchoun, Chlef, and highway section).

In the present study, two different geometrical models (Model-A and Model-B) have been suggested in order to assess the effects of three different parameters namely: (1) physical parameter (Min (200kPa) and Max (600kPa) loads were applied to simulate the traffic circulation) (SETRA, 2000), (2) mechanical parameter (subbase layer with and without treatment by adding 8% lime as an additive and (3) geometrical parameter (0.9m thickness was used for untreated subbase layer and both 0.3m and 0.6m thicknesses (SETRA, 2000) were used for lime-treated subbase layer, respectively) on the behaviour of the road structure, found by its researchers, where the following conclusions were drawn:

- In model-A (untreated subbase layer), different calculation phases were created in order to evaluate the safety coefficients with two loads min (200 kPa) and max (600 kPa) applied to the road surface.
- The displacement of the untreated subbase layer it demonstrates that the minor load (200 kPa) was applied just on the left side (3rd position) because it is occupied by light vehicles.
- Heavy goods vehicles generally occupying the 1st position of the road (right side) where the major load (600 kPa) has been applied.
- In untreated soil (model-A) applied for two max loads (200kPa) and (600kPa) can cause inadmissible displacements or deformations, which necessitates the treatment of the subbase layer with mineral additives or to reinforce it with a soil of columns treated with lime.

- The Safety Coefficient (FS) obtained with the load min (200 kPa) and load max (600 kPa) for model-A (untreated ground) less than (1) are insufficient to withstand the different loads for the short (5 days) and long calculations (200 days) term.
- In the case where lime-treated columns are absent; the lime-treated subbase layer with 0.3m thickness shows that the application of the two loads of 200 kPa and 600 kPa caused displacements of $71 \cdot 10^{-3}$ m and $132.1 \cdot 10^{-3}$ m, respectively. However, the application of the same loads (200 kPa and 600 kPa) caused displacements of $51.9 \cdot 10^{-3}$ m and $97.7 \cdot 10^{-3}$ m while increasing the lime-treated subbase layer up to 0.6m thickness.
- In the case of the presence of lime-treated columns, the subbase layer with 0.3m thickness shows that the application of 200 kPa on the road surface caused displacements of $21.2 \cdot 10^{-3}$ m, $36.8 \cdot 10^{-3}$ m and $60.1 \cdot 10^{-3}$ m respectively with the spaced columns distance of 0.7, 1.4 and 2.1m. However, with the same thickness, the application of 600 kPa on the road surface caused displacements of $34.2 \cdot 10^{-3}$ m, $55.9 \cdot 10^{-3}$ m and $83.4 \cdot 10^{-3}$ m with the same spaced columns distance.
- In the case of a 0.3 m thick lime-treated subbase layer, it is obvious to observe that whatever the load applied and whatever the value of the spacing between the treated columns with lime, the displacements are very low compared to those of the same stabilized layer with columns treated with lime.
- The untreated subbase layer (0.9m) and those of the same layer treated with lime at 8% with differences in thickness (0.3m and 0.6m), displacement increases with increasing load. However, for both loads, displacement decreases with increasing thickness of the subbase.
- In the case of a subbase layer treated with lime (0.3 m thickness), all displacements are greater than the limit value (3cm) mentioned in SETRA (2000) except in the case where this was based on poles spaced 0.7m apart in the presence of a load of 200 kPa.
- For a 0.6 m thickness lime-treated subbase layer, without exception, all displacements are less than the limit value.

2. Recommendations

- The subbase layer treated with lime with 0, 6 m thickness with columns of 2.1 m apart can be considered the most economical, therefore, has sufficient safety coefficient (FS) and the displacement is less than the limit value (SETRA).
- A subbase layer treated with lime, applied for two loads min and max, does not cause serious deformation problem compared to untreated subbase layer.
- To avoid considerable deformation and short road lifespan, the soil may need treatment with lime or even other binders.

List of References

List of references

- **ASTM. (2000).** Standard test methods for soil test, West Conshohocken, PA, ASTM – American Society for Testing and Materials.
- **Brinkgreve, R.B.J. (2003).** PLAXIS v8 reference manual, Delft University of Technology & PLAXIS by The Netherlands.
- **B40. (1977).** Etudes générales techniques et économiques des aménagements routiers. Normes techniques d'aménagement des routes (NTAR), Ministère des travaux publics, Algérie.
- **Duncan, J.M and Chang, Y.Y. (1970).** Nonlinear analysis of stress and strain in soils. Journal of the Soil Mechanics and Foundations Division. ASCE, Vol.96, pp.1629.
- **Fédéric V. (2015).** Road Geotechnic Study, Lyon-France, March;
- **Gadouri H, Harichane K, Ghrici M. (2017a).** Assessment of sulphates effect on pH and pozzolanic reactions of soil–lime–natural pozzolana mixtures. Int J Pavement Eng 20:1–14. <https://doi.org/10.1080/10298436.2017.1337119>.
- **Gadouri H, Harichane K, Ghrici M. (2017b).** A comparison study between $\text{CaSO}_4 \cdot 2\text{H}_2\text{O}$ and Na_2SO_4 effects on geotechnical properties of clayey soils stabilised with mineral additives to recommend adequate mixtures as materials for road pavements. Int J Geotech Eng. 13(1): 61–82. <https://doi.org/10.1080/19386362.2017.1320850>.
- **Gadouri H. (2017).** Influence of sulphates on the stabilization of clayey soils using mineral additives. Ph.D thesis, Medea University, Algeria. https://www.researchgate.net/publication/330912668_Influence_of_sulphates_on_the_stabilization_of_clayey_soils_using_mineral_additives.
- **Guide Technique LCPC-SETRA, (1994).** Conception et dimensionnement des structures de chaussée, France.
- **Harichane, K., Ghrici, M., and Kenai, S., 2011a.** Effect of curing period on shear strength of cohesive soils stabilized with combination of lime and natural pozzolana. *International Journal of Civil Engineering*, 9, (2), 90–96.
- **Harichane, K., and Ghrici, M., 2009.** *Effect of combination of lime and natural pozzolana on the plasticity of soft clayey soils*, 2nd International Conference on New Developments in Soil Mechanics and Geotechnical Engineering, 30 May 2009, Near East University, Nicosia, North Cyprus.
- **Jean-Michel C. (2017).** La structure de la chaussée, CNFPT, France <https://www.wikiterritorial.cnfpt.fr/xwiki/bin/view/vitrine/La%20structure%20de%20la%20chauss%C3%A9e%20>.
- **Levasseur, S. (2007).** Inverse geotechnical analysis: development of a method based on genetic algorithms. Doctoral thesis, Joseph University Fourier - Grenoble I.

- **Manoj Anaokar and Sharad Mhaiskar. (2019).** Numerical analysis of lime stabilized capping under embankments based on expansive subgrades. *Heliyon*, Vol. 5 N° e02473, pp. 1-9. <https://doi.org/10.1016/j.heliyon.2019.e02473>.
- **Mathew. T.V and Krishna Rao K.V. (2006).** Introduction to transportation engineering: Environmental impact assessment for sustainable transport, India.
- **Mestat, P. (2002).** Elastoplastic modelling of soils. In *Elasto-plasticity of soils and rocks. Behaviour model of soils and rocks 1*. Under the direction of P.Y. Hicher and J.F. Shao. Hermès science.
- **Mugdha P. (2000).** Transportation-engineering/highway/materials-used-for-the-construction-of-roads-methods-process-layers-and-road-pavement/48549 (IS: 217-1988: Specification for cutback bitumen, Bureau of Indian Standards, New Delhi, 1993).
- **Narasimha and Rajasekaran (1994).** Lime injection technique to improve the behaviour of soft marine clays. *Ocean Engineering*, Vol. 21, No 1, pp. 29-43, 1994.
- **Nova, R. (2005).** Foundations of soil mechanics. Hermes Science.
- **Sadok, S. (2015).** Study of geogrid reinforcement of a road platform. Magister's thesis, University of Tébéssa, p.11-18 <https://pt.scribd.com/document/440498475/Etude-de-renforcement-par-geogrilles-d-une-plateforme-routiere-pdf>.
- **Schanz, T, Vermeer, P.A and Bonnier, P.G. (1999).** Formulation and verification of the hardening soil model. In *Computational Geotechnics*, pp. 281–290.
- **Selvaraj, S. I. (2012).** Review on the use of instrumented pavement test data in validating flexible pavement mechanistic load response models. *Procedia-Social and Behavioral Sciences*, 43, 819-831.
- **Shighiba, H.A. (2007).** Study of the effect of pavement absorption in a tire-pavement model". Magisters' thesis, Department of Mechanics, University of Blida, Algeria, p.35-37.
- **TRIAW. S. (2006).** Mechanistic-empirical dimensioning of pavement structures: Application to the Séo-Diourbel section. PFE, Ecole supérieure Polytechnique, Dakar (Senegal), p.27-28.